JMIRx Bio

Overlay journal for preprints with post-review manuscript marketplace
Volume 2 (2024) ISSN Editor in Chief: Edward Meinert, MA (Oxon), MSc, MBA, MPA, PhD, CEng, FBCS, EUR ING

Contents

Peer Review Reports

Peer-Review Reports

Authors’ Response to Peer Reviewss

Original Papers

Peer Review Report

Peer Review of "Establishing Antimicrobial Resistance Surveillance in the Water and Environment Sector in a Resource-Limited Setting: Methodical Qualitative and Quantitative Description of Uganda's Experience From 2021 to 2023"

Hojjat Borhany[1], MSc

Politecnico di Milano, Milan, Italy

Related Articles:

Companion article: https://preprints.jmir.org/preprint/50588

Companion article: https://bio.jmirx.org/2024/1/e58949/

Companion article: https://bio.jmirx.org/2024/1/e50588/

(JMIRx Bio 2024;2:e58901) doi:10.2196/58901

KEYWORDS

antimicrobial resistance; surveillance system; water and environment sector

This is a peer-review report submitted for the paper "Establishing Antimicrobial Resistance Surveillance in the Water and Environment Sector in a Resource-Limited Setting: Methodical Qualitative and Quantitative Description of Uganda's Experience From 2021 to 2023"

Round 1 Review

Specific Comments

Major Comments

This paper [1] describes:

1. A stepwise and governmental approach for establishing antimicrobial resistance (AMR) surveillance in the environment and aquatic sector in a country with a resource-limited setting. This includes leveraging on previous experiments in the human and animal sector, and experimental methodology, namely, conventional culture-based bacteriology techniques, which is aligned with the current available equipment and infrastructure at the country scale.
2. The rationality of the passive and active monitoring was well presented and discussed. The quantification of antimicrobial susceptibility in priority microbial isolates were major findings in the study area, as they may cause a silent but life-threatening pandemic. However, no indicator was presented for the assessment of the limitation of the generated AMR data and the scale resolution associated the monitoring sites and sampling locations as well as experimental methodologies.
3. It also lacks a numerical comparison between the AMR values reported for the microbial isolates collected from point sources and nonpoint sources. The readability of the text is very satisfactory; however, there are still some parts that could be further improved!

Minor Comments

1. The Objective section was missed in the structured abstract.
2. The abbreviations should be relocated before the reference section.
3. The map of the study area with the georeferenced location of the monitoring sites along with the compactness of the surveillance site per unit of area were not presented!
4. No indicator was presented for the assessment of the limit of generated AMR data.
5. Comparisons of many AMR values are reported to be similar to other studies, while a significant difference as high as two times was noticed during the peer review. It is recommended to include the values from other studies in the table to facilitate the comparison. Rewrite this section.
6. Some points like "The program needs to be consolidated and expanded to include more sentinel sites, sample types, advanced AMR surveillance methodologies and techniques, and the surveillance of antimicrobial residues" presented in the conclusions are not supported in the main area of the paper.
7. Some information in the abstract, like 27% (n=160) of recovered isolates exhibited multidrug resistance and extensive drug resistance, was never presented in the main text.

8. The Data Analysis section was totally unclear to me. Mainly, I cannot understand what steps were taken to analyze the data. It is recommended that the author adds some description with regard to that.

Conflicts of Interest

None declared.

Reference

1. Katumba G, Mwanja H, Mayito J, Mbolanyi B, Isaasi F, Kibombo D, et al. Establishing antimicrobial resistance surveillance in the water and environment sector in a resource-limited setting: methodical qualitative and quantitative description of Uganda's experience from 2021 to 2023. JMIRx Bio 2024. [doi: 10.2196/50588]

Abbreviations

AMR: antimicrobial resistance

Edited by T Leung; submitted 27.03.24; this is a non–peer-reviewed article;accepted 27.03.24; published 07.05.24.

Please cite as:
Borhany H
Peer Review of "Establishing Antimicrobial Resistance Surveillance in the Water and Environment Sector in a Resource-Limited Setting: Methodical Qualitative and Quantitative Description of Uganda's Experience From 2021 to 2023"
JMIRx Bio 2024;2:e58901
URL: https://bio.jmirx.org/2024/1/e58901
doi:10.2196/58901
PMID:

Peer-Review Report

Peer Review of "Establishing Antimicrobial Resistance Surveillance in the Water and Environment Sector in a Resource-Limited Setting: Methodical Qualitative and Quantitative Description of Uganda's Experience From 2021 to 2023"

Gerald Mboowa[1], PhD

Makerere University, Kampala, Uganda

Related Articles:

Companion article: https://preprints.jmir.org/preprint/50588

Companion article: https://bio.jmirx.org/2024/1/e58949/

Companion article: https://bio.jmirx.org/2024/1/e50588/

(JMIRx Bio 2024;2:e58903) doi:10.2196/58903

KEYWORDS

antimicrobial resistance; surveillance system; water and environment sector

This is a peer-review report submitted for the paper "Establishing Antimicrobial Resistance Surveillance in the Water and Environment Sector in a Resource-Limited Setting: Methodical Qualitative and Quantitative Description of Uganda's Experience From 2021 to 2023"

Round 1 Review

General Comments

This paper [1] is timely and presents data on antimicrobial resistance (AMR) surveillance in the water and environment sector in a resource-limited setting.

Specific Comments

Methodology

"A stepwise approach was employed. Governance structures were streamlined and sector-specific AMR surveillance guiding documents developed" -> "were developed"

"Conslusion" -> Check the spelling.

"CONFLICTS OF INTEREST" -> "CONFLICT OF INTEREST"

Antimicrobial Resistance Governance Establishment and Enhancement

"To streamline the AMR governance in the water and environment sector, a sector-specific AMR technical working group (TWG) was instituted with identified a focal person to coordinate the surveillance activities in the sector." (Rewrite this.)

Major Comments

Enhancement of the Microbiology Capacity of the National Water Quality Reference Laboratory

I would like to see a description of the testing platforms in this lab and plans for genomic surveillance of AMR since it reveals more about the complexity, evolution, and transmission of these pathogens as seen here.

Minor Comments

AMR Data Generation

"The developed sector-specific AMR surveillance documents were pretested." (How was this done?")

Discussion

Figure 1: It would be important to share this data via a public dashboard like here [2]. "Liguori et al. have described the methods as fairly standardized, and an avenue for further analysis of the recovered isolates including sensitivity testing, sequence-based typing and whole genome sequencing, which aid in detecting and identifying antibiotic-resistant genes and genetic elements [3]." And virulence factors [4].

Authors should also discuss making a sentence on the contribution of environmental wastewater sequencing.

As a way forward, I wish to request the authors set up a public dashboard to share this important AMR surveillance data to stakeholders beyond the TWG as seen here [5].

Conflicts of Interest

None declared.

Editorial notice: A peer reviewer conflict of interest was identified prior to publication: They work at the same institution or organization as an author. They have published with an author during the past 5 years.

References

1. Katumba G, Mwanja H, Mayito J, Mbolanyi B, Isaasi F, Kibombo D, et al. Establishing antimicrobial resistance surveillance in the water and environment sector in a resource-limited setting: methodical qualitative and quantitative description of Uganda's experience from 2021 to 2023. JMIRx Bio 2024. [doi: 10.2196/50588]
2. MAAP country reports. African Society for Laboratory Medicine. URL: https://aslm.org/what-we-do/maap/maap-country-reports [accessed 2024-04-22]
3. Liguori K, Keenum I, Davis BC, Calarco J, Milligan E, Harwood VJ, et al. Antimicrobial resistance monitoring of water environments: a framework for standardized methods and quality control. Environ Sci Technol 2022 Jul 05;56(13):9149-9160. [doi: 10.1021/acs.est.1c08918] [Medline: 35732277]
4. Kiyaga S, Kyany'a C, Muraya AW, Smith HJ, Mills EG, Kibet C, et al. Genetic diversity, distribution, and genomic characterization of antibiotic resistance and virulence of clinical strains in Kenya. Front Microbiol 2022;13:835403. [doi: 10.3389/fmicb.2022.835403] [Medline: 35369511]
5. National situation of antimicrobial resistance and consumption analysis from 2016-2018. African Society for Laboratory Medicine. URL: https://aslm.org/wp-content/uploads/2023/07/AMR_REPORT_UGANDA.pdf?x89467 [accessed 2024-04-22]

Abbreviations

AMR: antimicrobial resistance
TWG: technical working group

Edited by T Leung; submitted 27.03.24; this is a non–peer-reviewed article;accepted 27.03.24; published 07.05.24.

Please cite as:
Mboowa G
Peer Review of "Establishing Antimicrobial Resistance Surveillance in the Water and Environment Sector in a Resource-Limited Setting: Methodical Qualitative and Quantitative Description of Uganda's Experience From 2021 to 2023"
JMIRx Bio 2024;2:e58903
URL: https://bio.jmirx.org/2024/1/e58903
doi:10.2196/58903
PMID:

Peer-Review Report

Peer Review of “Roles of Progranulin and FRamides in Neural Versus Nonneural Tissues on Dietary Restriction–Related Longevity and Proteostasis in C. elegans (Preprint)”

Anonymous

Related Article:

Companion article: https://www.biorxiv.org/content/10.1101/2024.02.06.579250v1

(JMIRx Bio 2024;2:e60570) doi:10.2196/60570

KEYWORDS

C. elegans; dietary restriction; lifespan; heat shock; proteostasis; neurodegeneration; motility

This is a peer-review report submitted for the preprint “Roles of Progranulin and FRamides in Neural Versus Nonneural Tissues on Dietary Restriction–Related Longevity and Proteostasis in C. elegans.”

Round 1 Review

General Comments

The manuscript titled “Roles of progranulin and FRamides in neural versus non-neural tissues on dietary restriction-related longevity and proteostasis in C. elegans” by Mir et al [1] examines the role of FMRFamide-like neuropeptides in dietary restriction (DR)–mediated lifespan extension. To achieve this goal, the authors measured the survivability of animals under ad libitum (AL) and DR after knocking down these peptides specifically in the neuronal tissue or systemically (Figures 1 and 2). The authors did not obtain any significant results in these experiments and further performed other experiments to examine the impact of *pgrn-1* and *flp* knockdown in maintaining proteostasis in *eat-2* mutants (Figure 3) and influencing locomotion in the Alzheimer model of neurotoxicity (Figure 4). The data from all these experiments did not reveal any role for *pgrn-1* or *flp* genes in DR-dependent lifespan extension and proteostasis.

Specific Comments

Major Comments

1. The premise of this study was that the authors found that *pgrn-1* and *flp* genes exhibited increased recruitment to polysomes upon DR. These data imply that these genes are translated to higher levels upon DR. Hence, increasing the levels of these under AL should recapitulate a DR-like state. However, the authors decided to examine the phenotypes associated with the knockdown of these genes. However, their data did not show any significant changes in DR-dependent lifespan enhancement. Hence, the logic of performing the experiments in Figures 3 and 4 is unclear.

2. There is no data to indicate the level (-fold decrease) of the FRamides or progranulin after RNA interference.

3. The lifespan experiments corresponding to Figure 2 have been performed two times, and the data are noted in Supplementary Table 3. However, the data from the two repeats (for *flp-5*, *flp-14*) are not reproducible, with one experiment showing a significant difference in lifespan under AL and DR and the second repeat showing no significant difference. These data indicate nonreproducibility, and ideally, no inference should be drawn from them without repeating them.

4. Supplementary Figure 2 data and conclusions are drawn from a single experiment only.

5. The title of the paper reflects that progranulin and FRamides play a role in DR-mediated extension of lifespan; however, all the results noted indicate the opposite (lines 205 and 206, 213-217, 336-339, and 345-348). Hence, the rationale for continuing to assess the role of these genes in the DR pathway by performing experiments in Figures 3 and 4 is unclear. Moreover, the authors also concluded that knocking down the expression of *pgrn-1* or *flp* does not have any role in proteostasis, and their role in neural proteotoxicity is complex (lines 369-372). Based on the data from Figure 4, the authors conclude that downregulation of *pgrn-1* or *flp* has minimal or no effect on motility during adulthood under DR conditions. Overall, the findings indicate that though there is increased translation of *pgrn-1* or *flp* genes upon DR, these genes do not function as DR effectors.

Hence, a more appropriate title would be “Progranulin and FRamides do not play a role in DR-related longevity and proteostasis.” Moreover, a more detailed explanation of the results in Figures 3 and 4 might be helpful for the readers to understand the role of these genes in motility and why there are differences in young and late ages. Unfortunately, I cannot recommend this manuscript for publication in its current state.

Conflicts of Interest

None declared.

Editorial Notice

The authors of the preprint under review declined the opportunity to revise the preprint in response to the feedback in the peer reviews and publish it in the journal JMIRx Bio. The editors thank the peer reviewers for providing their feedback on this preprint.

Reference

1. Mir DA, Cox M, Horrocks J, Ma Z, Rogers A. Roles of progranulin and FRamides in neural versus non-neural tissues on dietary restriction-related longevity and proteostasis in C. elegans. bioRxiv. Preprint posted online on February 8, 2024 2024 [FREE Full text]

Abbreviations

AL: ad libitum
DR: dietary restriction

Edited by G Eysenbach; submitted 15.05.24; this is a non–peer-reviewed article;accepted 15.05.24; published 17.06.24.

Please cite as:
Anonymous
Peer Review of "Roles of Progranulin and FRamides in Neural Versus Nonneural Tissues on Dietary Restriction–Related Longevity and Proteostasis in C. elegans (Preprint)"
JMIRx Bio 2024;2:e60570
URL: https://bio.jmirx.org/2024/1/e60570
doi:10.2196/60570
PMID:

Peer-Review Report

Peer Review of “Roles of Progranulin and FRamides in Neural Versus Nonneural Tissues on Dietary Restriction–Related Longevity and Proteostasis in C. elegans (Preprint)”

Anonymous

Related Article:

Companion article: https://www.biorxiv.org/content/10.1101/2024.02.06.579250v1

(JMIRx Bio 2024;2:e60571) doi:10.2196/60571

KEYWORDS

C. elegans; dietary restriction; lifespan; heat shock; proteostasis; neurodegeneration; motility

This is a peer-review report submitted for the preprint “Roles of Progranulin and FRamides in Neural Versus Nonneural Tissues on Dietary Restriction–Related Longevity and Proteostasis in C. elegans*.”*

Round 1 Review

General Comments

Mir et al [1] is a study designed to understand the role of progranulin and FRamindes in neural and nonneural tissues through a dietary restriction approach.

The idea of using multiple mutants to understand the effect of *flp-5*, *flp-14*, *flp-15*, and *pgrn-1* is interesting. While I like the overall idea and the experimental setup, I have a few questions regarding the study.

Specific Comments

1. I would have liked to see another control where wild-type worms were taken and heat treated at 35 °C alongside an unheated control group. This way I could have seen a more direct and indirect comparison between the groups.

2. I would have liked to understand the reason behind carrying out motility assays at 25 °C when the worms were maintained at 20 °C. Is it because it is ideal?

3. It could be that I might have read it wrong, but to me, the labels in Figures 1, 2, and S2 seem to be off. They don’t match the alphabetical order, or I might be missing something here.

4. For the motility assay, where they compared the GRU102 strain against GRU102 crossed with TU3335, I see that all the results were compared to one universal control. I would have liked to see mutant controls alongside the GRU102 and GRU102 crossed with TU3335. Again, by doing this, I would have had a direct comparison of the control, mutant controls, and mutants under conditions. Here, I cannot see how the mutants were performing on day 1 as the authors show the mutant data started from day 4.

Conflicts of Interest

None declared.

Editorial Notice

The authors of the preprint under review declined the opportunity to revise the preprint in response to the feedback in the peer reviews and publish it in the journal JMIRx Bio. The editors thank the peer reviewers for providing their feedback on this preprint.

Reference

1. Mir DA, Cox M, Horrocks J, Ma Z, Rogers A. Roles of progranulin and FRamides in neural versus non-neural tissues on dietary restriction-related longevity and proteostasis in C. elegans. bioRxiv. Preprint posted online on February 8, 2024 2024 [FREE Full text]

Edited by G Eysenbach; submitted 15.05.24; this is a non–peer-reviewed article;accepted 15.05.24; published 17.06.24.

Please cite as:
Anonymous
Peer Review of "Roles of Progranulin and FRamides in Neural Versus Nonneural Tissues on Dietary Restriction–Related Longevity and Proteostasis in C. elegans (Preprint)"
JMIRx Bio 2024;2:e60571
URL: https://bio.jmirx.org/2024/1/e60571
doi:10.2196/60571
PMID:

Peer Review Report

Peer Review of “Establishment of a Novel Fetal Ovine Heart Cell Line by Spontaneous Cell Fusion: Experimental Study”

Arjama Mukherjee[1]

Indian Association for the Cultivation of Science, Kolkata, India

Related Articles:

Companion article: https://preprints.jmir.org/preprint/53721

Companion article: https://bio.jmirx.org/2024/1/e62911/

Companion article: https://bio.jmirx.org/2024/1/e53721/

(JMIRx Bio 2024;2:e62905) doi:10.2196/62905

KEYWORDS

immortal; cell; cells; biology; heart; cardiology; SNP; SNPs; nucleotide; nucleotides; polymorphism; polymorphisms; cellular; cardiocyte; cardiocytes; gene; genes; genetic; genetics; RNA; rRNA; genome; genomes; genotype; genotyping; genotypes; mutations; mutational

This is a peer-review report submitted for the paper “Establishment of a Novel Fetal Ovine Heart Cell Line by Spontaneous Cell Fusion: Experimental Study.”

Round 1 Review

General Comments

The paper [1] is well researched, innovative, and the methodologies are clear. There are some minor suggestions from my side.

1. Can you provide more details on the specific morphological characteristics observed during the fusion event that led to immobilization? Were there any distinct features or markers associated with the fused cells compared to nonfused cells?

2. Apart from morphological changes, were there any functional assays or markers used to confirm the immortalized phenotype of the fetal ovine heart–Saudi Arabia (FOH-SA) cell line? How were these characteristics compared to primary heart cell cultures?

3. The paper mentions a large-scale genetic conversion leading to high homozygosity in single-nucleotide polymorphism genotypes. What are the potential implications of this genetic conversion on the behavior and stability of the cell line, particularly in terms of its use in vaccine production and biotechnological applications?

4. How was the FOH-SA cell line authenticated at the European Collection of Authenticated Cell Cultures? Were there any specific criteria or standards used to verify the identity and purity of the cell line, especially considering its potential for patenting and commercialization?

5. Beyond vaccine production, what other potential applications or research areas do you envision for the FOH-SA cell line? Are there any specific experiments or collaborations planned to further explore its capabilities and characteristics?

Conflicts of Interest

None declared.

Reference

1. Suleiman K, Aljulidan M, Hussein G, Alkhalaf H. Establishment of a novel fetal ovine heart cell line by spontaneous cell fusion: experimental study. JMIRx Bio 2024. [doi: 10.2196/53721]

Abbreviations

FOH-SA: fetal ovine heart–Saudi Arabia

Edited by G Eysenbach; submitted 04.06.24; this is a non–peer-reviewed article;accepted 04.06.24; published 18.07.24.

Please cite as:
Mukherjee A
Peer Review of "Establishment of a Novel Fetal Ovine Heart Cell Line by Spontaneous Cell Fusion: Experimental Study"
JMIRx Bio 2024;2:e62905
URL: https://bio.jmirx.org/2024/1/e62905
doi:10.2196/62905
PMID:

Peer Review Report

Peer Review of “Establishment of a Novel Fetal Ovine Heart Cell Line by Spontaneous Cell Fusion: Experimental Study”

Hira Rafi[1], PhD

Feinberg School of Medicine, Northwestern University, Chicago, IL, United States

Related Articles:

Companion article: https://preprints.jmir.org/preprint/53721

Companion article: https://bio.jmirx.org/2024/1/e62911/

Companion article: https://bio.jmirx.org/2024/1/e53721/

(JMIRx Bio 2024;2:e63336) doi:10.2196/63336

KEYWORDS

immortal; cell; cells; biology; heart; cardiology; SNP; SNPs; nucleotide; nucleotides; polymorphism; polymorphisms; cellular; cardiocyte; cardiocytes; gene; genes; genetic; genetics; RNA; rRNA; genome; genomes; genotype; genotyping; genotypes; mutations; mutational

This is a peer-review report submitted for the paper “Establishment of a Novel Fetal Ovine Heart Cell Line by Spontaneous Cell Fusion: Experimental Study.”

Round 1 Review

1. Enhancing the presentation for clarity and coherence in outlining the study’s goals and results would improve the paper [1].

2. A more detailed exploration into the cell fusion phenomenon, focusing on the mechanisms of spontaneous fusion, could enrich the study.

3. Investigating and discussing the involvement of specific fusion proteins or cellular factors could yield deeper insights into cell fusion processes.

4. By broadening the comparison to encompass additional immortal cell lines, the study could offer a more comprehensive understanding of its findings’ implications.

5. A comparative analysis of how different cell lines undergo immortalization, their genetic integrity, and their response to viral infections could provide a more nuanced understanding.

6. Extending the functional characterization of the fetal ovine heart–Saudi Arabia (FOH-SA) cell line to include its capability for differentiation and response to various external factors would add value.

7. The paper would benefit from an examination of the FOH-SA cell line’s genetic stability through extended culture durations and numerous passages.

8. Detailing the cell line’s potential for broader biotechnological uses, such as in gene therapy or tissue engineering, would underscore its utility.

9. A discussion on the safety and regulatory aspects related to the cell line’s application in vaccine production, including tumorigenicity risks and quality control adherence, is essential.

10. Incorporating schematic illustrations to summarize the key findings and the spontaneous cell fusion development process would enhance the paper’s visual clarity.

11. Providing details on data and material accessibility, including making sequencing data and cell culture protocols available, would facilitate study replication and transparency.

Round 2 Review

Your manuscript now provides clearer insights and greater detail, which significantly enhances the understanding of the cell line’s characteristics and its potential applications in biotechnology and medicine. The additional data and clarifications have adequately addressed the questions raised, ensuring the work’s robustness and relevance to the field. I believe your findings will make a valuable contribution to the scientific community.

Conflicts of Interest

None declared.

Reference

1. Suleiman K, Aljulidan M, Hussein G, Alkhalaf H. Establishment of a novel fetal ovine heart cell line by spontaneous cell fusion: experimental study. JMIRx Bio 2024. [doi: 10.2196/53721]

Abbreviations

FOH-SA: fetal ovine heart–Saudi Arabia

Edited by G Eysenbach; submitted 17.06.24; this is a non–peer-reviewed article;accepted 19.06.24; published 18.07.24.

Please cite as:
Rafi H
Peer Review of "Establishment of a Novel Fetal Ovine Heart Cell Line by Spontaneous Cell Fusion: Experimental Study"
JMIRx Bio 2024;2:e63336
URL: https://bio.jmirx.org/2024/1/e63336
doi:10.2196/63336
PMID:

Peer-Review Report

Peer Review of “In-Silico Works Using an Improved Hovorka Equations Model and Clinical Works on the Control of Blood Glucose Levels in People With Type 1 Diabetes: Comparison Study”

Ross Gore[1], PhD

Office of Enterprise Research and Innovation, Old Dominion University, Norfolk, VA, United States

Related Articles:

Companion article: https://www.biorxiv.org/content/10.1101/2022.09.23.509189v1

Companion article: https://bio.jmirx.org/2024/1/e64442

Companion article: https://bio.jmirx.org/2024/1/e43662/

(JMIRx Bio 2024;2:e63851) doi:10.2196/63851

KEYWORDS

blood glucose level; closed-loop system; Hovorka model; in-silico work; meal disturbance; type 1 diabetes mellitus

This is a peer-review report submitted for the paper “In-Silico Works Using an Improved Hovorka Equations Model and Clinical Works on the Control of Blood Glucose Levels in People With Type 1 Diabetes: Comparison Study.”

Round 1 Review

General Comments

The paper [1] simulates the ability of a new version of the Hovorka model to simulate the blood glucose level (BGL) of type 1 diabetes (T1D) for 3 patients with meal disturbances for 24 hours. The simulation was done using MATLAB software, and the BGL profile from both simulation and clinical works were compared and analyzed. While the *P* values for the simulation and clinical data were <.05, indicating that the simulation work using the improved Hovorka equations was acceptable for predicting the BGL, results showed that the BGLs for all 3 people with T1D were lower in the simulation work compared to the clinical work.

Specific Comments

Major Comments

1. The paper is well written, the experiments seem correctly designed, and the results seem reasonable. However, the most interesting result is that the simulated BGL results were consistently lower than the clinical results. While the authors discuss some clinical reasons for this systematic difference the hypotheses are not terribly compelling. I think it is also necessary to discuss that the simulation/model may have some systematic bias due to the assumptions of its construction. The model may be an effective low BSL baseline estimate for a patient as opposed to an effective expected value estimate.

In some sense, this is an unexpected result from the model, but it does not make the model invalid. Explicitly stating this, characterizing it in an established taxonomy of unexpected behaviors for simulations, and discussing how the model can still be valid would improve the paper and increase its maturity, in terms of its application of modeling and simulation.

Papers/books to support this effort:

- Mittal S, Diallo S, Tolk A.*Emergent Behavior in Complex Systems Engineering: A Modeling and Simulation Approach*. John Wiley & Sons; 2018.
- Gore R, Reynolds PF. An exploration-based taxonomy for emergent behavior analysis in simulations. Presented at: 2007 Winter Simulation Conference; December 9-12, 2007; Washington, DC.

2. The paper refers to many tables (1-6) that are not present in the text. The data in these tables are needed for the presentation of the material (ie, they need to be present in the paper) and certainly should be present if referenced by the authors.

3. The importance of the issue (T1D) and regulating BGLs has the potential to impact millions of people. In addition, being able to estimate this (even a low-end estimate) with modeling reduces material costs, time, and patient risk. However, this context establishing the impact and importance of the paper is missing. Adding this will help readers appreciate the impact (and cite) the paper.

Minor Comments

4. In the replication crisis era, the MATLAB software the scripts used to create the graphics should be provided to the reader and reviewers.

5. The abstract reads as if it was written continuously (ie, subsections infer context from previous subsections). This is not how JMIR abstracts are written. The subsections within the abstract should be able to be read independently.

Conflicts of Interest

None declared.

Reference

1. Som AM, Sohadi NAM, Nor NSM, Ali SA, Ahmad MA. In-silico works using an improved Hovorka equations model and clinical works on the control of blood glucose levels in people with type 1 diabetes: comparison study. JMIRx Bio 2024;2(1):e43662 [FREE Full text] [doi: 10.2196/43662]

Abbreviations

BGL: blood glucose level
T1D: type 1 diabetes

Edited by T Leung; submitted 01.07.24; this is a non–peer-reviewed article;accepted 16.07.24; published 15.08.24.

Please cite as:
Gore R
Peer Review of "In-Silico Works Using an Improved Hovorka Equations Model and Clinical Works on the Control of Blood Glucose Levels in People With Type 1 Diabetes: Comparison Study"
JMIRx Bio 2024;2:e63851
URL: https://bio.jmirx.org/2024/1/e63851
doi:10.2196/63851
PMID:

Peer-Review Report

Peer Review of “In-Silico Works Using an Improved Hovorka Equations Model and Clinical Works on the Control of Blood Glucose Levels in People With Type 1 Diabetes: Comparison Study”

Anonymous

Related Articles:

Companion article: https://www.biorxiv.org/content/10.1101/2022.09.23.509189v1

Companion article: https://bio.jmirx.org/2024/1/e64442

Companion article: https://bio.jmirx.org/2024/1/e43662/

(JMIRx Bio 2024;2:e64403) doi:10.2196/64403

KEYWORDS

blood glucose level; closed-loop system; Hovorka model; in-silico work; meal disturbance; type 1 diabetes mellitus

This is a peer-review report submitted for the paper “In-Silico Works Using an Improved Hovorka Equations Model and Clinical Works on the Control of Blood Glucose Levels in People With Type 1 Diabetes: Comparison Study.”

Round 1 Review

General Comments

This paper [1] presents a preliminary validation with clinical data of a new glucose-insulin model proposed by the authors in other publications. The paper is well organized and discusses a topic of interest in the field of artificial pancreas.

The authors conclude that the new model is a good predictor for blood glucose levels. However, they also mention that the model yields better glucose metrics than the observed clinical data. In my opinion, these two statements are contradictory, so I would request authors to elaborate on this point more.

Specific Comments

I am afraid that I am doubtful of some methodological aspects of the paper, so I need more justification for them. These concerns are listed in Major Comments. In addition, minor typos and other suggestions are presented in Minor Comments.

Major Comments

1. I would be grateful if the author completed the description of the data collection. It is unclear whether the study was deliberately designed to validate the “improved Hovorka model,” or in contrast, data were initially collected for other purposes. Additionally, I could not find if the study was performed at each patient’s home or, instead, it was a controlled study in the hospital. In addition, I missed information about insulin therapy (closed-loop or open-loop). Finally, in the Results section (line 140), the authors state that the high glucose levels observed in the clinical data may be because of exercise. Does it mean that the study protocol allows the patients to practice physical activity?

2. Preliminary validations of widely used glucose-insulin models such as Hovorka’s [2] or Dalla-Man’s [3] used short-duration trials (less than a day) but with frequent measurement to gain more considerable insight into glucose variations. However, the experiment devised in this manuscript has a longer duration but much less frequent measurements. As the authors state in the Results section, line 139, this lack of measurements may mislead the calculated time in normoglycemia. Could the authors explain why they did not design an experiment with more frequent measurements?

3. The authors indicated that three insulin rates were simulated (lines 75 and 76), and insulin boluses were adjusted by trial and error to optimize the glucose profile (line 101). Nevertheless, I could not find the insulin rates and boluses used in the clinical trial. Were they the same as for the simulation? If not, could you justify this decision, please? In my opinion, using different insulin inputs in the model than in the actual patient will lead to noncomparable outputs.

4. It is unclear how the authors performed the regression statistical analysis (line 135). Did they compare specific blood glucose samples in the clinical data to the corresponding simulated data points, or did they compare some fitting error metric like the root mean square error or glucose performance metric such as the time in range? In addition, it would be helpful if the authors provided which type of regression model they

employed (eg, linear model, generalized model, multilevel model).

5. The authors concluded that the model "is acceptable to predict the BGL for people with T1D" (line 137). However, they also stated that "all patients showed improvement in BGL for the in-silico works." In my opinion, these two statements are contradictory: if the in-silico model did not reproduce, with acceptable errors, the glucose profiles observed in the clinical trial, then the model cannot be considered a good predictor. Could the author explain this point more, please?

Minor Comments

6. I could not find any information about how the authors identify the model's parameters. Could the author describe, please, how the model was calibrated?

7. I could not find any referenced table in the manuscript.

8. Lines 17-19: In the introduction, it seems that the authors presented the "improved Hovorka model" to address the poor performance achieved by current artificial pancreas systems. Could the authors please elaborate more on how the model they presented will enhance the performance of existing control algorithms?

9. The authors used "workers" in several places in the manuscript. Did they mean "works"?

10. Lines 43 and 44: Equation 1 seems to be missing the last term.

11. Lines 63 and 64: I think equation 8 contains a typo. Should the second "=" be removed?

12. Figures 2-4: The collected clinical data comprises six glucose samples per patient. However, data was represented with a continuous line. In my opinion, this representation leads to a misleading interpretation (eg, glucose follows a horizontal line in some periods, which is unrealistic). I suggest the authors mark the actual blood samples as in a scatter plot.

13. Figures 2-4: I think the x-axes should be in hours, not in minutes.

Round 2 Review

First, I would like to thank the authors for completing the clinical trial and statistical analysis description and for addressing all my comments on the previous submission. Unfortunately, I am afraid that I still have some methodological doubts regarding the comparison between the in-silico results and the clinical results. Therefore, I suggest a further revision of the manuscript.

Specific Comments

My principal methodological concerns are listed in the Major Comments section. Other doubts or typos are presented in the Minor Comments section.

Major Comments

1. If I understood well, the insulin infusion rate used to simulate the "Improved Hovorka model" (variable u(t) in equation 6) is different from the infusion rate administered to the actual patients in the clinical trial. On the one hand, virtual patients have received an insulin infusion rate calculated from a closed-loop algorithm (the enhanced model-based predicted control). On the other hand, actual patients seem to follow an open-loop therapy (multiple drug injections). Lastly, the authors also state (lines 361 and 362) that the timing of insulin bolus is different in both settings. Could the authors explain these discrepancies, please? If the goal is to compare the prediction ability of the "Improved Hovorka model," why have the authors not simulated the model with the same insulin therapy used for the clinical trial?

2. From the regression analysis results (lines 406-409), the authors seem to conclude that the model is "applicable in predicting BGL" because the *P* value is <.01. However, I cannot see the relation between a significant *P* value and a better prediction. From the clear description the authors provided of the multiple regression analysis, I think the authors fitted the following linear model:

improved_hovorka_glucose = insulin·beta1 + meal·beta2 + e

where "improved_hovorka_glucose" is the output of the "Improved Hovorka model," "insulin" and "meal" correspond to the values of the infusion rate and meal amount in that model, "beta1" and "beta2" are coefficients to be estimated in the analysis, and "e" is the normal distributed residuals. A *P* value <.05 means that data supports the rejection of the null hypothesis that beta1 = beta2 = 0 [2]. Thus, a significant *P* value indicates that the "insulin" and/or the "meal" inputs can explain the variations observed in "improved_hovorka_glucose." However, I cannot see how one can conclude anything from the prediction accuracy of the "Improved Howorka model" from the fact that beta1≠0 or beta2≠0. Could the author explain this point, please?

Minor Comments

3. Equation 5: The term exp(t/maxG) should be exp(-t/maxG).

4. Equation 6: In line 103, the authors define u(t) as insulin bolus. However, in line 180, the authors refer to infusion rates. Could the author check the consistency of this definition?

Round 3 Review

I would like to thank the authors for their efforts in replying to my comments. Unfortunately, I still do not understand the article's contribution regarding comparing clinical data. As stated by the authors, clinical data and in-silico results are not comparable due to the different methodologies and protocols applied to obtain the data; therefore, I wonder if including the clinical data set analysis is justified. In addition, I have doubts about under which conditions the authors have simulated the model, for instance, if the simulation included any kind of variability.

Specific Comments

Major Comments

1. Since clinical data results and in-silico data are incomparable, could the authors justify the motivation for including the clinical data in the article?

2. In lines 191-193, the authors indicate that comparing the in-silico data with the clinical data would help determine the model's accuracy in mimicking the actual glucose. I believe this statement is incompatible with the fact that both clinical and in-silico data were obtained following incomparable protocols and methodologies.

3. Have the authors thought about modifying the simulation of the model to make the results more comparable with the clinical data? For instance, I would suggest they simulate the model with the same bolus, basal insulin, and meal carbohydrates utilized in the clinical trial. Then, they could compare the model output with each glucose measurement.

4. In the Discussion section (lines 374-378) and the conclusion (line 404), the authors concluded from Table 13 that the patients have less sensitivity in the morning. Since Table 13 corresponds to the results of the virtual patients in the in-silico analysis, I wonder whether the authors have included any kind of circadian variability in the simulation, for instance, some sinusoidal variability in ka1, kw1, kw11, ka2, kw2, kw22, ka3, kw3, or kw33. If this is not the case and these parameters were kept constant in the simulation, I suggest authors better justify this apparent increase in insulin sensitivity.

5. The authors said the insulin bolus was computed by trial and error. Since one of the article's goals is determining the optimal bolus, it would be advisable to detail the method followed to calculate it.

Round 4 Review

I would like to thank the authors for replying to my comments. Unfortunately, I still believe the work has two principal limitations preventing me from accepting the manuscript. The main one is that the differences in protocols and conditions between the clinical and simulation works make it, in my opinion, unfeasible to address the goal of determining "the accuracy and effectiveness of the in-silico model in mimicking real-world BGL dynamics." The second one is that insufficient information is reported to reproduce the calculation of the optimal bolus in the in-silico simulations.

Conflicts of Interest

None declared.

References

1. Som AM, Sohadi NAM, Nor NSM, Ali SA, Ahmad MA. In-silico works using an improved Hovorka equations model and clinical works on the control of blood glucose levels in people with type 1 diabetes: comparison study. JMIRx Bio 2024;2(1):e43662 [FREE Full text] [doi: 10.2196/43662]
2. Hovorka R, Shojaee-Moradie F, Carroll PV, Chassin LJ, Gowrie IJ, Jackson NC, et al. Partitioning glucose distribution/transport, disposal, and endogenous production during IVGTT. Am J Physiol Endocrinol Metab 2002 May;282(5):E992-E1007 [FREE Full text] [doi: 10.1152/ajpendo.00304.2001] [Medline: 11934663]
3. Man CD, Micheletto F, Lv D, Breton M, Kovatchev B, Cobelli C. The UVA/PADOVA type 1 diabetes simulator: new features. J Diabetes Sci Technol 2014 Jan;8(1):26-34 [FREE Full text] [doi: 10.1177/1932296813514502] [Medline: 24876534]

Edited by G Eysenbach; submitted 16.07.24; this is a non–peer-reviewed article;accepted 16.07.24; published 15.08.24.

Please cite as:
Anonymous
Peer Review of "In-Silico Works Using an Improved Hovorka Equations Model and Clinical Works on the Control of Blood Glucose Levels in People With Type 1 Diabetes: Comparison Study"
JMIRx Bio 2024;2:e64403
URL: https://bio.jmirx.org/2024/1/e64403
doi:10.2196/64403
PMID:

Authors' Response to Peer Reviews

Authors' Response to Peer Reviews of "Establishing Antimicrobial Resistance Surveillance in the Water and Environment Sector in a Resource-Limited Setting: Methodical Qualitative and Quantitative Description of Uganda's Experience From 2021 to 2023"

Godfrey Katumba[1*], MSc; Herman Mwanja[2*], BEHS; Jonathan Mayito[2*], MBChB, MMed; Betty Mbolanyi[1], MSc; Fred Isaasi[2], MPH; Daniel Kibombo[2], MPH; Judith Namumbya[1], MSc; David Musoke[3], PhD; Jonathan Kabazzi[2,4], BMLS; Musa Sekamatte[5], MPH; Lillian Idrakua[1], MSci; Richard Walwema[2], MBA; Mohammed Lamorde[2], PhD; Francis Kakooza[2], PhD; Simon Etimu[1], MSci

[1]Ministry of Water and Environment, Government of Uganda, Kampala, Uganda
[2]Infectious Diseases Institute, Makerere University, Kampala, Uganda
[3]School of Public Health, Makerere University, Kampala, Uganda
[4]National Health Laboratory and Diagnostics Services, Ministry of Health, Kampala, Uganda
[5]One Health Coordination Office, Ministry of Health, Kampala, Uganda
[*]these authors contributed equally

Corresponding Author:
Herman Mwanja, BEHS
Infectious Diseases Institute
Makerere University
Makerere University Main-Campus
Kampala
Uganda
Phone: 256 0770781589
Email: hmwanja@idi.co.ug

Related Articles:

Companion article: https://preprints.jmir.org/preprint/50588

Companion article: https://bio.jmirx.org/2024/1/e58901/

Companion article: https://bio.jmirx.org/2024/1/e58903/

Companion article: https://bio.jmirx.org/2024/1/e50588/

(JMIRx Bio 2024;2:e58949) doi:10.2196/58949

KEYWORDS

antimicrobial resistance; surveillance system; water and environment sector

This is the authors' response to peer-review reports for "Establishing Antimicrobial Resistance Surveillance in the Water and Environment Sector in a Resource-Limited Setting: Methodical Qualitative and Quantitative Description of Uganda's Experience From 2021 to 2023".

Round 1 Review

Reviewer B [1]

General Comments

This paper [2] is timely and presents data on antimicrobial resistance surveillance in the water and environment sector in a resource-limited setting.

Specific Comments

Methodology

"A stepwise approach was employed. Governance structures were streamlined and sector-specific AMR surveillance guiding documents developed" -> "were developed"

"Conslusion" -> Check the spelling.

Response: This section was revised and now reads "The Government of Uganda, through the MWE, with support from the Infectious Diseases Institute at Makerere University through the Fleming Fund Country Grant 2 project, instituted a step-wise approach with incremental targets and sequential phases from August 2021. This involved establishing a foundation; consolidating and refining gains; scaling up and further expansion of the surveillance system." Please see page 3 of the revised manuscript.

The spelling for "Conclusion" was also corrected. Please see page 9 of the revised manuscript.

"CONFLICTS OF INTEREST" -> "CONFLICT OF INTEREST"

Response: The suggested edit has been adopted. Please see page 10 of the revised manuscript.

Antimicrobial Resistance Governance Establishment and Enhancement

"To streamline the AMR governance in the water and environment sector, a sector-specific AMR technical working group (TWG) was instituted with identified a focal person to coordinate the surveillance activities in the sector." (Rewrite this.)

Response: This statement has been rewritten and now reads "A sector-specific AMR technical working group (TWG) and a focal person position were established to coordinate AMR containment efforts including surveillance activities in the sector."

Major Comments

Enhancement of the Microbiology Capacity of the National Water Quality Reference Laboratory

I would like to see a description of the testing platforms in this lab and plans for genomic surveillance of antimicrobial resistance (AMR) since it reveals more about the complexity, evolution, and transmission of these pathogens as seen here.

Response: The current testing platforms were described in the Methodology section under the "Pre-test and rollout of the AMR surveillance documents sub-section." Please see page 3 of the revised manuscript.

Minor Comments

AMR Data Generation

"The developed sector-specific AMR surveillance documents were pretested." (How was this done?)

Response: The steps followed during the pretest were included. This section now reads "The developed sector specific AMR surveillance documents were pre-tested through an active survey. This involved collection of samples from the Kampala-Wakiso region and analysing them at the NWQRL. Nine strategic surface water (non-point sources) and waste water (point sources) sampling sites were identified in Kampala and Wakiso and fifteen grab samples collected using the standard procedures as stipulated in the different surveillance documents. The samples were transported to the NWQRL under appropriate conditions and analysed using standard conventional culture-based procedures. The lessons learned during the pre-test were used to refine the surveillance documents." Please see page 3 of the revised manuscript.

Discussion

Figure 1: It would be important to share this data via a public dashboard like here [3]. "Liguori et al. have described the methods as fairly standardized, and an avenue for further analysis of the recovered isolates including sensitivity testing, sequence-based typing and whole genome sequencing, which aid in detecting and identifying antibiotic-resistant genes and genetic elements [4]." And virulence [5] factors.

Response: The section on data availability was added to the manuscript and reads "The data generated from the water and environment sector is a preserve of the Uganda MWE. It can be accessed by placing a request and concept on use to the Commissioner Water Quality Management Department in the Directorate of Water Resources Management, MWE." Please see page 9 of the revised manuscript.

Authors should also discuss making a sentence on the contribution of environmental wastewater sequencing.

Response: This has been included as advised and reads as "Thus, the AMR surveillance systems in the sector require appropriate expansion to include whole genome sequencing and environmental wastewater sequencing." Please see page 8 of the revised manuscript.

As a way forward, I wish to request the authors set up a public dashboard to share this important AMR surveillance data to stakeholders beyond the TWG as seen [6] here.

Response: The section on data availability was added to the manuscript and reads as "The data generated from the water and environment sector is a preserve of the Uganda MWE. It can be accessed by placing a request and concept on use to the Commissioner Water Quality Management Department in the Directorate of Water Resources Management, MWE." Please see page 9 of the revised manuscript.

Reviewer BS [7]

Specific Comments

Major Comments

This paper describes:

1. A stepwise and governmental approach for establishing AMR surveillance in the environment and aquatic sector in a country with a resource-limited setting. This includes leveraging on previous experiments in the human and animal sector, and experimental methodology, namely, conventional culture-based

bacteriology techniques, which is aligned with the current available equipment and infrastructure at the country scale.

2. The rationality of the passive and active monitoring was well presented and discussed. The quantification of antimicrobial susceptibility in priority microbial isolates were major findings in the study area, as they may cause a silent but life-threatening pandemic. However, no indicator was presented for the assessment of the limitation of the generated AMR data and the scale resolution associated the monitoring sites and sampling locations as well as experimental methodologies.

3. It also lacks a numerical comparison between the AMR values reported for the microbial isolates collected from point sources and nonpoint sources. The readability of the text is very satisfactory; however, there are still some parts that could be further improved!

Response: A comparison of the resistance observed among isolates collected from point and nonpoint sources was done. This section has been included and it reads as "Overall, there was no significant difference between the resistance observed in E. coli and Klebsiella spp isolates recovered from point and non-point sources. Among the Enterococcus spp isolates, a significant difference (OR 5.318182 (95% CI 1.793498-15.76977), p=0.003) was observed in the resistance to chloramphenicol between the isolates recovered from point and non-point sources. The Enterococcus isolates recovered from point sources were five times more likely to be resistant to chloramphenicol than those recovered from non-point sources." Please see page 6 of the revised manuscript.

Minor Comments

1. The Objective section was missed in the structured abstract.

Response: The Objective section has been included in the structured abstract, and it reads as "To describe Uganda's experience in establishing AMR surveillance in the Water and Environment sector." Please see page 1 of the revised manuscript.

2. The abbreviations should be relocated before the reference section.

Response: The list of abbreviations and acronyms used in the manuscript has been provided before the References section. Please see page 10 of the revised manuscript.

3. The map of the study area with the georeferenced location of the monitoring sites along with the compactness of the surveillance site per unit of area were not presented!

Response: A map of the study area has been developed and provided as a figure PNG file.

4. No indicator was presented for the assessment of the limit of generated AMR data.

Response: An explanation for this has been provided in the Discussion section. It reads "The representativeness of the AMR data generated is still limited as the active surveys are conducted in only the Kampala- Wakiso region. Therefore, the data may not be sufficient to generalize the prevalence of AMR in Uganda's water and environment sector. However, the data marks the first efforts to generate AMR data in the sector, but more efforts are required to increase the quantity of the sector AMR data." Please see page 9 of the revised manuscript.

5. Comparisons of many AMR values are reported to be similar to other studies, while a significant difference as high as two times was noticed during the peer review. It is recommended to include the values from other studies in the table to facilitate the comparison. Rewrite this section.

Response: The section has been rewritten as suggested. Please see page 7 of the revised manuscript.

6. Some points like "The program needs to be consolidated and expanded to include more sentinel sites, sample types, advanced AMR surveillance methodologies and techniques, and the surveillance of antimicrobial residues" presented in the conclusions are not supported in the main area of the paper.

Response: The Methodology and Results sections were revised to include the suggestions. Please see pages 3-7 of the revised manuscript.

7. Some information in the abstract, like 27% (n=160) of recovered isolates exhibited multidrug resistance and extensive drug resistance, was never presented in the main text.

Response: This text in the abstract was changed. The statement now reads "Up to 254 (64%) of the priority pathogens recovered exhibited multi and extensive resistance to the different antibiotics set." Please see pages 1 and 7 of the revised manuscript.

8. The Data Analysis section was totally unclear to me. Mainly, I cannot understand what steps were taken to analyze the data. It is recommended that the author adds some description with regard to that.

Response: The Data section was revised and more description was added. The section now reads "Microsoft Excel 2016 and Stata 16 were used for data entry, cleaning and analysis. Percentage resistance of the isolates to each antibiotic was generated and visuals (charts and graphs) developed. The Chi-square test and binary logistic regression were used to test whether resistance of the priority pathogens (E. coli, Klebsiella and Enterococcus spp) to the different antibiotics were significantly different across the point and non-point sources. A p-value of less than 0.05 indicated a significant statistical difference." Please see pages 4 of the revised manuscript.

Conflicts of Interest

None declared.

References

1. Mboowa G. Peer review of "Establishing Antimicrobial Resistance Surveillance in the Water and Environment Sector in a Resource-Limited Setting: Methodical Qualitative and Quantitative Description of Uganda's Experience From 2021 to 2023". JMIRx Bio 2024. [doi: 10.2196/58903]
2. Katumba G, Mwanja H, Mayito J, Mbolanyi B, Isaasi F, Kibombo D, et al. Establishing antimicrobial resistance surveillance in the water and environment sector in a resource-limited setting: methodical qualitative and quantitative description of Uganda's experience from 2021 to 2023. JMIRx Bio 2024. [doi: 10.2196/50588]
3. MAAP country reports. African Society for Laboratory Medicine. URL: https://aslm.org/what-we-do/maap/maap-country-reports [accessed 2024-04-22]
4. Liguori K, Keenum I, Davis BC, Calarco J, Milligan E, Harwood VJ, et al. Antimicrobial resistance monitoring of water environments: a framework for standardized methods and quality control. Environ Sci Technol 2022 Jul 05;56(13):9149-9160. [doi: 10.1021/acs.est.1c08918] [Medline: 35732277]
5. Kiyaga S, Kyany'a C, Muraya AW, Smith HJ, Mills EG, Kibet C, et al. Genetic diversity, distribution, and genomic characterization of antibiotic resistance and virulence of clinical strains in Kenya. Front Microbiol 2022;13:835403 [FREE Full text] [doi: 10.3389/fmicb.2022.835403] [Medline: 35369511]
6. National situation of antimicrobial resistance and consumption analysis from 2016-2018. African Society for Laboratory Medicine. URL: https://aslm.org/wp-content/uploads/2023/07/AMR_REPORT_UGANDA.pdf?x89467 [accessed 2024-04-22]
7. Borhany H. Peer review of "Establishing Antimicrobial Resistance Surveillance in the Water and Environment Sector in a Resource-Limited Setting: Methodical Qualitative and Quantitative Description of Uganda's Experience From 2021 to 2023". JMIRx Bio 2024. [doi: 10.2196/58901]

Abbreviations

AMR: antimicrobial resistance
TWG: technical working group

Edited by T Leung; submitted 28.03.24; this is a non–peer-reviewed article;accepted 28.03.24; published 07.05.24.

Please cite as:
Katumba G, Mwanja H, Mayito J, Mbolanyi B, Isaasi F, Kibombo D, Namumbya J, Musoke D, Kabazzi J, Sekamatte M, Idrakua L, Walwema R, Lamorde M, Kakooza F, Etimu S
Authors' Response to Peer Reviews of "Establishing Antimicrobial Resistance Surveillance in the Water and Environment Sector in a Resource-Limited Setting: Methodical Qualitative and Quantitative Description of Uganda's Experience From 2021 to 2023"
JMIRx Bio 2024;2:e58949
URL: https://bio.jmirx.org/2024/1/e58949
doi:10.2196/58949
PMID:

Authors' Response to Peer Reviews

Authors' Response to Peer Reviews of "Establishment of a Novel Fetal Ovine Heart Cell Line by Spontaneous Cell Fusion: Experimental Study"

Khalid Suleiman[1], BVSc, MVSc, PhD; Mutaib Aljulidan[1], BSc; Gamaleldin Hussein[1], BVSc, MVSc, PhD; Habib Alkhalaf[1], BVSc, MVSc

Veterinary Vaccine Production Centre, Ministry of Environment, Water and Agriculture, Riyadh, Saudi Arabia

Corresponding Author:
Khalid Suleiman, BVSc, MVSc, PhD
Veterinary Vaccine Production Centre
Ministry of Environment, Water and Agriculture
PO Box 15831
Riyadh, 11454
Saudi Arabia
Phone: 966 501305563
Email: kmsuleiman67@gmail.com

Related Articles:

Companion article: https://preprints.jmir.org/preprint/53721

Companion article: https://bio.jmirx.org/2024/1/e63336/

Companion article: https://bio.jmirx.org/2024/1/e62905/

Companion article: https://bio.jmirx.org/2024/1/e53721/

(JMIRx Bio 2024;2:e62911) doi:10.2196/62911

KEYWORDS

immortal; cell; cells; biology; heart; cardiology; SNP; SNPs; nucleotide; nucleotides; polymorphism; polymorphisms; cellular; cardiocyte; cardiocytes; gene; genes; genetic; genetics; RNA; rRNA; genome; genomes; genotype; genotyping; genotypes; mutations; mutational

This is the authors' response to peer-review reports for "Establishment of a Novel Fetal Ovine Heart Cell Line by Spontaneous Cell Fusion: Experimental Study."

Round 1 Review

Reviewer CU [1]

1. Enhancing the presentation for clarity and coherence in outlining the study's goals and results would improve the paper [2].

Response: We have carefully addressed the issues and revised the manuscript.

2. A more detailed exploration into the cell fusion phenomenon, focusing on the mechanisms of spontaneous fusion, could enrich the study.

Response: It is true that studying the mechanisms of spontaneous cell fusion would have enriched the study, however, that would require additional research tools such as flow cytometry to separate the two morphological cell types and to explore the nature and markers of each cell type.

3. Investigating and discussing the involvement of specific fusion proteins or cellular factors could yield deeper insights into cell fusion processes.

Response: We still keep stock of cells before cell fusion, and we hope to collaborate with specialized international research centers so as to investigate the event of spontaneous cell fusion at the molecular level.

4. By broadening the comparison to encompass additional immortal cell lines, the study could offer a more comprehensive understanding of its findings' implications.

Response: The available data about the Vero cell line allowed us to compare some of its data with these of fetal ovine heart–Saudi Arabia (FOH-SA). Future studies could include additional immortal cell lines.

5. A comparative analysis of how different cell lines undergo immortalization, their genetic integrity, and their response to viral infections could provide a more nuanced understanding.

Response: The exact mechanisms that led to spontaneous immortalization of most animal cell lines remained unexplained, and the results of this study gave an explanation of how the Vero cell line was established, and this might encourage researchers to further investigate into this area.

6. Extending the functional characterization of the FOH-SA cell line to include its capability for differentiation and response to various external factors would add value.

Response: Such an investigation would be of great value since external factors would affect the cell density and ultimately the target product such as viruses.

7. The paper would benefit from an examination of the FOH-SA cell line's genetic stability through extended culture durations and numerous passages.

Response: In this study, we investigated the extended culture incubation at 37 °C of one passage, but we did not examine its genetic stability.

8. Detailing the cell line's potential for broader biotechnological uses, such as in gene therapy or tissue engineering, would underscore its utility.

Response: The cell line being permissive to many animal viruses, it might be a good future candidate for expression of vector viruses and plasmids and hence its possible utility in gene therapy.

9. A discussion on the safety and regulatory aspects related to the cell line's application in vaccine production, including tumorigenicity risks and quality control adherence, is essential.

Response: Depending on the fact that the Vero cell line was found to be tumorigenic at a high passage number (232), we cautiously used this to produce vaccines at passages 40-70; nonetheless, the safety of the cell line in vaccine production and its tumorigenicity should be investigated.

10. Incorporating schematic illustrations to summarize the key findings and the spontaneous cell fusion development process would enhance the paper's visual clarity.

Response: We have added a schematic summary of the spontaneous cell fusion event to the manuscript. Thank you very much.

11. Providing details on data and material accessibility, including making sequencing data and cell culture protocols available, would facilitate study replication and transparency.

Response: We have added a subsection for data and material availability to the manuscript.

Reviewer DA [3]

General Comments

The paper is well researched, innovative, and the methodologies are clear. There are some minor suggestions from my side.

1. Can you provide more details on the specific morphological characteristics observed during the fusion event that led to immobilization? Were there any distinct features or markers associated with the fused cells compared to nonfused cells?

Response: During the study, we observed the following additional morphological characteristics:

1. The population of epithelial-like cells constituted about 70%-75% of the cell population, while the fibroblast-like cells represented about 25%-30%. This may partially explain the increased proliferation rate of the fibroblast-like cells at passages 27 and 28 just before the point of fusion.
2. The size of cells after cell fusion is comparatively smaller than the size of cells before cell fusion. The figure, which was a trial to document the transformation event before we had a phase contrast microscope, clearly shows the difference in shape, size, and intensity of growth between the cells before transformation (Figure A, passage 26), the filamentous growth at passages 29, 30, 31, and 32 (Figure B), and cells after transformation (Figure C, passage 33).

2. Apart from morphological changes, were there any functional assays or markers used to confirm the immortalized phenotype of the FOH-SA cell line? How were these characteristics compared to primary heart cell cultures?

Response: Apart from the morphological changes and absence of signs of senescence after prolonged passage, we did not investigate specific markers or functional assays.

3. The paper mentions a large-scale genetic conversion leading to high homozygosity in single-nucleotide polymorphism (SNP) genotypes. What are the potential implications of this genetic conversion on the behavior and stability of the cell line, particularly in terms of its use in vaccine production and biotechnological applications?

Response: In general, the change in SNP genotype may alter the amino acid sequence (nonsynonmous SNP) or may not cause a change in the amino acid sequence (synonymous SNP). In this regard, we are particularly interested in investigating the status of the interferon gene cluster, which might partially explain the permissiveness of the cell line to animal viruses.

4. How was the FOH-SA cell line authenticated at the European Collection of Authenticated Cell Cultures? Were there any specific criteria or standards used to verify the identity and purity of the cell line, especially considering its potential for patenting and commercialization?

Response: Authentication of animal cell lines at culture collection is done by DNA barcoding of the cytochrome C oxidase gene to verify the animal species of the cell line and the test will detect the presence of any contaminating cells from other species.

The cell line deposit at ATCC (International Depository Authority) is certified as the "Original Deposit," and according to Budapest Treaty Rule 11, samples of the deposit can be furnished to a third-party by a written authorization from the depositor. An international company has already requested a nonexclusive licensing for the cell line.

5. Beyond vaccine production, what other potential applications or research areas do you envision for the FOH-SA cell line? Are there any specific experiments or collaborations planned to further explore its capabilities and characteristics?

Response: In collaboration with national or international research centers, we will look forward to studying:

- The whole genome sequence and the mutation events after cell fusion that led to immortalization,
- Comparative study of the mitochondria genome of FOH-SA and Vero cell lines, and
- The molecular events of spontaneous cell fusion.

References

1. Rafi H. Peer review of "Establishment of a Novel Fetal Ovine Heart Cell Line by Spontaneous Cell Fusion: Experimental Study". JMIRx Bio 2024. [doi: 10.2196/63336]
2. Suleiman K, Aljulidan M, Hussein G, Alkhalaf H. Establishment of a novel fetal ovine heart cell line by spontaneous cell fusion: experimental study. JMIRx Bio 2024. [doi: 10.2196/53721]
3. Mukherjee A. Peer review of "Establishment of a Novel Fetal Ovine Heart Cell Line by Spontaneous Cell Fusion: Experimental Study". JMIRx Bio 2024. [doi: 10.2196/62905]

Abbreviations

FOH-SA: fetal ovine heart–Saudi Arabia
SNP: single-nucleotide polymorphism

Edited by T Leung; submitted 04.06.24; this is a non–peer-reviewed article;accepted 04.06.24; published 18.07.24.

Please cite as:
Suleiman K, Aljulidan M, Hussein G, Alkhalaf H
Authors' Response to Peer Reviews of "Establishment of a Novel Fetal Ovine Heart Cell Line by Spontaneous Cell Fusion: Experimental Study"
JMIRx Bio 2024;2:e62911
URL: https://bio.jmirx.org/2024/1/e62911
doi:10.2196/62911
PMID:

Authors' Response to Peer Reviews

Authors' Response to Peer Reviews of "In-Silico Works Using an Improved Hovorka Equations Model and Clinical Works on the Control of Blood Glucose Levels in People With Type 1 Diabetes: Comparison Study"

Ayub Md Som[1*], MSc, PhD; Nur Amanina Mohd Sohadi[1*], BEng, MSc; Noor Shafina Mohd Nor[2*], MB BCh BAO, BMedSc, MRCP; Sherif Abdulbari Ali[1*], MSc, PhD; Mohd Aizad Ahmad[1*], BEng, MSc, PhD

[1]School of Chemical Engineering, College of Engineering, Universiti Teknologi MARA, Shah Alam, Malaysia

[2]Department of Peadiatrics, Faculty of Medicine, Universiti Teknologi MARA, Sungai Buloh, Malaysia

[*]all authors contributed equally

Corresponding Author:
Ayub Md Som, MSc, PhD
School of Chemical Engineering
College of Engineering
Universiti Teknologi MARA
Block 5, Level 10 Engineering Complex
Shah Alam, 40450
Malaysia
Phone: 60 173211463
Email: ayub522@uitm.edu.my

Related Articles:

Companion article: https://www.biorxiv.org/content/10.1101/2022.09.23.509189v1

Companion article: https://bio.jmirx.org/2024/1/e63851

Companion article: https://bio.jmirx.org/2024/1/e64403

Companion article: https://bio.jmirx.org/2024/1/e43662/

(JMIRx Bio 2024;2:e64442) doi:10.2196/64442

KEYWORDS

blood glucose level; closed-loop system; Hovorka model; in-silico work; meal disturbance; type 1 diabetes mellitus

This is the authors' response to peer-review reports for "In-Silico Works Using an Improved Hovorka Equations Model and Clinical Works on the Control of Blood Glucose Levels in People With Type 1 Diabetes: Comparison Study."

Round 1 Review

Reviewer AN [1]

General Comments

The paper [2] simulates the ability of a new version of the Hovorka model to simulate the blood glucose level (BGL) of type 1 diabetes (T1D) for 3 patients with meal disturbances for 24 hours. The simulation was done using MATLAB software, and the BGL profile from both simulation and clinical works were compared and analyzed. While the P values for the simulation and clinical data were <.05, indicating that the simulation work using the improved Hovorka equations was acceptable for predicting the BGL, results showed that the BGLs for all 3 people with T1D were lower in the simulation work compared to the clinical work.

Response: Thank you for the compliments.

Specific Comments

Major Comment

1. The paper is well written, the experiments seem correctly designed, and the results seem reasonable. However, the most interesting result is that the simulated BGL results were consistently lower than the clinical results. While the authors

discuss some clinical reasons for this systematic difference the hypotheses are not terribly compelling. I think it is also necessary to discuss that the simulation/model may have some systematic bias due to the assumptions of its construction. The model may be an effective low BSL baseline estimate for a patient as opposed to an effective expected value estimate.

In some sense, this is an unexpected result from the model, but it does not make the model invalid. Explicitly stating this, characterizing it in an established taxonomy of unexpected behaviors for simulations, and discussing how the model can still be valid would improve the paper and increase its maturity, in terms of its application of modeling and simulation.

Papers/books to support this effort:

- *Mittal S, Diallo S, Tolk A.*Emergent Behavior in Complex Systems Engineering: A Modeling and Simulation Approach. *John Wiley & Sons; 2018.*
- *Gore R, Reynolds PF. An exploration-based taxonomy for emergent behavior analysis in simulations. Presented at: 2007 Winter Simulation Conference; December 9-12, 2007; Washington, DC.*

Response: Thank you for the compliments and constructive comments. We have taken the recommendations seriously by explaining it in greater length in the revised manuscript as follows:

Discussion section (lines 335-352): “The comparison of BGL against time between clinical and in-silico works can be challenging, especially when clinical data is limited, and in this case the CGM device is not used. Thus, the BGL profiles are different since patients in the clinical work use conventional method to monitor their BGL i.e. SMBG and MDI; therefore, only a snapshot of BGL at a particular time available for comparison as seen in Figures 5 to 7. Studies have shown that the use of CGM device can improve time in range in the clinical settings, thus improve the BGL profiles [3,4].

“In this case, the only available data point is the focus since the clinical data is limited and does not cover the entire time span. While BGL simulations can be helpful for predicting how a T1D patient’s BGL may change under different conditions, they are not always accurate. This is because the mathematical models used in the simulations are based on assumptions about how the body works, and these assumptions may not always hold for every individual. Additionally, the simulation may not consider all of the complex factors that can affect BGL, such as exercise, stress or illness. BGL monitoring can also be subjected to errors and variability in clinical settings. Factors such as the accuracy of the glucose meter or sensor, the timing and frequency of measurements, and the variability of patients' responses to interventions (meals, physical activities, and medication for example) can all affect the reliability and accuracy of clinical BGL monitoring.”

2. The paper refers to many tables (1-6) that are not present in the text. The data in these tables are needed for the presentation of the material (ie, they need to be present in the paper) and certainly should be present if referenced by the authors.

Response: Tables 1-6 are included in the revised manuscript plus their respective references. More tables have also been added to give insightful information to further support the findings and conclusion.

3. The importance of the issue (T1D) and regulating BGLs has the potential to impact millions of people. In addition, being able to estimate this (even a low-end estimate) with modeling reduces material costs, time, and patient risk. However, this context establishing the impact and importance of the paper is missing. Adding this will help readers appreciate the impact (and cite) the paper.

Response: Thank you for the constructive comments.

This statement was added in the revised manuscript as recommended.

Introduction section (lines 16-19): “The importance of the issue (T1D) and regulating BGL by means of the APD has the potential to impact millions of people. In addition, being able to estimate this (even a low-end estimate) with modelling work reduces materials cost, time and patient risk.”

Minor Comments

4. In the replication crisis era, the MATLAB software the scripts used to create the graphics should be provided to the reader and reviewers.

Response: Some examples of the scripts used in MATLAB are provided to the reader and reviewers in the revised manuscript in the case of enhanced model-based predicted control (eMPC) applications for the control system algorithm. Please refer to Figures 6 and 7 (lines 191 and 192).

5. The abstract reads as if it was written continuously (ie, subsections infer context from previous subsections). This is not how JMIR abstracts are written. The subsections within the abstract should be able to be read independently.

Response: Thank you for the comments. All necessary corrections have been made in the revised abstract:

“Background: People with Type 1 Diabetes (T1D) depend on external insulin to regulate their BGL within the normoglycemic range between 4.0 to 7.0 mmol/L. T1D patients routinely conduct self-monitoring of blood glucose (SMBG) through finger pricks prior to insulin injections. Artificial Pancreas (AP) is an innovative device that mimics the function of a healthy pancreas. Despite its recent advancement, the control algorithms used in the AP are still lagging in delivering the proper insulin dosage to T1D patients. Previous researchers attempted to improve the interrelation between parameters and variables in the original Hovorka model equations, later known as improved Hovorka model equations; however, the improved model equations have not yet been tested in terms of its usability to regulate and control the BGL in safe range for two or more people with T1D.

“Objectives: This study aimed to simulate the improved Hovorka model equations using actual patients’ data via MATLAB programming coupled with enhanced model-based predicted control (eMPC) and determine the optimum bolus insulin. The

study then compares the performance results obtained from in-silico and clinical works.

"Methods: Three actual patients' data were collected from Clinic 1, Clinical Training Centre, Universiti Teknologi MARA (UiTM) Hospital, Sungai Buloh, Selangor upon getting approval from UiTM Ethics Committee. The inclusion criteria of subjects were namely; T1D patients, age range between 11 to 14 years old, highly dependent on insulin injection with four or more finger pricks or self-monitoring of blood glucose (SMBG) for BGL measurements per day. T1D patients attended the clinic every three months and require blood taking as routine follow-up care. The T1D patients typically receive meals three times per day; breakfast, lunch, and dinner. As for data analysis of patients between clinical and in-silico works, *P*-value via multiple linear regression (MLR) was used to model the relationship between meal, insulin, and BGL.

"Results: Based on observation, in order of breakfast, lunch, and dinner: the optimum bolus insulins for patient 1 were 83.33, 33.33 and 16.67 mU/min; patient 2 were 66.67, 50.01 and 33.33 mU/min, and patient 3 were 100.02, 83.33, and 66.67 mU/min, respectively. As for the in-silico works using improved Hovorka model equations, results revealed that the percentages of time for their BGL on target in patients 1, 2, and 3 were at 79.59%, 87.76%, and 71.43%, respectively, as compared to the clinical works with less than 50%. All patients in both clinical and in-silico works had a significantly small *P*-value ($P<0.01$), which indicated there was strong relationship between the independent variables (meals and insulin) and the dependent variable (BGL).

"Conclusions: In conclusion, the in-silico work using the improved Hovorka model equations can be applicable in simulating BGL with meal disturbances for people with T1D."

Anonymous [5]

General Comments

This paper [1] presents a preliminary validation with clinical data of a new glucose-insulin model proposed by the authors in other publications. The paper is well organized and discusses a topic of interest in the field of artificial pancreas.

The authors conclude that the new model is a good predictor for blood glucose levels. However, they also mention that the model yields better glucose metrics than the observed clinical data. In my opinion, these two statements are contradictory, so I would request authors to elaborate on this point more.

Response: Thank you for the compliments and constructive comments. We have taken the recommendations seriously by explaining it in greater length in the revised manuscript as follows:

Discussion section (lines 335-352): "The comparison of BGL against time between clinical and in-silico works can be challenging, especially when clinical data is limited, and in this case the CGM device is not used. Thus, the BGL profiles are different since patients in the clinical work use conventional method to monitor their BGL i.e. SMBG and MDI; therefore, only a snapshot of BGL at a particular time available for comparison as seen in Figures 5 to 7. Studies have shown that the use of CGM device can improve time in range in the clinical settings, thus improve the BGL profiles [3,4].

"In this case, the only available data point is the focus since the clinical data is limited and does not cover the entire time span. While BGL simulations can be helpful for predicting how a T1D patient's BGL may change under different conditions, they are not always accurate. This is because the mathematical models used in the simulations are based on assumptions about how the body works, and these assumptions may not always hold for every individual. Additionally, the simulation may not consider all of the complex factors that can affect BGL, such as exercise, stress or illness. BGL monitoring can also be subjected to errors and variability in clinical settings. Factors such as the accuracy of the glucose meter or sensor, the timing and frequency of measurements, and the variability of patients' responses to interventions (meals, physical activities, and medication for example) can all affect the reliability and accuracy of clinical BGL monitoring."

Specific Comments

I am afraid that I am doubtful of some methodological aspects of the paper, so I need more justification for them. These concerns are listed in Major Comments. In addition, minor typos and other suggestions are presented in Minor Comments.

Response: Thank you for the comment.

Major Comments

1. I would be grateful if the author completed the description of the data collection. It is unclear whether the study was deliberately designed to validate the "improved Hovorka model," or in contrast, data were initially collected for other purposes. Additionally, I could not find if the study was performed at each patient's home or, instead, it was a controlled study in the hospital. In addition, I missed information about insulin therapy (closed-loop or open-loop). Finally, in the Results section (line 140), the authors state that the high glucose levels observed in the clinical data may be because of exercise. Does it mean that the study protocol allows the patients to practice physical activity?

Response: Thank you for the constructive comments. Apparently, the study was deliberately designed to validate the improved Hovorka model using the actual patients' data. As for the clinical data, the actual patients took their BGL via self-monitoring of blood glucose (SMBG; finger prick) at patients' homes during breakfast, lunch, and dinner times. These finding results were then compared with the findings through simulation or in-silico works (via MATLAB) using the improved Hovorka model proposed by the authors. No physical activity was allowed in the study protocols. For more information of the study protocols and data collection, please refer to the Methods section as outlined in the revised manuscript.

Methods section (lines 32-59):

"Ethics Approval on Data Collection for Clinical Works

"Ethical approval for this study (Ref No: REC/435/19) was granted by the University Teknologi MARA (UiTM) Ethics Committee before data collection was commenced (reference

letter: 600-TNCPI (5/1/6) dated 29 October 2019). Data collection and patients' information required in this study were obtained from Clinic 1, Clinical Training Centre (CTC), UiTM Medical Specialist Centre, UiTM Hospital, Sungai Buloh, Selangor. Information sheets were given, and formal consent for participation from the parents or legal guardians of T1D patients was obtained since the subjects were all minors. During the appointment, parents or guardians of participants, i.e., T1D patients, were allowed to ask questions before signing the consent form. The participants could withdraw from the study at any time without penalty. Participants' details, such as names or other personal identifiers, remain confidential in the researcher's data.

"A total of three (3) T1D patients were recruited following informed consent. The inclusion criteria of subjects were namely; T1D patients, age range between 11 to 14 years old, highly dependent on insulin injection with four or more finger pricks or self-monitoring of blood glucose (SMBG) for BGL measurements per day, multiple daily injections (MDI) of insulin, and with well-documented bolus insulin requirement. Exclusion criteria were T1D patients with evidence of hypoglycaemia unawareness, known or suspected allergy to insulin, established neuropathy, nephropathy, and retinopathy. T1D patients attended the clinic every three months and require blood taking as routine follow-up care. The amount of blood taken by the paediatrician was 5mL for fasting glucose and fasting insulin each and was taken once only. The additional data required include namely; patient's name, age, gender, race, body weight, body mass index (BMI), type and amounts of meals consumed specifically carbohydrates (CHO), meal time and duration, T1D history (years diagnosed with T1D), fasting plasma glucose level, fasting plasma insulin level, bolus insulin administered, and other relevant information. The T1D patients typically receive meals three times per day; breakfast, lunch, and dinner. The actual patients' data were termed clinical data (clinical work) throughout the study."

Methods section (lines 74-78):

"Mathematical Model for In-silico Works

"Improved Hovorka equations [6,7] based on Hovorka model [8] are specifically designed for people with T1D. The diagram of the improved Hovorka equations model is illustrated as shown in Figure 1. The model has two inputs: meal disturbances and bolus insulin. It consists of three subsystems: the glucose subsystem, insulin subsystem, and insulin action subsystem."

Lines 161-165: "Consequently, all simulated data via in-silico works for the three people with T1D were collected and plotted so as to produce such profiles of BGL versus time for each patient, respectively. Upon completion of data collection and construction of sufficient BGL versus time profiles for both clinical and in-silico works, these two finding results were then analysed and compared for any similarity and difference purposes."

2. Preliminary validations of widely used glucose insulin models such as Hovorka's [9] or Dalla-Man's [10] used short-duration trials (less than a day) but with frequent measurement to gain more considerable insight into glucose variations. However, the experiment devised in this manuscript has a longer duration but much less frequent measurements. As the authors state in the Results section, line 139, this lack of measurements may mislead the calculated time in normoglycemia. Could the authors explain why they did not design an experiment with more frequent measurements?

Response: Thank you for the constructive comments. We did not design such an experiment with more frequent measurement for the case of the clinical works because all three patients were not in continuous glucose monitoring (CGM) regime as yet. A CGM device has not been used for all patients with T1D in our clinic at the Universiti Teknologi MARA (UiTM) hospital as we only asked them to use SMBG via finger prick. However, these can be explained as follows:

Discussion section (lines 335-352): "The comparison of BGL against time between clinical and in-silico works can be challenging, especially when clinical data is limited, and in this case the CGM device is not used. Thus, the BGL profiles are different since patients in the clinical work use conventional method to monitor their BGL i.e. SMBG and MDI; therefore, only a snapshot of BGL at a particular time available for comparison as seen in Figures 5 to 7. Studies have shown that the use of CGM device can improve time in range in the clinical settings, thus improve the BGL profiles [3,4].

"In this case, the only available data point is the focus since the clinical data is limited and does not cover the entire time span. While BGL simulations can be helpful for predicting how a T1D patient's BGL may change under different conditions, they are not always accurate. This is because the mathematical models used in the simulations are based on assumptions about how the body works, and these assumptions may not always hold for every individual. Additionally, the simulation may not consider all of the complex factors that can affect BGL, such as exercise, stress or illness. BGL monitoring can also be subjected to errors and variability in clinical settings. Factors such as the accuracy of the glucose meter or sensor, the timing and frequency of measurements, and the variability of patients' responses to interventions (meals, physical activities, and medication for example) can all affect the reliability and accuracy of clinical BGL monitoring."

3. The authors indicated that three insulin rates were simulated (lines 75 and 76), and insulin boluses were adjusted by trial and error to optimize the glucose profile (line 101). Nevertheless, I could not find the insulin rates and boluses used in the clinical trial. Were they the same as for the simulation? If not, could you justify this decision, please? In my opinion, using different insulin inputs in the model than in the actual patient will lead to noncomparable outputs.

Response: Thank you for the constructive comments. The insulin rates and boluses for both clinical and in-silico works were the same based on the meals amount taken during breakfast, lunch, and dinner for each patient as described as follows:

Discussion section (lines 354-370): "Bolus insulin is used to control BGL at mealtime. The best time for insulin injection depends on the type of insulin used and the individual's need in order to achieve optimal BGL targets to reduce the

complications of diabetes. The insulin is typically injected subcutaneously, either with a syringe or an insulin pen, and taken shortly before or after a meal [11]. The amount of bolus insulin needed depends on factors such as age, body weight, the amount of CHO in the meal consumed, insulin sensitivity, and physical activity [12-14]. These factors help patients to determine the appropriate dose of bolus insulin needed.

"Patients in the clinical work were given insulin during mealtime as opposed to the in-silico work in which the insulin was injected 30 minutes prior to a meal. Additionally, it is important to consider the timing of bolus insulin administration. Giving bolus insulin too early before a meal or too late after a meal can result in hypoglycaemia and hyperglycaemia, respectively. So, the bolus insulin administration was timed appropriately to match the timing of CHO intake.

"In this study, all patients used a rapid-acting insulin to manage their BGL during mealtime. This is to ensure their BGL would not deviate too far from the normoglycemic range, i.e., 4.0 to 7.0 mmol/L, after each meal. Table 15 summarises the amount of bolus insulin administered for all patients in the in-silico work. The optimum amount of bolus insulin was obtained on a trial-and-error basis. The aim is to get the BGL within or closer to the normoglycemic range while avoiding hypoglycaemia episodes as much as possible."

4. It is unclear how the authors performed the regression statistical analysis (line 135). Did they compare specific blood glucose samples in the clinical data to the corresponding simulated data points, or did they compare some fitting error metric like the root mean square error or glucose performance metric such as the time in range? In addition, it would be helpful if the authors provided which type of regression model they employed (eg, linear model, generalized model, multilevel model).

Response: Thank you for the constructive comments. The regression statistical analysis was performed as described below:

Method section (Data Analysis of Patients Using Microsoft Excel subsection; lines 199-229): "Data analysis was done using relevant data collected. Previously, the BGL profiles for both works were created. The BGL profiles in the clinical work were done manually by inserting data related and plotting the BGL profiles using Microsoft Excel 2016. Conversely, the BGL profiles in the silico work were generated using MATLAB software. From there, the pattern of BGL profiles was observed and identified, such as the time of day when BGL tends to be the highest or lowest, the frequency of hypoglycemic and hyperglycemic events, and the variability of BGL. The BGL profiles were used to evaluate the patient's glycemic control over the selected time frame by calculating the average BGL and the percentage of time spent in different glycemic ranges, such as hypoglycaemia, normoglycaemia, and hyperglycaemia, and among other things.

"Thus, Microsoft Excel 2016 was used to facilitate the data analysis work. The following data were used such as the amounts of meals (g CHO), meal time and duration, amount of plasma insulin and plasma glucose. Regression analysis was selected for data analysis, i.e., a statistical method generally used to analyse the relationship between two or more variables. Multiple linear regression (MLR) is a type of regression analysis that was done to analyse the relationship between two or more independent variables and a dependent variable. In this case, the two independent variables were the amounts of meals consumed and insulin administered, while the dependent variable was the predicted BGL. The following steps were performed to obtain MLR.

"The first step was to enter the data into the Excel spreadsheet with one column for the dependent variable and one or more columns for the independent variables. Then, from the data tab, data analysis containing various analysis tools was selected. The regression analysis was chosen where the selected input of the y range was the BGL outcome, and the inputs of the x range were meals consumed and insulin administered. A new worksheet tab appeared, giving the summary output of regression statistics and other relevant information. The probability value (*P*-value) and coefficient of determination (R-squared, R2) are important statistical measures used in regression analysis. The *P*-value was used to test the research hypothesis whether to reject or support the null hypothesis. A small *P*-value ($P<0.05$) indicates the relationship between the variables are significant and the null hypothesis is rejected. The R-squared (R2) measures how much the independent variables explain the variation in the dependent variable. A high value of R-squared indicates a better fit of the model to the data."

5. The authors concluded that the model "is acceptable to predict the BGL for people with T1D" (line 137). However, they also stated that "all patients showed improvement in BGL for the in-silico works." In my opinion, these two statements are contradictory: if the in-silico model did not reproduce, with acceptable errors, the glucose profiles observed in the clinical trial, then the model cannot be considered a good predictor. Could the author explain this point more, please?

Response: Thank you for the constructive comments. Your query can be explained as follows:

Discussion section (lines 329-352): "Observing the BGL trend for all patients in both works, the in-silico work performed better in managing BGL as compared to the clinical work. Patients in the clinical work rarely achieved the glycemic target, 4.0 to 7.0 mmol/L. Patients 1 and 2 only achieved the target range during morning and evening, respectively, whereas patient 3 was none at all. The patients in the in-silico work were able to achieve the glycemic target more than 70% of the time as compared to the clinical which is less than 50%.

"The comparison of BGL control between clinical data and in-silico works can be challenging, especially when clinical data is limited, and in this case the CGM device is not used. Thus, the BGL profiles are different since patients in clinical works use conventional method to monitor their BGL i.e. SMBG and MDI, therefore, only a snapshot of BGL at a particular time available for comparison (as seen in Figures 5-7). Studies had shown that the use of CGM device can improve the time in targt range in the clinical work, thus improve the BGL profiles [3,4].

"In this case, the only available data point is the focus since the clinical data is limited and does not cover the entire time span.

While BGL simulations can be helpful for predicting how a T1D patient's BGL may change under different conditions, they are not always accurate. This is because the mathematical models used in the simulations are based on assumptions about how the body works, and these assumptions may not always hold for every individual. Additionally, the simulation may not consider all of the complex factors that can affect BGL, such as exercise, stress or illness. BGL monitoring can also be subjected to errors and variability in clinical settings. Factors such as the accuracy of the glucose meter or sensor, the timing and frequency of measurements, and the variability of patients' responses to interventions (meals, physical activities, and medication for example) can all affect the reliability and accuracy of clinical BGL monitoring."

Minor Comments

6. I could not find any information about how the authors identify the model's parameters. Could the author describe, please, how the model was calibrated?

Response: All model parameters are taken from the previous studies, and they are all provided in the form of tables (Tables 5 and 6) as shown in the revised manuscript.

7. I could not find any referenced table in the manuscript.

Response: All tables are included with respective references in the revised manuscript.

8. Lines 17-19: In the introduction, it seems that the authors presented the "improved Hovorka model" to address the poor performance achieved by current artificial pancreas systems. Could the authors please elaborate more on how the model they presented will enhance the performance of existing control algorithms?

Response: Thank you for your query.

The improved Hovorka model has been added with additional parameters to its original Hovorka model; for example, the following equations are newly added to the original model as follows:

(dQ_1 (t))/dt=EGP_0+U_G+0.01Q_2+[x_1 k_w1+x_2 k_w2+x_3 k_w3]-F_R Q_1-[〖F_01〗^C/(V_G G(t))] Q_1-0.002Q_1 (Eq.1)

(dQ_2 (t))/dt=[k_w11 x_1 (t)+k_w22 x_2 (t)+k_w33 x_3 (t)]+EGP_0 [k_w1 x_1 (t)+k_w2 x_2 (t)+k_w3 x_3 (t)]-k_12 Q_2 (Eq.2)

(dI(t))/dt=(U_I (t))/V_I -k_e I(t)- [k_w1 x_1 (t) + k_w2 x_2 (t) + k_w3 x_3 (t)] (Eq.8)

[dx_1/dt]=k_a1 x_1 (t)+k_w1 I(t)+k_w11 I(t) (Eq.10)

[dx_2/dt]=k_a2 x_2 (t)+k_w2 I(t)+k_w22 I(t) (Eq.11)

[dx_3/dt]=k_a3 x_3 (t)+k_w3 I(t)+k_w33 I(t) (Eq.12)

All these parameters and their values are included and described as shown in Tables 5 and 6 in the revised manuscript. It is also good to note that all these added equations are solely the original works of the authors based on their previous works in this artificial pancreas area (please refer to references [6,7,15-19] in the revised manuscript). The authors came up with parameter additions in the improved Hovorka equations model after carrying out a system identification technique on all parameters involved in the original Hovorka model. It was observed that by introducing the additional parameters in the improved Hovorka equations, there had been better interaction and interconnection between the accessible compartment and nonaccessible compartment in its glucose-insulin dynamics. Consequently, it gives a better control algorithm so as to yield optimum performance in regulating BGL for people with T1D.

9. The authors used "workers" in several places in the manuscript. Did they mean "works"?

Response: Workers means researchers who carry out the works.

10. Lines 43 and 44: Equation 1 seems to be missing the last term.

Response: Equation 1 has been corrected. Please refer to line 80 in the revised manuscript.

11. Lines 63 and 64: I think equation 8 contains a typo. Should the second "=" be removed?

Response: Equation 8 has been corrected. Please refer to line 100 in the revised manuscript.

12. Figures 2-4: The collected clinical data comprises six glucose samples per patient. However, data was represented with a continuous line. In my opinion, this representation leads to a misleading interpretation (eg, glucose follows a horizontal line in some periods, which is unrealistic). I suggest the authors mark the actual blood samples as in a scatter plot.

Response: Thank you for the constructive comments. Data analyses in determining percentage on target (normoglycemic range) for both clinical and in-silico works were carried out using Microsoft Excel, and it requires a continuous line; therefore, we decided to stick to our decision. We might shift to CGM applications once available in our clinic.

13. Figures 2-4: I think the x-axes should be in hours, not in minutes.

Response: Thank you for the comments. All figures mentioned have been changed to "hours" in the revised manuscript.

Round 2 Review

Anonymous

First, I would like to thank the authors for completing the clinical trial and statistical analysis description and for addressing all my comments on the previous submission. Unfortunately, I am afraid that I still have some methodological doubts regarding the comparison between the in-silico results and the clinical results. Therefore, I suggest a further revision of the manuscript.

Response: Thank you for the compliments and constructive comments.

Specific Comments

My principal methodological concerns are listed in the Major Comments section. Other doubts or typos are presented in the Minor Comments section.

Major Comments

1. If I understood well, the insulin infusion rate used to simulate the "Improved Hovorka model" (variable u(t) in equation 6) is different from the infusion rate administered to the actual patients in the clinical trial. On the one hand, virtual patients have received an insulin infusion rate calculated from a closed-loop algorithm (the eMPC). On the other hand, actual patients seem to follow an open-loop therapy (multiple drug injections). Lastly, the authors also state (lines 361 and 362) that the timing of insulin bolus is different in both settings. Could the authors explain these discrepancies, please? If the goal is to compare the prediction ability of the "Improved Hovorka model," why have the authors not simulated the model with the same insulin therapy used for the clinical trial?

Response: Thank you for your comment. We fully agree and appreciate your deep concern on the design of the methodology adopted in this study. Yes, there are so many limitations and constraints faced throughout the course of this study; among others, CGM was not used, limited data was available for patients, etc, which, in turn, forced us to use two different protocols; namely, the closed-loop algorithm (eMPC) was used for the in-silico test, whereas an open-loop therapy was used for the clinical validation. These issues have been clarified in different sections of the manuscript as follows:

Abstract (has been inserted, accordingly): "Methods: Three actual patients' data were collected from Clinic 1, Clinical Training Centre, Universiti Teknologi MARA (UiTM) Hospital, Sungai Buloh, Selangor upon getting approval from UiTM Ethics Committee. The inclusion criteria of subjects were namely; T1D patients, age range between 11 to 14 years old, highly dependent on insulin injection with four or more finger pricks or self-monitoring of blood glucose (SMBG) for BGL measurements per day. The T1D patients typically receive meals three times per day; breakfast, lunch, and dinner. In a nutshell, closed-loop algorithm (eMPC) was used for the in-silico test whereas an open-loop therapy was used for the clinical validation. As for data analysis of patients, *P*-value via multiple linear regression (MLR) was used to model the relationship between meal, insulin, and BGL.

"Results: In order of breakfast, lunch, and dinner: the optimum bolus insulins for patient 1 were 83.33, 33.33 and 16.67 mU/min; patient 2 were 66.67, 50.01 and 33.33 mU/min, and patient 3 were 100.02, 83.33, and 66.67 mU/min, respectively. As for the in-silico works; results revealed that the percentages of time for their BGL on target in patients 1, 2, and 3 were at 79.59%, 87.76%, and 71.43%, respectively, as compared to the clinical works with less than 50%. A small *P*-value ($P<0.01$) indicated that the variables were significant. However, when comparison was made on the BGL profile; both profiles were not comparable due to different methodology adopted in the design of the study.

"Conclusions: In conclusion, the in-silico work using the improved Hovorka model equations was not comparable to the clinical works to simulate BGL with meal disturbances for people with T1D."

Discussion section (lines 396 and 397): "However, when comparison was made on the BGL profile; both profiles were not comparable due different methodology adopted in the design of the study."

Conclusion section (lines 414-416): "In conclusion, the in-silico work using the improved Hovorka model equations was not comparable to the clinical works to simulate BGL with meal disturbances for people with T1D due to different methodology adopted for both works."

2. From the regression analysis results (lines 406-409), the authors seem to conclude that the model is "applicable in predicting BGL" because the P value is <.01. However, I cannot see the relation between a significant P value and a better prediction. From the clear description the authors provided of the multiple regression analysis, I think the authors fitted the following linear model:

$$improved\_hovorka\_glucose = insulin \cdot beta1 + meal \cdot beta2 + e$$

where "improved_hovorka_glucose" is the output of the "Improved Hovorka model," "insulin" and "meal" correspond to the values of the infusion rate and meal amount in that model, "beta1" and "beta2" are coefficients to be estimated in the analysis, and "e" is the normal distributed residuals. A P value <.05 means that data supports the rejection of the null hypothesis that beta1 = beta2 = 0 [9]. Thus, a significant P value indicates that the "insulin" and/or the "meal" inputs can explain the variations observed in "improved_hovorka_glucose." However, I cannot see how one can conclude anything from the prediction accuracy of the "Improved Howorka model" from the fact that beta1≠0 or beta2≠0. Could the author explain this point, please?

Response: Thank you for your comment. I am sorry that I may have to reserve my answer for this specific comment. Due to weaknesses in the methodology being adopted for comparison purposes for both works, these results might have happened. However, I have corrected my statements in different sections on the revised manuscript in order to clarify those issues as follows:

Lines 394-397: "Based on Table 14, all patients in both clinical and in-silico works have a small *P*-value ($P<0.01$), which indicates the variables are significant. However, when comparison was made on the BGL profile; both profiles were not comparable due different methodology adopted in the design of the study."

Lines 414-416: "In conclusion, the in-silico work using the improved Hovorka model equations was not comparable to the clinical works to simulate BGL with meal disturbances for people with T1D due to different methodology adopted for both works."

Minor Comments

3. Equation 5: The term exp(t/maxG) should be exp(-t/maxG).

Response: Thank you for your comment. Equation 5 has been corrected as suggested. Please refer to lines 89 and 90.

4. Equation 6: In line 103, the authors define u(t) as insulin bolus. However, in line 180, the authors refer to infusion rates. Could the author check the consistency of this definition?

Response: Thank you for your comment. The u(t) definition has been used consistently as "Insulin infusion rate" throughout the manuscript. Therefore, the said term has been changed which can be found in line 98 as follows: "u(t) (mU/min) is insulin infusion rate."

Round 3 Review

Anonymous

I would like to thank the authors for their efforts in replying to my comments. Unfortunately, I still do not understand the article's contribution regarding comparing clinical data. As stated by the authors, clinical data and in-silico results are not comparable due to the different methodologies and protocols applied to obtain the data; therefore, I wonder if including the clinical data set analysis is justified. In addition, I have doubts about under which conditions the authors have simulated the model, for instance, if the simulation included any kind of variability.

Response: Thank you for the compliments and constructive comments.

We thought that we had answered these queries in the first and second detailed response reports in greater lengths (please refer to those reports), and we reserve not to deliberate them again at this point.

Specific Comments

Major Comments

1. Since clinical data results and in-silico data are incomparable, could the authors justify the motivation for including the clinical data in the article?

Response: Thank you for the comments. Yes, the clinical data are equally important in this study since the actual patients' demographic profiles are based on their age group, body weight, daily meal intakes, etc. All these information have been taken into account in the calculations for the in-silico results, accordingly.

2. In lines 191-193, the authors indicate that comparing the in-silico data with the clinical data would help determine the model's accuracy in mimicking the actual glucose. I believe this statement is incompatible with the fact that both clinical and in-silico data were obtained following incomparable protocols and methodologies.

Response: The authors are still in the opinion that this work is considered as a preliminary study attempting to apply the improved Hovorka equations (the authors' own previous work) using actual patients' data in the calculations of the in-silico works for glucose mimicking purposes. Even though both studies (in-silico vs clinical) have used different methodologies and protocols due to study/data limitation, the same actual patients' datasets are used throughout the simulation study, and we believe it should be acceptable for mathematical modeling purposes (in-silico). However, further research needs to be carried out when CGM is available in our clinics.

3. Have the authors thought about modifying the simulation of the model to make the results more comparable with the clinical data? For instance, I would suggest they simulate the model with the same bolus, basal insulin, and meal carbohydrates utilized in the clinical trial. Then, they could compare the model output with each glucose measurement.

Response: Thank you for the compliments and constructive comments.

Yes, we have thought about it, and this should be the way forward for our further research work.

4. In the Discussion section (lines 374-378) and the conclusion (line 404), the authors concluded from Table 13 that the patients have less sensitivity in the morning. Since Table 13 corresponds to the results of the virtual patients in the in-silico analysis, I wonder whether the authors have included any kind of circadian variability in the simulation, for instance, some sinusoidal variability in ka1, kw1, kw11, ka2, kw2, kw22, ka3, kw3, or kw33. If this is not the case and these parameters were kept constant in the simulation, I suggest authors better justify this apparent increase in insulin sensitivity.

Response: Thank you for the compliments and constructive comments.

Since this study is very preliminary in nature, we are unable to conduct our simulation as suggested. However, we will take that into consideration seriously into our research works in the future.

5. The authors said the insulin bolus was computed by trial and error. Since one of the article's goals is determining the optimal bolus, it would be advisable to detail the method followed to calculate it.

Response: We thought that we had answered these queries in the first and second detailed response reports in greater lengths (please refer to those reports), and we reserve not to deliberate them again at this point.

Round 4 Review

Anonymous

I would like to thank the authors for replying to my comments. Unfortunately, I still believe the work has two principal limitations preventing me from accepting the manuscript. The main one is that the differences in protocols and conditions between the clinical and simulation works make it, in my opinion, unfeasible to address the goal of determining "the accuracy and effectiveness of the in-silico model in mimicking real-world BGL dynamics." The second one is that insufficient information is reported to reproduce the calculation of the optimal bolus in the in-silico simulations.

Response: Thank you for the comments. All corrections stated as limitations of the study are included in the revised manuscript.

Limitations of the Study (lines 398-414): "Apparently, there are two main limitations discovered from the study which, in

turn, make it unfeasible to address the goal of determining the accuracy and effectiveness of the in-silico model in mimicking real-world BGL dynamics. Firstly, it was due to different protocols and conditions adopted in the methodology for the clinical and simulation works. As stated earlier, the open loop therapy was used in the clinical work for evaluation purposes; whereas the closed loop algorithm with MPC was used in the in-silico test. In order to address this limitation for future works, it is primarily essential to modify the simulation of the model to make the results more comparable with the clinical data. For instance, it is suggested that in the simulation work, the improved Hovorka equations model could be simulated using the same bolus, basal insulin, and meal CHO utilized in the clinical trial. By doing so, they could compare the model output with each glucose measurement, preferably when CGM is available at our clinic for future use. Secondly, insufficient information was reported to reproduce the calculation of the optimal bolus in the in-silico simulations. This happened due to the insulin bolus was computed by trial and error as programmed earlier in its closed loop algorithm. Since one of the main goals of the study is to determine the optimal bolus insulin, it would be advisable to detail the method followed to calculate it in the development of its new control algorithm for future works."

Conflicts of Interest

None declared.

References

1. Gore R. Peer review of "In-Silico Works Using an Improved Hovorka Equations Model and Clinical Works on the Control of Blood Glucose Levels in People With Type 1 Diabetes: Comparison Study". JMIRx Bio 2024;2(1):e63851 [FREE Full text] [doi: 10.2196/63851]
2. Som AM, Sohadi NAM, Nor NSM, Ali SA, Ahmad MA. In-silico works using an improved Hovorka equations model and clinical works on the control of blood glucose levels in people with type 1 diabetes: comparison study. JMIRx Bio 2024;2(1):e43662 [FREE Full text] [doi: 10.2196/43662]
3. Marigliano M, Pertile R, Mozzillo E, Troncone A, Maffeis C, Morotti E, et al. Satisfaction with continuous glucose monitoring is positively correlated with time in range in children with type 1 diabetes. Diabetes Res Clin Pract 2023 Oct;204:110895. [doi: 10.1016/j.diabres.2023.110895] [Medline: 37673191]
4. Nefs G, Bazelmans E, Marsman D, Snellen N, Tack CJ, de Galan BE. RT-CGM in adults with type 1 diabetes improves both glycaemic and patient-reported outcomes, but independent of each other. Diabetes Res Clin Pract 2019 Dec;158:107910 [FREE Full text] [doi: 10.1016/j.diabres.2019.107910] [Medline: 31678626]
5. Anonymous. Peer review of "In-Silico Works Using an Improved Hovorka Equations Model and Clinical Works on the Control of Blood Glucose Levels in People With Type 1 Diabetes: Comparison Study". JMIRx Bio 2024;2(1):e64403 [FREE Full text] [doi: 10.2196/64403]
6. Yusof NFM, Som AM, Ibrehem AS, Ali SA. Parameter addition in interaction of glucose and insulin for type 1 diabetes. 2012 Presented at: IEEE-EMBS Conference on Biomedical Engineering and Sciences; Langkawi, Malaysia; December 17-19, 2012.
7. Som AM, Yusof NFMBM, Ali SA, Fuzil NS. Meal disturbance effect on blood glucose control for type 1 diabetes using improved Hovorka equations. Key Eng Materials 2019 Mar;797:158-167. [doi: 10.4028/www.scientific.net/kem.797.158]
8. Hovorka R, Canonico V, Chassin LJ, Haueter U, Massi-Benedetti M, Orsini Federici M, et al. Nonlinear model predictive control of glucose concentration in subjects with type 1 diabetes. Physiol Meas 2004 Aug;25(4):905-920. [doi: 10.1088/0967-3334/25/4/010] [Medline: 15382830]
9. Hovorka R, Shojaee-Moradie F, Carroll PV, Chassin LJ, Gowrie IJ, Jackson NC, et al. Partitioning glucose distribution/transport, disposal, and endogenous production during IVGTT. Am J Physiol Endocrinol Metab 2002 May;282(5):E992-1007 [FREE Full text] [doi: 10.1152/ajpendo.00304.2001] [Medline: 11934663]
10. Man CD, Micheletto F, Lv D, Breton M, Kovatchev B, Cobelli C. The UVA/PADOVA type 1 diabetes simulator: new features. J Diabetes Sci Technol 2014 Jan;8(1):26-34 [FREE Full text] [doi: 10.1177/1932296813514502] [Medline: 24876534]
11. Cengiz E, Danne T, Ahmad T, Ayyavoo A, Beran D, Ehtisham S, et al. ISPAD Clinical Practice Consensus Guidelines 2022: insulin treatment in children and adolescents with diabetes. Pediatr Diabetes 2022 Dec;23(8):1277-1296. [doi: 10.1111/pedi.13442] [Medline: 36537533]
12. Bell KJ, King BR, Shafat A, Smart CE. The relationship between carbohydrate and the mealtime insulin dose in type 1 diabetes. J Diabetes Complications 2015;29(8):1323-1329. [doi: 10.1016/j.jdiacomp.2015.08.014] [Medline: 26422396]
13. Ozaslan B, Patek SD, Fabris C, Breton MD. Automatically accounting for physical activity in insulin dosing for type 1 diabetes. Comput Methods Programs Biomed 2020 Dec;197:105757 [FREE Full text] [doi: 10.1016/j.cmpb.2020.105757] [Medline: 33007591]
14. Weinstock RS. Patient education: type 1 diabetes: insulin treatment (beyond the basics). UpToDate. 2022. URL: https://www.uptodate.com/contents/type-1-diabetes-insulin-treatment-beyond-the-basics [accessed 2024-08-06]

15. Yusof NFM, Som AM, Ibrehem AS, Abdulbari Ali S. System identification in modified diabetic model for nanochip controller. Adv Materials Res 2014 Jun;938:299-304. [doi: 10.4028/www.scientific.net/amr.938.299]
16. Som AM, Yusof NFM, Ali SA, Sohadi NM, Maarof AM, Nor NSM. In-silico works on the control of blood glucose level for type 1 diabetes mellitus (T1DM) using improved hovorka equations. Int J Pharm Med Biol Sci 2020;9(4):144-151. [doi: 10.18178/ijpmbs.9.4.144-151]
17. Sohadi NAM, Som AM, Nor NSM, Ali SA, Pacana NDA. Control of blood glucose level for type 1 diabetes mellitus using improved Hovorka equations: comparison between clinical and in-silico works. Afr J Diabetes Med 2020 Dec;29(1):1-11.
18. Som AM, Yusof NFM, Ali SA, Zawawi N. Simulation work on blood glucose control for type 1 diabetes using modified Hovorka equations. Pertanika J Sci Technol 2019;27(4):1527-1538.
19. Yusof NFM, Som AM, Ibrehem AS, Ali SA. A review of mathematical model describing insulin delivery system for type 1 diabetes. J Appl Sci 2014 Jun 15;14(13):1465-1468. [doi: 10.3923/jas.2014.1465.1468]

Abbreviations

BGL: blood glucose level
CGM: continuous glucose monitoring
eMPC: enhanced model-based predicted control
SMBG: self-monitoring of blood glucose
T1D: type 1 diabetes
UiTM: Universiti Teknologi MARA

Edited by T Leung; submitted 17.07.24; this is a non–peer-reviewed article;accepted 17.07.24; published 15.08.24.

Please cite as:
Som AM, Sohadi NAM, Nor NSM, Ali SA, Ahmad MA
Authors' Response to Peer Reviews of "In-Silico Works Using an Improved Hovorka Equations Model and Clinical Works on the Control of Blood Glucose Levels in People With Type 1 Diabetes: Comparison Study"
JMIRx Bio 2024;2:e64442
URL: https://bio.jmirx.org/2024/1/e64442
doi:10.2196/64442
PMID:

Authors' Response to Peer Reviews

Authors' Response to Peer Review of "Exploring the Accuracy of Ab Initio Prediction Methods for Viral Pseudoknotted RNA Structures (Preprint)"

Vasco Medeiros[1], BSc, MSc, AS; Jennifer Pearl[2], BSc, AS; Mia Carboni[3], BSc; Stamatia Zafeiri[1], BSc, MSc

[1]Stevenage Bioscience Catalyst, Stevenage, United Kingdom
[2]Stanford University, Santa Clara, CA, United States
[3]University of Turin, Torino, Italy

Corresponding Author:
Vasco Medeiros, BSc, MSc, AS
Stevenage Bioscience Catalyst
Gunnels Wood Rd Stevenage
Stevenage, SG1 2FX
United Kingdom
Phone: 44 07534150352
Email: vasco.miguel.medeiros@gmail.com

Related Articles:

Companion article: https://www.biorxiv.org/content/10.1101/2024.03.21.586060v1

Companion article: https://bio.jmirx.org/2024/1/e65154

Companion article: https://bio.jmirx.org/2024/1/e58899/

(JMIRx Bio 2024;2:e67586) doi:10.2196/67586

KEYWORDS

pseudoknots; viral RNA; MFE prediction; MEA prediction; virus; virology; computational biology; minimal free energy prediction; maximum expected accuracy prediction

Live PREreview [1]

Summary

The study [2] examines the performance of 5 RNA-folding engines for predicting complex viral pseudoknotted RNA structures. This research fills a critical gap in the field by comparing the efficiency of minimal free energy (MFE) and maximum expected accuracy (MEA) using a curated dataset of 26 viral RNA sequences with known secondary structures. Contrary to prevailing assumptions favoring MEA models, their findings reveal that pKiss, an MFE-folding engine, outperforms Vsfold 5 in terms of the sensitivity, positive predictive value (PPV), and F_1-score, while laying emphasis on the importance of the PPV and sensitivity parameters in understanding and determining the superior accuracy of pKiss to predict correct base pairs and minimize incorrect predictions. The authors also point out that the engine still needed additional data to achieve high accuracy as well as a better understanding of thermodynamics at the intracellular level.

The statistical analyses used to evaluate the results were 2-way ANOVA and Tukey multiple comparisons test, which provided robust insights into the performance differences among the tested engines. The research integrates bioinformatics with statistics and advanced data science methodologies to promote our understanding of computational RNA biology. The study provides important insights into the relative advantages and disadvantages of both approaches in predicting pseudoknotted RNA structures by contrasting MFE models and MEA models. It also highlights avenues for future research to focus on the development of more sophisticated energy models and MFE engines, like pKiss, to enhance prediction capabilities, especially in the context of viral replication and gene regulation, which may lead to a better understanding of the functional roles of pseudoknotted RNA structures. Overall, this research

contributes significantly to the field of computational and molecular biology.

Below, we list major and minor concerns that were discussed by participants of the live review, and where possible, we provide suggestions on how to address those issues.

List of Major Concerns and Feedback

It would be helpful to provide more context on why percent error was chosen as the primary metric for evaluating different engines, considering alternatives like mean absolute error (MAE) and mean squared error (MSE) could enhance the analysis. For instance, MAE is robust against outliers, making it a valuable metric, especially when outlier removal is part of the process. Although MAE is less sensitive to extreme values, it can offer a useful qualitative check on the models. On the other hand, the mean MSE's sensitivity to outliers can be advantageous when the spread of the forecast is important. Including these metrics could provide a more comprehensive evaluation.

Response: It should be noted that the percent error (%) in this case is in fact analogous to the MAE (as described in equation 1) and is represented as such in Figure 4A. Hence, the two are used interchangeably, which is clarified on pages 8 and 10 and within the supplementary materials on page 23. The reviewer's suggestion to use MSE, in addition to MAE was heeded, and the following values for MSE were calculated and exhibited in the newly generated Figure 4B. The utility of MSE and MAE was expounded on in the Discussion section on page 15. It should be noted that a prerequisite for applying MSE is that all data be normally distributed, which was tested for and confirmed.

It should also be noted that MSE (or root mean square error) equals the residuals' SD, calculating the variance between the observed and expected values. This makes it unnecessary to calculate and display the SD of the MSE within Figure 4B.

The authors have conducted a comprehensive and insightful study, revealing important differences in prediction accuracy between Vsfold 5 and pKiss. One area that could further enhance the manuscript is the exploration of how auxiliary parameters (eg, Mg2+ binding, dangling end options, H-type penalties) are managed across the various RNA-folding engines utilized. For example, Vsfold 5, although being an MEA model, may encounter challenges if its handling of Mg2+ binding or dangling ends significantly diverges from what is optimal for the studied RNAs. The authors' observation in section 3.1 that "the low percent error exhibited by pKiss could be the result of the pseudoknot 'enforce' constraint, but it is more likely that this outcome was multivariable, equating to the Turner energy model used, and the sensitive auxiliary parameters enforced by the program" is particularly insightful. This highlights the complexity of RNA structure prediction algorithms. To build on these findings, a structured comparative analysis of parameter handling across different software tools could be highly beneficial. This analysis would not only clarify why certain engines performed better than others but also help in identifying best practices or potential biases in prediction methodologies. Such an addition would significantly strengthen the study's conclusions and provide valuable guidance for future research in RNA structure prediction.

Response: This major criticism has been addressed. Though not all auxiliary parameters like Mg2+ binding and dangling end options were explored (given that the amount of data this would generate could warrant an entirely new paper/manuscript) several auxiliary parameters were modified and compared to the original percent error (%)/MAE of pKiss (Figure 4A).

These include overall pKiss function, altering the "enforce" setting to the "MFE" setting, which computes the single energetically best secondary structure (column 2, S2.1), altering the strategy from "pKiss C" (slow, low memory, but thorough) to "pKiss A" (fast but sloppy; column 3, S2.2), altering the exclusion of lonely base pairs to the inclusion of lonely base pairs (column 4, S2.8), altering the H-type penalty from 9 to 18 (column 5 S2.3), and altering the K-type penalty from 12 to 24 (column 5, S2.4). pKiss was chosen to explore these parameters, given that it is the most accurate out of all other folding software.

Testing these auxiliary parameters, displaying them in graphical format, and expounding upon them in the Discussion section of this report (page 15) helps eliminate potential biases and shows how sensitive these functions can be and why certain engines are better than others.

To build on these findings, a structured comparative analysis of parameter handling across different software tools could be highly beneficial. This analysis would not only clarify why certain engines performed better than others but also help in identifying best practices or potential biases in prediction methodologies. Such an addition would significantly strengthen the study's conclusions and provide valuable guidance for future research in RNA structure prediction.

In section 3.1 of the manuscript, no significant difference in percent error was identified. However, it does not specify the statistical test employed nor the method used for adjusting P values, which are essential details for validating the results. Additionally, the term "Vij" is introduced early in the manuscript but is not contextualized until page 13. Providing this context earlier would enhance the reader's understanding.

Response: Both before and after the PREreview criticisms were considered and implemented, the statistical tests employed in this paper were expounded on. Statistical analyses used throughout the paper (2-way ANOVA testing, outlier identification, normality, lognormality tests, etc) were summarized at the end of the Materials and Methods section (page 10). Moreover, any specific statistical test used for any dataset/figure was discussed in depth within the figure

descriptions and, if relevant to the reader, discussed even more in depth within the Discussion section of the manuscript.

The term V(i,j) (the real symmetric contact matrix) was contextualized earlier within the paper, as per the reviewers' suggestion (pages 2 and 3), and the math behind its utility is explained in greater depth.

> *It would be beneficial if "false positive" and "false negative" were more clearly defined, particularly in the context of mRNA detection. To improve clarity, the authors might consider specifying that sensitivity is the appropriate measure for detecting mRNA among known positives, while specificity is the appropriate measure for detecting mRNA among known negatives, where the probability of false positives is 1 – specificity. Additionally, using the Youden index (J), which is defined as sensitivity + specificity – 1, could provide a helpful summary of detection accuracy. This index ranges from –1 (indicating 100% incorrect detection) to 1 (indicating 100% correct detection), offering a clear metric for assessing performance [3].*

Response: False positives (pairings that do not fall under Matthews' [4] parameters) and false negatives (base pairs missed by the prediction software) were more clearly defined on page 8 of the manuscript in the context of all metrics used and in the context of MAE/percent error (%). They were also discussed in greater depth on page 9 and on page 16, in the context of Youden's index. The specificity and sensitivity used to detect known negatives and known positives, respectively, are further discussed in greater depth within sections 2.4, 3.2, 3.3, and 4.2 of the original manuscript.

The reviewers' suggestion to use the Youden index (J; a more sensitive metric than F_1 scoring) was implemented. The equation for the Youden index (J) was provided on page 9, with figures for J values of the 26 experimentally derived pseudoknotted models from each of the 5 folding software displayed on page 13 (including raw values and normalized values), the results of which were then expounded on in the Discussion section.

While J is most often represented in a receiver operating characteristic curve, the authors are displaying the mean (SD) of J values across folding software for the sake of clarity and visual representation, given that 130 receiver operating characteristic curves would prove visually confusing. It should also be noted that data were normalized and put into graphical format (Figure 6B) again for visual clarification. This eliminates negative values for J (as negative values for J are not defined).

> *Providing the link to the dataset will allow better compliance with open science practices. Please add the link to the dataset as it appears to be missing from the reviewed version of the manuscript. When sharing the dataset, it would be important to also include the associated metadata and appropriate documentation that matches the methods described in the manuscript. For guidelines on how to share data so that it's as reusable as it can be, authors may refer to the Findability, Accessibility, Interoperability, and Reuse (FAIR) principles of data sharing [5].*

Response: The link to both the dataset, the RNA pseudoknot folding software web servers, and the manner in which each was implemented to said dataset have been provided, complying with open science practices. They can be located within the supplemental materials, the DOI and URL of which can be found on page 17 of the original manuscript (DOI: 10.17605/OSF.IO/7QVKN [6]). They are located within the Open Science Framework an open-source cloud-based project management platform (for ease of access). The FAIR Principles of Data Sharing was also broached, referenced on page 4 of the manuscript.

> *Figure 5B displays the PPV as three distinct blocks rather than continuous values, with varying sensitivity within these blocks. This nonrandom binning of PPV suggests the need for further investigation to understand the underlying causes.*

Response: This abnormal trend is accounted for within the manuscript and expounded upon within the Discussion section (page 12, last paragraph). It is explained that, while most MFE folding engines tend to have lower PPVs than sensitivity values (due to thermodynamics imposed by MFE algorithms overshooting the number of canonical base pairings), pKiss and NUPACK do not follow this trend. This is because updated software such as this implements a more accurate assessment of the thermodynamic properties of the structure, removing unwanted pairs and improving overall performance [7].

> *In the Discussion section, the authors stated "We have provided evidence suggesting that MEA software is not always the optimal method of topological prediction when applied to short viral pseudoknotted RNA." This is a significant claim and would benefit greatly from specific references to support the evidence provided in the study. Citing the relevant figures and results that support this claim would significantly enhance comprehension and readability. For example, "As demonstrated in Figure 4, the MEA software Vsfold 5 exhibited higher percent errors in predicting knotted base pairs compared to MFE software like pKiss." Additionally, referencing previous studies that have reported similar findings or that discuss the limitations of MEA methods in RNA structure prediction in the Discussion section would strengthen the credibility of the authors' claims by showing that similar limitations have been observed by other researchers. This helps readers understand that the study is building upon existing knowledge. For instance, "Previous studies have also highlighted the limitations of MEA methods in RNA folding predictions, particularly for pseudoknotted structures (in-text citations)."*

Response: The authors recognize this as the most valuable criticism the reviewers have made and have addressed it accordingly. The length of the Discussion section was increased from 389 words to 1235 words, including a more in-depth analysis of the results and statistical significance of said results,

as it applies to MEA software being suboptimal (at times) when compared to its MFE counterparts. Nine different references to in-text figures or supplementary materials were added; relevant literature was additionally cited, and previous studies were discussed and compared to the results of the paper.

However, it should also be noted that previous studies highlighting the limitations of MEA methods when applied to RNA folding have not been cited, given that this is a novel approach to exploring ab initio RNA prediction algorithms. Though RNA prediction algorithms have been explored in great depth in previous literature, none (to the author's knowledge) have compared MFE and MEA prediction software against one another, and none have explored this software when applied to short-stranded (20-150nt) viral pseudoknotted RNAs.

List of Minor Concerns and Feedback

> *Overall, the reviewers really appreciated how clearly the figures and results were presented. Below are some minor suggested improvements [7].*
>
> *In the Abstract section: Please identify the abbreviation PPV as positive predictive value.*

Response: The acronym for positive predictive value (PPV) was defined in the abstract as per the editor's suggestion (page 1).

> *Page 3, first paragraph after Figure 1: Definitions of pseudoknot should be referenced.*

Response: On page 3, an official definition for a pseudoknot was referenced by Brierley et al [8]. Moreover, two more definitions were posited by the authors on the very same page.

> *Page 3, second paragraph after Figure 1: Please identify the NMR abbreviation as nuclear magnetic resonance.*

Response: Nuclear magnetic resonance (NMR) was abbreviated, and the acronym was defined. Please note that, given the new additions to the manuscript, this clarification is now found on page 4 of the manuscript, rather than page 3.

> *Page 7: The manuscript acknowledges the skewness in the data and provides a rationale for its presence. It's noted that this skewness impacts the training and testing phases, often contributing to false positives and false negatives. It would be beneficial if the authors could elaborate on how they addressed data imbalance, particularly in relation to reducing false positives and false negatives. This additional detail would enhance the understanding of the methods used to manage data skewness and improve model performance.*

Response: The reviewer is correct in stating that the manuscript acknowledges the skewness in data and that it provides a rationale for its presence on page 7:

"This skewness (regarding the class of RNA) is intentional, and true to nature, given that hairpin-type pseudoknots (H-type) are more common by far [8]."

However, the reviewer is incorrect in saying that this skewness impacts the training and testing phases (which were not discussed within the manuscript) and is incorrect in saying that it contributes to false positives and false negatives (which it does not). This would be the case for deep learning algorithms and folding software that is malleable, in the sense that it can be trained and altered when inserting varying inputs. However, the folding software provided by each of the 5 web servers do not harbor any deep learning algorithm/training/machine learning, unlike other software such as ATTfold (which is referenced in the paper, page 16).

Page 8, second paragraph: "Mathews et al. 2019" should be corrected to "Mathews, 2019" [4].

Response: "Mathews et al 2019" was indeed changed to "Mathews 2019" [4], as per the editors' suggestion, on page 8 of the manuscript.

> *Page 8, equation 1: Add a "%" next to *100, giving the output of x%.*

The amendment was made, and equation 1 now has a % sign next to the 100 (100%).

> *Page 10, Figure 4: In the title, "accurcy" should be corrected to "accuracy."*

Response: In Figure 4, the typo "accuracy" was indeed corrected. Please note that, given new additions to the manuscript, this amendment can now be found on page 11, while the amendment itself is located in Figure 4A.

> *Page 10, Figure 4: The bar of the SD of Vienna (knotted) is not presented.*

Response: There being no SD bar present in the Vienna (knotted) control variable is actually correct. As stated on page 5 of the paper (as well as other instances within the manuscript), the Vienna RNAfold engine does not compute for pseudoknots, which is why it was implemented as a negative control. Its inability to compute pseudoknots axiomatically means that the percent error (%) for pseudoknot generation will always be 100%, leading to no SD whatsoever.

> *Page 10, Figure 4: The bars of the SD seem to be widely large, indicating significant variability in the results, so a test of the normality of data distribution should be performed before comparisons. This is also observed for the kinefold results in Figures 5 and 6.*

Response: Tests for normality (gaussian) and lognormality were conducted on all relevant figures:

- Figure 4 (A-B): Kolmogorov-Smirnov tests
- Figure 5: Shapiro-Wilk test
- Figure 6 (A-B): Shapiro-Wilk test and Kolmogorov-Smirnov tests
- Figure 7: Kolmogorov-Smirnov test

> *Page 12, Figure 6B: The color bar on the heat maps is missing.*

Response: Color bar on the heat map (now found on page 14 of the manuscript) was added.

References

1. Sadedri D, Nagesh V, Mahmoud RSG, Olatoye T, Arogundade FQ. Peer review of “Exploring the Accuracy of Ab Initio Prediction Methods for Viral Pseudoknotted RNA Structures (Preprint)”. JMIRx Bio 2024;2:e65154 [FREE Full text] [doi: 10.2196/65154]
2. Medeiros V, Pearl J, Carboni M, Zafeiri S. Exploring the accuracy of ab initio prediction methods for viral pseudoknotted RNA structures: retrospective cohort study. JMIRx Bio 2024:e58899. [doi: 10.2196/58899]
3. Youden index. ScienceDirect. 2010. URL: https://www.sciencedirect.com/topics/medicine-and-dentistry/youden-index [accessed 2024-10-23]
4. Mathews DH. How to benchmark RNA secondary structure prediction accuracy. Methods 2019 Jun 01;162-163:60-67 [FREE Full text] [doi: 10.1016/j.ymeth.2019.04.003] [Medline: 30951834]
5. FAIR principles. GO FAIR. URL: https://www.go-fair.org/fair-principles/ [accessed 2024-10-23]
6. Exploring the accuracy of ab initio prediction methods for viral pseudoknotted RNA structures. Open Science Framework. URL: https://osf.io/ujp5r [accessed 2024-10-23]
7. Do C, Woods D, Batzoglou S. CONTRAfold: RNA secondary structure prediction without physics-based models. Bioinformatics 2006 Jul 15;22(14):e90-e98. [doi: 10.1093/bioinformatics/btl246] [Medline: 16873527]
8. Brierley I, Pennell S, Gilbert RJC. Viral RNA pseudoknots: versatile motifs in gene expression and replication. Nat Rev Microbiol 2007 Aug;5(8):598-610 [FREE Full text] [doi: 10.1038/nrmicro1704] [Medline: 17632571]

Abbreviations

FAIR: Findability, Accessibility, Interoperability, and Reuse
MAE: mean absolute error
MEA: maximum expected accuracy
MFE: minimal free energy
MSE: mean squared error
NMR: nuclear magnetic resonance
PPV: positive predictive value

Edited by A Schwartz; submitted 15.10.24; this is a non–peer-reviewed article;accepted 15.10.24; published 05.11.24.

Please cite as:
Medeiros V, Pearl J, Carboni M, Zafeiri S
Authors' Response to Peer Review of “Exploring the Accuracy of Ab Initio Prediction Methods for Viral Pseudoknotted RNA Structures (Preprint)”
JMIRx Bio 2024;2:e67586
URL: https://bio.jmirx.org/2024/1/e67586
doi:10.2196/67586
PMID:

Original Paper

Exploring the Accuracy of Ab Initio Prediction Methods for Viral Pseudoknotted RNA Structures: Retrospective Cohort Study

Vasco Medeiros[1], BSc, MSc, AS; Jennifer Pearl[2], BSc, AS; Mia Carboni[3], BSc; Stamatia Zafeiri[1], BSc, MSc

[1]Stevenage Bioscience Catalyst, Stevenage, United Kingdom

[2]Stanford University, Santa Clara, CA, United States

[3]University of Turin, Torino, Italy

Corresponding Author:
Vasco Medeiros, BSc, MSc, AS
Stevenage Bioscience Catalyst
Gunnels Wood Rd Stevenage
Stevenage, SG1 2FX
United Kingdom
Phone: 44 07534150352
Email: vasco.miguel.medeiros@gmail.com

Related Articles:

Companion article: https://www.biorxiv.org/content/10.1101/2024.03.21.586060v1

Companion article: https://bio.jmirx.org/2024/1/e65154

Companion article: https://bio.jmirx.org/2024/1/e67586

Abstract

Background: The prediction of tertiary RNA structures is significant to the field of medicine (eg, messenger RNA [mRNA] vaccines, genome editing) and the exploration of viral transcripts. Though many RNA folding software programs exist, few studies have condensed their locus of attention solely to viral pseudoknotted RNA. These regulatory pseudoknots play a role in genome replication, gene expression, and protein synthesis.

Objective: The objective of this study was to explore 5 RNA folding engines that compute either the minimum free energy (MFE) or the maximum expected accuracy (MEA), when applied to a specified suite of viral pseudoknotted RNAs that have been previously confirmed using mutagenesis, sequence comparison, structure probing, or nuclear magnetic resonance (NMR).

Methods: The folding engines used in this study were tested against 26 experimentally derived short pseudoknotted sequences (20-150 nt) using metrics that are commonplace while testing software prediction accuracy: percentage error, mean squared error (MSE), sensitivity, positive predictive value (PPV), Youden's index (J), and F_1-score. The data set used in this study was accrued from the Pseudobase++ database containing 398 RNAs, which was assessed using a set of inclusion and exclusion criteria following PRISMA (Preferred Reporting Items for Systematic Reviews and Meta-Analyses) guidelines. Base pairings within a given RNA sequence were deemed correct or incorrect following Mathews' parameters.

Results: This paper reported RNA prediction engines with greater accuracy, such as pKiss, when compared to previous iterations of the software and when compared to older folding engines. This paper also reported that when assessed using metrics such as the F_1-score and the PPV, MEA folding software does not always outperform MFE folding software in prediction accuracy when applied to viral pseudoknotted RNA. Moreover, the results suggested that thermodynamic model parameters will not ensure accuracy if auxiliary parameters, such as Mg^{2+} binding, dangling end options, and hairpin-type penalties, are not applied.

Conclusions: This is the first attempt at applying a suite of RNA folding engines to a dataset solely comprised of viral pseudoknotted RNAs. The observations reported in this paper highlight the quality between difThis is the first attempt at applying a suite of RNA folding engines to a data set solely comprising viral pseudoknotted RNAs. The observations reported in this paper highlight the quality between different ab initio prediction methods, while enforcing the idea that a better understanding of intracellular thermodynamics is necessary for a more efficacious screening of RNAs.ferent ab initio prediction methods while

enforcing the idea that a better understanding of intracellular thermodynamics is necessary for a more efficacious screening of RNAs.

(JMIRx Bio 2024;2:e58899) doi:10.2196/58899

KEYWORDS

pseudoknot; viral RNA; MFE; minimum free energy; MFE prediction; MEA; maximum expected accuracy; MEA prediction; virus; virology; computational biology

Introduction

Computational biology is 1 of the key tools we possess to understand RNA folding and is used in pharmacokinetics, drug discovery, and pharmacology. In silico predictions of catalytic RNAs help narrow down and consolidate a surfeit of data, while expediting the search for potential drug targets. As of now, we know that catalytic RNA controls for ribozymes, riboswitches, messenger RNA (mRNA) vaccines, thermosensors, and essential elements of genome editing [1-4]. This is due to RNA's ability to fold itself into tertiary structures (pseudoknots), forming binding pockets and active site clefts that can act as targets for active pharmaceutical ingredients (APIs) [5]. As artificial intelligence (AI), computer processing, and data throughput continue to advance, we are witnessing these methodologies more frequently implemented in the field of virology [6]. This paper explores the different ways in which stochastic folding engines predict viral pseudoknotted RNAs and the accuracy of these approaches.

Pseudoknots are structural motifs found in almost all classes of RNA. Although most RNA forms planer secondary structures, these 3D structures embody up to 30% of tertiary nonplaner motifs in G+C-rich RNA sequences [7]. In the context of viruses, these pseudoknots control gene expression and protein synthesis. Many catalytic RNAs regulate the mechanisms of action associated with viral replication, viral translation, or both. An example of this can be seen in satellite viruses (eg, hepatitis delta virus, satellite tobacco necrosis virus 1) that encode ribozymes that are folded by pseudoknotted structures [8,9].

For decades, scientists have explored and created different prediction software to better elucidate the complicated nature of RNA folding. Though RNA is a biopolymer that folds in a specific manner, it can be difficult to discern which prediction algorithms, alignment sequences, or applied mathematics would result in the most accurate model. This difficulty becomes more apparent when noting how much the field has changed over the years and how small changes in the underlying formalisms and constraints can result in drastic differences in the final predicted structure.

RNA folding occurs through populated intermediates and is accomplished in a hierarchical manner, where secondary planer forms come prior to tertiary contacts [10]. This allows software engines to model both canonical and noncanonical base pairs, making it so the inputs within V(i,j) base pairs have a range of integer values (rather than binary values) dependent on the base pairs they form [11,12]. V(i,j) in this case is the real symmetric contact matrix of N×N, where N represents the number of nucleotides on a given polymer chain.

Using V(i,j), and other mathematical formalisms, derived from prior experimental data to model the effects of salinity, pH, temperature, loop entropies, and stacking formations, we can generate a "pseudo-energy model." This grants us a measure of the relative probability of different RNA secondary structures, expounding on the ensemble free energy, and the equilibrium concentrations of all possible structures, all of which correspond to the topological character of the RNA strand [13].

Within the RNA template, the first base at the 3' terminus is regarded as 1, and the final base found at the 5' terminus is regarded as N. In the total secondary structure, made up of V(i,j) base pairs, the index $1 \leq i < j \leq N$ should be set. Each integer within a given matrix will represent the i-th nucleotide being paired with the j-th nucleotide. The base pairs, (G-C), (A-U), and, at times, (G-U), dependent on the algorithm/software used, are the integer values that contribute to the matrix field. The entire structure of length N is regularly represented in Feynman diagrams, also known as arc and chord diagrams (Figure 1A,B [14-18]), where each nucleotide is represented as a point on the chain, while each arc represents a base pair forming between any nucleotides i and j.

Gilbert and coworkers [6] defined a pseudoknot as follows: "Pseudoknots are formed upon base pairing of a single-stranded region of RNA in the loop of a hairpin to a stretch of complementary nucleotides elsewhere in the RNA chain."

We proposed more specified definitions for the sake of clarity posing 1 definition of a pseudoknot as "a template of RNA in which nucleotides within a loop pair with regions that do not pertain to the helices that close said loop." Another definition could be "an RNA secondary structure that forms base pair regions upstream or downstream, resulting in stem-loop structures." Their topology is more varied than most other assemblies of RNA, presenting a challenge for in silico prediction software.

Although comparative approaches exist in the solving of optimal RNA structures [19,20], including web servers, such as KNetFold [21] and pAliKiss [22], this review focused on the ab initio topological predictions based primarily on the RNA secondary structure. The accuracy of these ab initio stochastic RNA folding software programs will be assessed in relation to a catalog of 26 distinct viral pseudoknotted RNAs taken from PseudoBase++ [23], whose wild-type structures have been previously determined via sequence comparison, structure probing, mutagenesis, and nuclear magnetic resonance (NMR). The RNA predictions generated in this paper, imparted by the underlying formalisms of the software, will result in structures that represent either the minimum free energy (MFE) or the

maximum expected accuracy (MEA) as both models are compared.

It can generally be posited that base pairs, when formed, lower the Gibbs free energy of a ribonucleic strand, making use of the attractive interactions between the complementary strands. MFE prediction algorithms assess these by solving for the maximum number of nucleotide pairings, via their thermodynamic properties, which generally results in the lowest energy form. It is important to note, however, that in nature, kinetic barriers, environmental conditions, and other factors may influence RNA folding intermediates, resulting in a physiologically favored RNA that does not coincide with the MFE structure [24].

Conversely, MEA models compute the final RNA structure via a partition function (a function that is used to calculate the thermodynamic properties of a system) that implements hard and soft constraints based on electrostatic interactions, stacking interactions, adjacent complementary base pairs, and other variables, depending on the software in question [24]. This results in a final structure that may not necessarily encompass the lowest-possible free energy of a system.

The current literature compares the accuracy of RNA folding software when applied to viral RNAs and cellular RNAs, suggesting there exists no difference in accuracy between the 2 [25]. These investigations have explored viral RNAs of various lengths, accounting for the positive predictive value (PPV), sensitivity, and F_1-scores. However, to the best of our knowledge, few papers exist that address the accuracy of RNA folding software when applied to viral pseudoknotted RNA transcripts alone. Moreover, the literature does not expound on the differences in accuracy regarding MEA and MFE modalities when applied to viral pseudoknotted RNA. This paper aimed to address this knowledge gap within the literature by forming a highly specific investigation of a data set of 26 short pseudoknotted sequences (20-150 nt), with updated versions of existing stochastic RNA prediction algorithms. This investigation addressed whether MEA prediction modalities are, in fact, more accurate than MFE modalities and which of the 5 folding software programs are more accurate when applied to the data set of 26 pseudoknotted RNAs.

Figure 1. Ways in which to model pseudoknotted RNA. (A) Circular arc and chord diagram of the viral tRNA-like brome mosaic virus [14,15]. (B) Planer arc and chord drawing of the viral tRNA-like brome mosaic virus made using the R-chie package [16]. (C) Planer representation of viral tRNA-like brome mosaic virus using nitrogenous bases [17]. (D) Three-dimensional model of tRNA-like brome mosaic virus in stick format made using PyMOL Molecular Graphics System version 2.0 [18]. tRNA: transfer RNA.

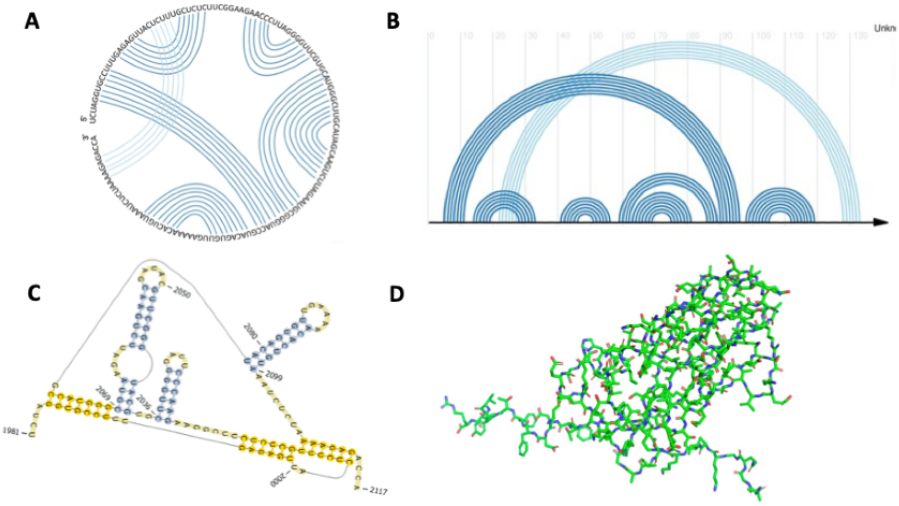

Methods

RNA Folding Engines, RNA Classes, and Genuses Assayed

The 5 RNA secondary structure prediction servers used in this paper are listed in Table 1.

See Sections S1-S5 in Multimedia Appendix 1 to view further details regarding the auxiliary parameters enforced by each software program. Access/links to the data set, as well as the 5 stochastic RNA folding web servers, are provided in Table S1 in Multimedia Appendix 1, in accordance with the FAIR (findability, accessibility, interoperability, and reusability) principles of data sharing.

The knowledge we possess pertaining to pseudoknots and their metabolic functions holds much of its origins in the study of viral biology, mounted on well-studied strains, such as flaviviruses, influenza viruses, and mosaic viruses [32-34]. These structures (Figure 2 [14,35-38]) encompass the regulatory elements of some viruses, controlling various phases of gene expression and function. Though many forms of pseudoknot classification have been conjectured [24,39,40], in this paper, all pseudoknots fall under 1 of the following 6 categories, building upon the grouping proposed by Legendre et al [24]:

- Hairpin-type (H-type) pseudoknot.
- Kissing hairpin–type (HHH-type) pseudoknot.
- Hairpin loop outer (HLout) pseudoknot: pertains to pseudoknots that form base pairs residing outside of a hairpin loop. This structure typically involves a larger loop enclosing the pseudoknot, which results in a more extended configuration.
- Hairpin loop inner (Hlin) pseudoknot: pertains to pseudoknots that form base pairs residing inside a hairpin

loop. The pseudoknot is nested within the loop structure, creating overlapping interactions within the loop itself.
- HLout,HLin pseudoknot.
- Loop-loop (LL) pseudoknot: forms between 2 distinct loops within the RNA structure. This base pair crossing results in steric interactions and stacking interactions across separate looped regions.

Table 1. MEA[a] and MFE[b] folding engines applied to viral RNA structures.

Name of the folding engine	Method of prediction	Thermodynamic model parameters	Pseudoknots enforced	Auxiliary parameters enforced	Study
Chiba Institute of Technology's Vsfold 5: RNA Secondary Structure Prediction Server	MEA	Jacobson-Stockmayer (standard parameters)	Yes	Kuhn length, Mg^{2+} binding, contiguous stems, minimum stem length, length of leading stem	Dawson et al [26]
Universitat Bielefeld's BiBiServ's (pKiss)	MFE	Turner model	Yes	H-type penalty, K-type penalty, maximal pseudoknot size, minimal hairpin length, lonely base pairs	Janssen and Giegerich [21]
Institut Curie's Kinefold	MFE	Turner model	No	Cotranscriptional fold, simulated molecular time, tracing and forcing helices	Xayaphoummine et al [27]
NUPACK 3.0	MFE	Turner model	No	Mg^{2+} binding, dangling end options, input of multiple interactions	Zadeh et al [28], Fornaceet al [29]
Vienna RNAfold[c]	MFE	Turner model	—[d]	Avoiding isolated base pairs, incorporation of G-quadruplex formation into the structure prediction algorithm, dangling end options, addition of modified base pairs	Hofacker et al [30]

[a]MEA: maximum expected accuracy.

[b]MFE: minimum free energy.

[c]The Vienna RNAfold engine does not compute for pseudoknots and is implemented as a negative control [31].

[d]Not applicable.

Figure 2. Six classes of pseudoknot. The figure depicts the class of pseudoknot (skeletal structure) on the right, with an example of an accepted structure on the left. (A) Simian retrovirus-1 [35]. (B) *Homo sapiens* signal recognition particle [36]. (C) *Escherichia coli* [37]. (D) *Palmaria palmatra* rRNA [38]. (E) Barley stripe mosaic virus [14]. (F) Pepper mild mottle virus [14]. H: hairpin; HHH: kissing hairpin; Hlin: hairpin loop inner; HLout: hairpin loop outer; LL: loop-loop; rRNA: ribosomal RNA.

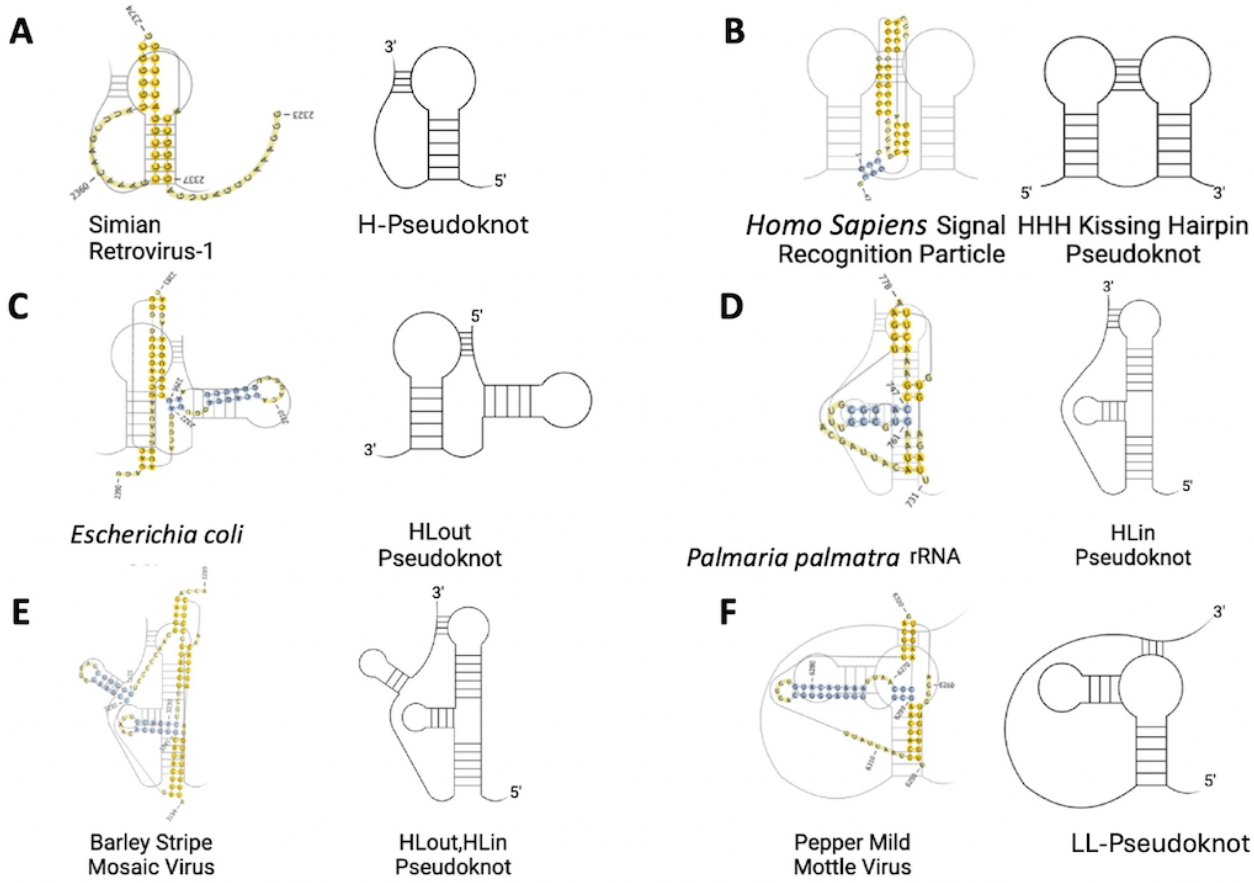

Given that most classified pseudoknots in data banks (both proteins and nucleic acids) have a genus of 1 [41], all pseudoknots expounded on in this investigation had a genus of 1. The “genus” of a pseudoknot refers to a mathematical concept that correlates to the topology of a surface. The genus is a positive integer value, which corresponds to the minimum number of handles of the embedding surface of a structure, or, more simply, the number of times the RNA molecule intersects with itself in 3D space. A genus of 0 means that the graph can be drawn without any crossing on a sphere. A genus of 1 means that the graph can be drawn on a torus (doughnut shape), without any base pairs crossing (Figure 3 [14,41-43]).

Figure 3. Depiction of genus 2, 1, and 0 RNAs. (A) Hepatitis delta virus ribozyme in 3D space and a planer arc and chord diagram [41,42]. (B) Tobacco rattle virus in 3D space and a planer arc and chord diagram [14]. (C) CCA sequence adding polymerase in 3D space and a planer arc and chord diagram [43].

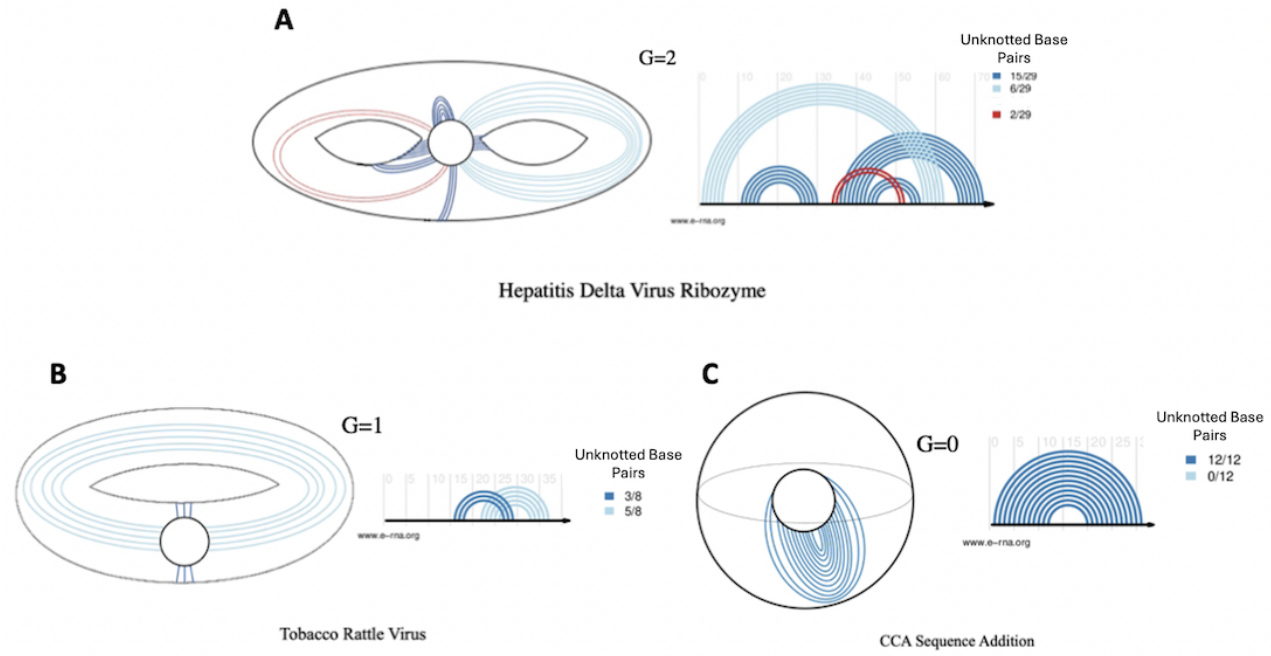

Generating a Viral Pseudoknotted RNA PseudoBase++ Data Set

For the 398 RNAs found in the Pseudobase++ database, 205 (51.5%) peer-reviewed papers referenced in these sites were vetted thoroughly following PRISMA (Preferred Reporting Items for Systematic Reviews and Meta-Analyses) guidelines [44]. The search identified 87 (42.4%) eligible studies. In addition to solely using pseudoknots of a genus 1 class, the computed MFE of all pseudoknots was also considered (see Table S2 in Multimedia Appendix 1). Any pseudoknot resulting in too high an MFE (P<.05, df=1) was excluded from the data set and considered an outlier. What remained were 26 (31.7%) RNAs of varying sizes from 20 to 150 nt, conforming to 1 of the 6 structures depicted in Figure 2 (see Table S3 in Multimedia Appendix 1 for further information about individual structures). Structures were derived from both plant and animal species, with each structure corresponding to a unique viral genome.

As mentioned previously, all pseudoknots expounded in this report fall under at least 1 of the 6 categories described in Figure 2. Of the 26 RNAs assessed, 17 (65.4%) consist of H-type pseudoknots, while the other 9 (34.6%) fall under 1 of the other configurations listed. This skewness is intentional, and true to nature, given that H-type pseudoknots are more common by far [6]. In addition, of the pseudoknotted RNAs assessed, 16 (61.5%) harbor viral transfer RNA (tRNA)–like motifs, 5 (19.2%) harbor viral 3' untranslated region (UTR)–like motifs, and 4 (15.4%) harbor viral frameshifts. Each motif plays an essential role in the replication of viruses and was thus included in the data set (see Table S3 in Multimedia Appendix 1 for further information). For example, the pseudoknotted UTRs of positive-strand RNA viruses regulate and initiate protein synthesis and replicase enzymes, L-shaped pseudoknots that resemble tRNAs propagate viral proteins, and viral frameshifts result in the production of unique proteins (especially in retroviruses) [6].

Assessing Prediction Software Efficacy Through Percentage Error and Mean Squared Error Metrics

Base pairings were deemed correct following Mathews' parameters [45]. Through this system, base pairing within a reference sequence of length N, between base pairs i and j (where $1 \leq i < j \leq N$), was considered correct if i was paired with either j, j – 1, or j + 1 or if j was paired with i, i – 1, or i + 1. If a pairing did not fall under these conditions, it was considered a false positive (FP). If a pairing that fell under these conditions was missed by a given prediction software program, it was classified as a false negative (FN). This model allows for some elasticity and leniency in prediction, deeming base pairing correct even if base pairs are displaced by 1 nucleotide either up- or downstream. This is the standard for in silico RNA computation. Further benchmarks used by Mathews [45] include the following:

- A large set of well-established reference/accepted structures to compare against experimentally derived data
- Tests for statistical significance
- Different RNA families/RNA types (see Table S3 in Multimedia Appendix 1) that should be used

First, the percentage error (represented in the results as the mean absolute error [MAE]) was used to assess the prediction accuracy of total base pairs and knotted base pairs. The percentage error is expressed as the absolute value of the difference between base pairings derived from 1 of the 5 RNA folding engines (Table 1) and base pairs from the PseudoBase++ database derived from sequence comparison, structure probing, and NMR, in percentage format:

This manner of assessment is robust against outliers and better suited to delineating between software that can or cannot predict pseudoknots.

The mean squared error (MSE) was applied to all experimental and control conditions. The MSE for a given folding engine is simply

where n is the number of data points, Y_i is observed values, and X_i is predicted values.

A better model will possess a better fit to the data should the resultant MSE be closer to 0. Often used in machine learning and regression analysis, this metric is appropriate when applied to evaluating the functioning of predictive models. However, these 2 metrics do not encompass a software program's ability to holistically assess both knotted and total base pairs in tandem. For this reason, many papers are instead opting for sensitivity (recall) and the PPV (precision) [45,46].

Assessing Prediction Software Efficacy Through Sensitivity, PPV, and Youden Index Metrics

Sensitivity and the PPV are common and important systems of measurement when predicting software accuracy. The former assesses a folding engine's ability to identify correct base pairs, while the latter assesses a software program's propensity to incorrectly identify base pairs (resulting in a value of 1-0).

Here, sensitivity reduces from 1 when an RNA folding engine misses pairings, while the PPV reduces from 1 the more an RNA folding engine predicts bases that are not of the original secondary structure. Though these metrics are commonplace in almost all branches of bioinformatics, such as genomic variant calling and drug targeting prediction [47,48], this report imposed them onto folding engines.

Youden index values (J) were also used to compare the accuracy of each model, with higher values being indicative of models with higher discriminative ability. Simply defined by the following equation:

this metric can range from –1 (denoting completely incorrect detection for a given group) to 1 (denoting completely correct detection for a given group). It is important to clarify that the value of J is often represented on a receiver operating characteristic (ROC) curve, with recall (true positive [TP] rate, T_{pr}, on the y axis and the FP rate [F_{pr}] on the x axis), when applied to 1 reference structure using 1 predictive model. However, this paper compared all relative J values imposed by all models across all 26 viral pseudoknotted RNAs in column format.

Assessing Prediction Software Efficacy Through F_1-Score Metrics

Once the PPV and sensitivity have been calculated, F_1-scores can then be derived for each structure. F_1-scores are a standard method used to evaluate prediction software [24,45,46,49] and assess the harmonic mean between sensitivity and the PPV by considering 3 of the 4 confusion matrix categories (TP, FP, and FN). It should be noted once more that for a base pairing prediction to be considered incorrect, it must fall outside the parameters established by Mathew [45], where base i is paired with j + (≥2) or j – (≥2) or base j is paired with i + (≥2) or i – (≥2)—or, in layperson terms, when the base pair is displaced by 2 nucleotides, either upstream or downstream, relative to the native structure.

F_1-scoring remains an archetype for binary classification problems [49] and integrates the boons of sensitivity and the PPV to produce a higher-caliber performance metric:

Normality and lognormality testing included Kolmogorov-Smirnov tests and Shapiro-Wilk tests to confirm normal (gaussian) distribution of data (α=.05). Robust outlier (ROUT) tests were used to identify outliers (Q=1%), and statistical analysis included 1-sample *t* tests, Wilcoxon tests, and 1- and 2-way ANOVA testing. Testing was performed using GraphPad Prism v.9.5 software (Graph-Pad Software), and accuracy metrics were reported as decimals.

Ethical Considerations

Ethical considerations were taken into regard for this study, though the authors have nothing to declare, given the in silico nature of this paper.

Results

Assessment of Percentage Error and Mean Squared Error Metrics

In this study, we tested the 5 folding engines used against 26 experimentally derived short pseudoknotted RNA sequences selected following PRISMA guidelines (Figure S1 in Multimedia Appendix 1). No significant difference in percentage error was observed between the total number of base pairs computed by all RNA folding algorithms (Figure 4), with the largest discernible difference between Vsfold 5 and Vienna (adjusted *P*=.99). This agrees with current studies, as the challenge biotechnicians face instead lies within predictions in O(N3) and O(N4) time and space, where N is the sequence length (using big O notation) [50]. Although certain algorithms can reduce higher-ordered structures to O(N3), thereby reducing computational complexity, a growing minimal N value correlates with more possible pseudoknots, making the algorithm less accurate [21].

The mean percentage error of total base pairs generated by each software program was 17.95%, with Vsfold 5 exhibiting the highest (mean 20.23%, SD 23.94%) and the negative control exhibiting the lowest (mean 15.07%, SD 12.35%) values, which was expected. Though the current literature now advocates for software that computes the MEA, rather than the MFE [24], the Vienna package is specifically designed to predict planer secondary structures.

A much higher percentage error was exhibited in knotted viral RNA structures produced by the MEA engine Vsfold 5, relative to its MFE-computing counterparts (apart from the negative control). Vsfold 5 was expected to give the lowest percentage error. However, the lowest percentage error for knotted base pairs was, instead, exhibited by MFE structures generated by pKiss (mean 22.37%, SD 24.2%), while Vsfold 5 retained a mean percentage error of 69.91% (SD 39.3%).

The values of the MSE drew parallels to those of the percentage error, with Vsfold 5 exhibiting the highest values of the experimental controls (382.29 for knotted bases and 37.85 for unknotted bases) and pKiss exhibiting the lowest values (48.4 for knotted bases and 6.88 for unknotted bases). Kolmogorov-Smirnov tests indicated that the data were normally distributed.

Figure 4. Percentage error and MSE. (A) Percentage error of total base pairs and knotted base pairs. Data correspond to the mean (SD) percentage error. The mean (SD) percentage error, across all 4 MFE RNA folding engines, was compared to that of the MEA computations of Vsfold 5, with statistical analysis performed using 2-way ANOVA, followed by a Tukey multiple-comparison test. ****P<.001 (df=4). The ROUT test was performed to identify outliers (Q=1%). (B) MSE (mean squared deviation). Kolmogorov-Smirnov tests performed on both "accuracy of unknotted/knotted base pairs" and "MSE" confirmed normal (gaussian) distribution of data (α=.05). MEA: maximum expected accuracy; MSE: mean squared error; ROUT: robust outlier.

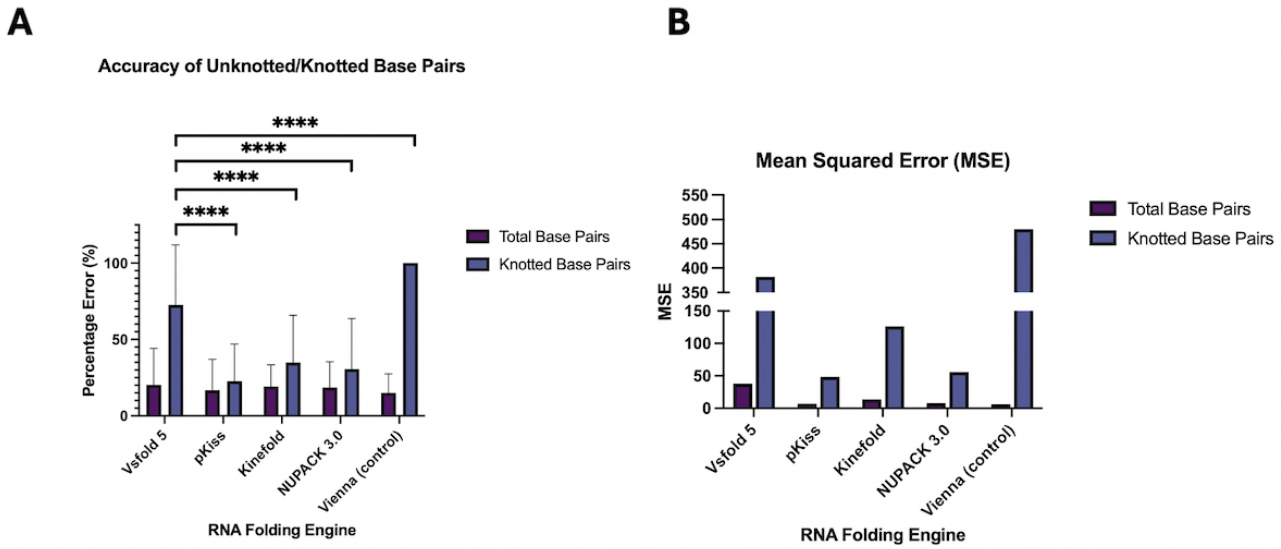

Sensitivity, PPV, and Youden Index of Folding Engines

The second metric used to assess RNA folding engines was sensitivity, coupled with the PPV. The highest mean sensitivity and PPV were derived from pKiss, with mean 0.88 (SD 0.14) and mean 0.82 (SD 0.16), respectively. Conversely, the lowest mean sensitivity and PPV were derived from Kinefold, with mean 0.14 (SD 0.23) and mean 0.171 (SD 0.31), respectively (Figure 5). Ultimately, pKiss outperformed the mean of the Vsfold 5 MEA prediction software by mean 0.296 with respect to sensitivity and by mean 0.176 with respect to the PPV.

We would like to note that PPV values derived from free-energy minimization (ie, MFE folding engines) have been shown to be lower than sensitivity values [51,52]. This is likely because structures accepted in the literature can be missing base pairs that may occur experimentally and because the thermodynamics imposed by MFE algorithms often overshoot the number of canonical base pairings (because it is the formation of base pairs that innately lowers the Gibbs free energy of a structure) [53]. However, this trend does not present itself in all 4 experimental conditions but only in pKiss and NUPACK 3.0. This is because updated software such as this implements a more accurate assessment of the thermodynamic properties of the structure, removing unwanted pairs and improving overall performance [54].

In addition to the PPV and sensitivity, the Youden index (sometimes denoted as J) provides an additional framework to assess detection accuracy. As shown in Figure 6, pKiss exhibited the highest J value in raw and normalized data sets (mean 0.713, SD 0.267, and mean 100.0, SD 19.1, respectively), while Kinefold exhibited the lowest J values in raw and normalized data sets (mean –0.68, SD 0.57, and mean 0.0, SD 41.0, respectively), reflecting the results in Figure 5.

Figure 5. Sensitivity and PPV of RNA folding engines on pseudoknotted viruses. (A) Data corresponding to the mean (SD) sensitivity and PPV across all 5 experimental conditions were compared to the sensitivity and PPV generated by Vsfold 5. Statistical analysis was performed using 2-way ANOVA, followed by a Tukey multiple-comparison test. ****P<.001 (df=1), **P≤.002 (df=1). The ROUT test was performed to identify outliers (Q=1%). (B) Sensitivity and PPV values plotted in a 1×1 matrix. The Shapiro-Wilk test confirmed normal (gaussian) distribution of data (α=.05). PPV: positive predictive value; ROUT: robust outlier.

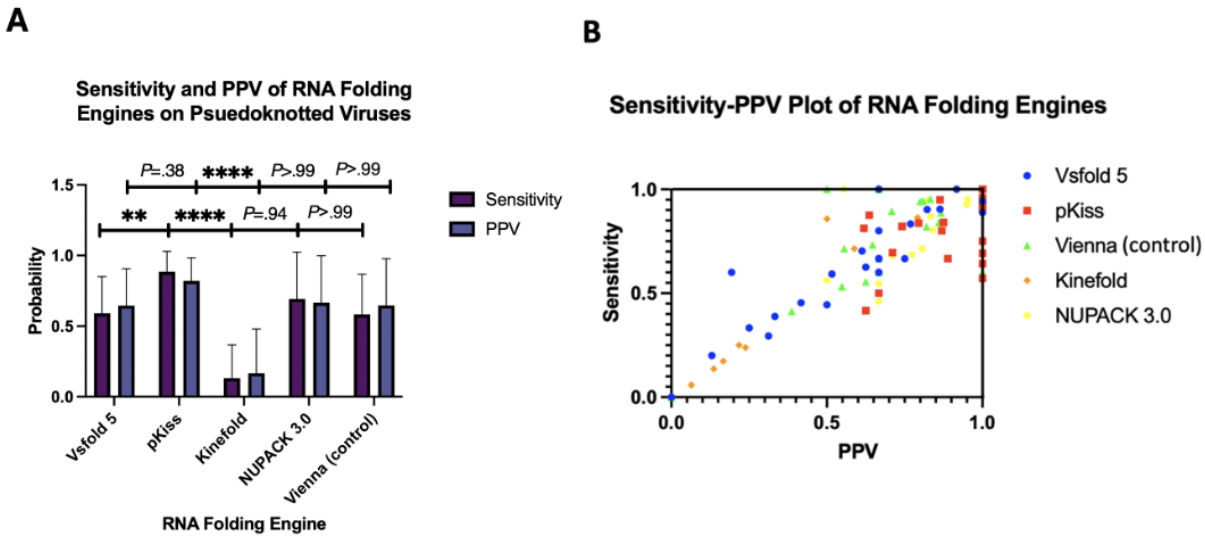

Figure 6. Youden index of RNA folding engines on pseudoknotted viruses. (A) Youden index of raw values. Data corresponding to the mean (SD) across all 5 experimental conditions. Row statistics were performed, alongside a 1-sample t test and Wilcoxon test (t4=0.7354). Data passed normality (gaussian) and logarithmic tests (which included the Shapiro-Wilk test and the Kolmogorov-Smirnov test). *P<.332, ****P<.001. (B) Graph displaying normalized data. This entailed the averaging of subcolumns and normalization of the means, where 0% is defined as the smallest mean in each data set and 100% is defined as the largest mean in each data set.

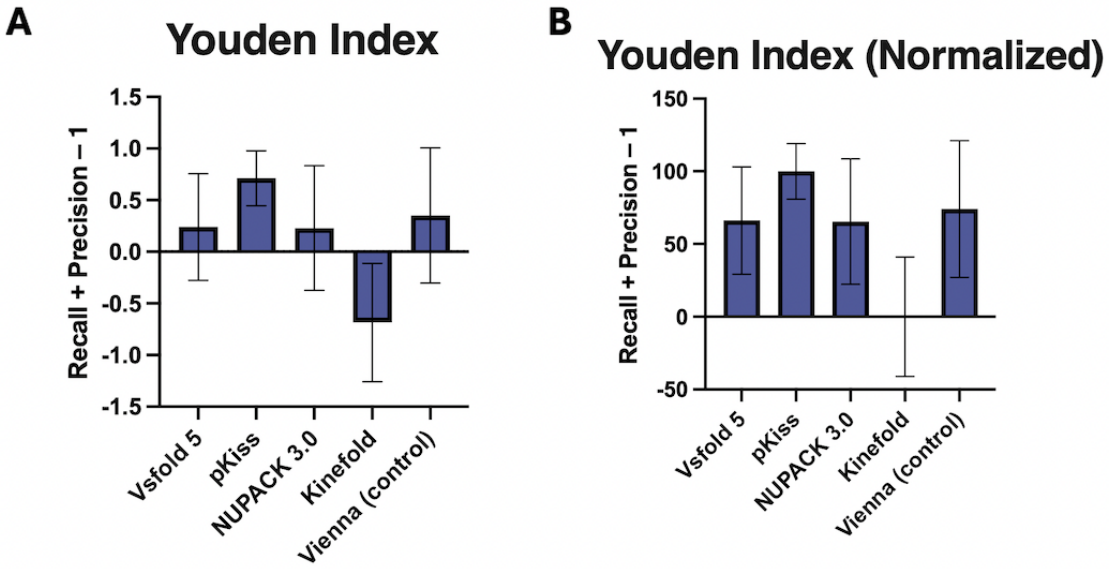

Quality of Prediction Software Assessed via F_1-Scoring

F_1-scores were derived from the sensitivity and PPV values (Figure 7). This modality is often adapted to assess prediction accuracy so long as the reference structure is given. Of all average F_1-scores generated from all 5 stochastic folding algorithms, the pKiss engine computed the largest values (mean 0.844, SD 0.138), while Kinefold computed the lowest values (mean 0.150, SD 0.273). Of all MFE folding algorithms used, pKiss was the only one to significantly outperform the mean F_1-score of the Vsfold 5 MEA engine by a value of 0.235. Outliers were found in Vsfold 5, Kinefold, and NUPACK 3.0, corresponding to large data sets.

Figure 7. F_1-scores of the Pseudobase++ database. (A) Mean (SD) F_1-scores depicted as a bar graph. (B) Individual F_1-scores generated by all software programs depicted as a heatmap, with white equating to the best performance (F_1-score=1) and black equating to the worst performance (F_1-score=0). Data corresponding to the mean (SD) F_1-scores. Mean (SD) F_1-scores across all 5 experimental conditions were compared to those of Vsfold 5, with statistical analysis performed using 2-way ANOVA, followed by a Tukey multiple-comparison test. ****P<.001, **P≤.002. The ROUT test was performed to identify outliers (Q=1%). The Kolmogorov-Smirnov test was performed, confirming that pKiss was the only experimental condition to conform to normal (gaussian) distribution (α=.05).

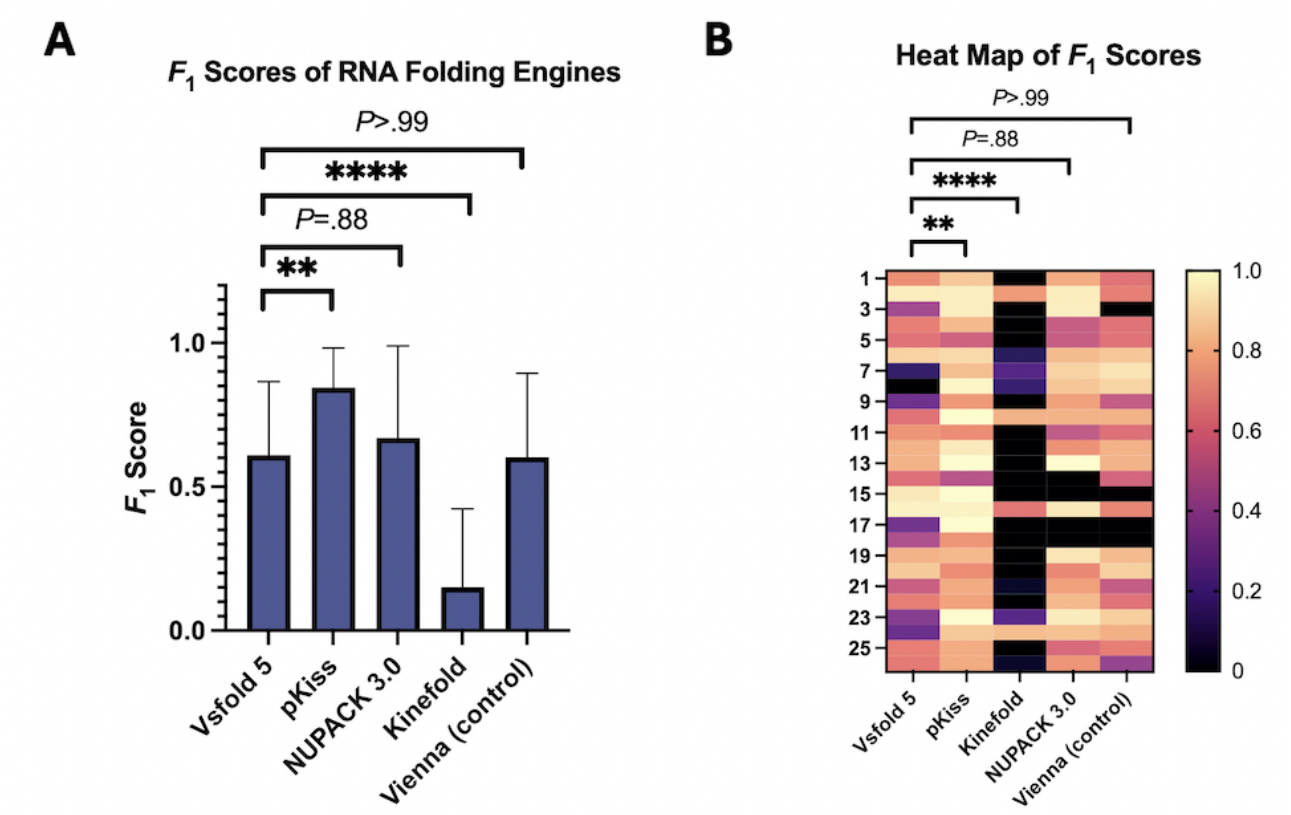

Discussion

Principal Findings

The primary aims of this study were to evaluate how MEA folding modalities compare to MFE folding modalities in the context of pseudoknotted viral RNAs and to see which of the 4 experimental conditions (folding software) provides the most accurate models. Although differences in the percentage error (MAE) of "total base pair" predictions were nonsignificant across all software programs (which was expected), the differences in the percentage error of "knotted base pair" predictions were vastly different across the software programs.

The pKiss MFE folding engine exhibited the highest prediction accuracy across all MFE and MEA folding engines and across all performance metrics used (percentage error of total base pairs and knotted base pairs, MSE, sensitivity, PPV, Youden index, F_1-scores), outperforming the MEA folding software Vsfold 5 on all accounts. In contrast, Kinefold exhibited the lowest values for sensitivity, PPV, Youden index, and F_1-scores, even when compared to the control. We have provided evidence suggesting that MEA software is not always the optimal method of topological prediction when applied to short viral pseudoknotted RNAs.

Origins of Stochastic RNA Folding Engines

The underlying functions and computational modalities for RNA prediction algorithms have greatly evolved since Nussinov's dynamic programming algorithm [55], a formalism derived in 1978 and arguably the genesis of predictive RNA folding, whereby:

Here,

Using these systems, it is possible to generate MFE predictions in kcal/mol of a structure via tracebacking, resulting in a probabilistic model of the nature of the RNA template in vivo. This original scheme has been amended many times over, with Zuker's algorithm [56] being the most notable change—an amendment that is still used to this day.

The realization of these formalisms coincides with the discovery of the first pseudoknotted plant viruses discovered in the early 1980s. Today, they make up many of the pseudoknots found in various online databases/databanks and are recognized as common motifs that allow for viral mRNA function, ribosome function, and replication [6]. The inherent vastness of viral RNA in nature and, consequently, within pseudoknot databases (like

those taken from PseudoBase++ [23] and the RNA Secondary Structure and Statistical Analysis Database (RNA STRAND [57]) was the primary rationale for this investigation.

Evaluation of Percentage Error and MSE Performance Metrics

MEA software outperformed MFE software. The first metric used to evaluate the accuracy of the 5 RNA folding engines was the percentage error of total base pairs and knotted base pairs. These values were computed first by considering all total base pairs in the given model (purple) and then again by considering only pseudoknotted base pairs (blue), as shown in Figure 4A. To reiterate, the difference in percentage error between the total number of base pairs computed by all RNA folding algorithms was nonsignificant (as expected), while pKiss (an MFE model) resulted in a lower percentage error for knotted bases (mean 22.37%, SD 24.2%) when compared to its MEA counterpart Vsfold 5 (mean 69.91%, SD 39.3%). Although some might assume that the lower percentage error exhibited by pKiss could be the result of the pseudoknot "enforce" constraint embedded in the software, it is more likely that this outcome was multivariable, equating to the Turner energy model used and the sensitive auxiliary parameters enforced by the program (refer to Table 1 and Section S2 in Multimedia Appendix 1). This was later tested and proven, showing that small changes within the auxiliary parameters resulted in drastic changes in pseudoknot prediction accuracy (refer to Figure S2 in Multimedia Appendix 1).

The MSE was additionally used, as it is a commonplace tool for assessing predictive models (especially those models that incorporate continuous variables), as shown in Figure 4B. A prerequisite for applying the MSE is that observations are normally distributed [58], which was confirmed using the Kolmogorov-Smirnov test. It was found that for knotted bases, Vsfold 5 resulted in the highest MSE value (382.29), while pKiss resulted in the lowest MSE value (48.4). This greatly buttresses the claim that MFE software may, at times, result in a more favorable model, especially when considering the MSE's sensitivity to outliers.

Evaluation of Sensitivity, PPV, and Youden Index Performance Metrics

With all 26 viral RNAs considered, the highest mean sensitivity and PPV were derived from pKiss, with values of 0.88 (SD 0.14) and 0.82 (SD 0.16), respectively. These values trump those of prior versions, reporting lesser sensitivity (mean 0.80, SD 0.24) and PPV (mean 0.75, SD 0.27) [24].

It is important to emphasize the increase in both the PPV and sensitivity of the newer folding engines listed in Table 1 when compared to older folding engines previously reported in the literature. Such examples include ProbKnot, with a mean sensitivity of 0.693 and a mean PPV of 0.613 [54], and PKNOTS (the older version of pKiss), with older papers reporting a mean sensitivity of 0.828 and a mean PPV of 0.789 and newer papers reporting a mean sensitivity of 0.855 and a mean PPV of 0.808 [59]. Papers promoting RNA software that shares MEA and MFE properties, such as BiokoP dating back 5 years prior, have also reported lesser sensitivity (mean 0.81, SD 0.22) and PPV (mean 0.75, SD 0.26) values [24]. Note that confounding variables between this paper and the referenced literature are minimal, as all reports screened for a diverse set of RNA pseudoknots.

Concerning J, we saw that pKiss continued to show the highest mean value of 0.713 (SD 0.267) for raw values (Figure 6A). Though this metric is similar to the F_1-score, in the sense that it incorporates sensitivity and the PPV, it optimally predicts the probability cutoff by increasing the difference between TP and FP rates. This system of measurement remains inherently more sensitive than F_1-scoring, with minimums and maximums ranging from 1 to –1 rather than from 1 to 0 [60].

Regarding the raw data set, we know that a value of 0 indicates that the experimental variable tested (eg, folding software) has no diagnostic value, while a value of 1 indicates a perfect test, yielding no FPs or FNs. Therefore, pKiss, the MFE model, outperformed Vsfold 5, the MEA model, by a significant amount (mean 0.713, SD 0.267, vs mean 0.241, SD 0.516), enforcing the idea that MEA models are not always the optimal method for topological prediction. It should also be noted that J values were normalized and put into graphical format (Figure 6B) for visual clarification via elimination of negative values (as negative values for J are not defined).

Quality of Prediction Software Assessed via F_1-Scoring

Among the F_1-scores (Figure 7), the pKiss MFE folding engine computed the most promising values (mean 0.844, SD 0.138), significantly outperforming the mean F_1-score computed by the Vsfold 5 MEA engine by a value of 0.235. These values exceed those of previously reported folding engines, such as CCJ and ProbKnot with mean F_1-scores of 0.644 and 0.738, respectively, while, at the same time, underperforming when compared to deep learning algorithms, such as ATTfold with a mean F_1-score of 0.966 [46,61]. Moreover, in all the 5 RNA folding engines assessed, the F_1-score derived from pKiss was the most consistent by far (most symmetrical, with the least amount of skewness), being the only one to have passed the Kolmogorov-Smirnov test for gaussian distribution (α=.05).

It is important to keep in mind that minor improvements have been made to previous MFE reports, although they still underperform existing deep learning and machine learning algorithms.

Of the metrics that were used under the remits of this investigation, none demonstrated that the MEA algorithm used, Vsfold 5, was inherently superlative to its MFE counterparts. This suggests that some short viral pseudoknotted RNAs (20-150 nt) may often result in their lowest free-energy model (granted that salinity, Mg^{2+} concentration, and other environmental variables remain constant). This conclusion is shared among viral pseudoknotted RNAs that are of different structures (eg, H-type, LL-type) and of different motifs (eg, viral tRNA-like, viral 3 UTR).

It should be noted that the thermodynamics within the cell, as well as the many auxiliary folding pathways of RNA, become muddled when the extensive cellular environment is explored

in vivo. This is where ab initio and comparative approaches come into play. However, one should consider that in silico studies will often lack direct cellular relevance, as researchers remain aloof to the broader physiological consequences of change [5]. Therefore, it should be emphasized that both in vitro and in silico approaches are necessary to explore the nature of viral RNAs.

Limitations

Error is inherently fixed to in silico predictions such as these. In nature, kinetic barriers, environmental conditions, and other factors may influence RNA folding intermediates, resulting in a physiologically favored RNA that does not coincide with the predicted results, even if these natural factors are accounted for. Though the methodologies provide novel data to better help us understand genus 1, short (20-150 nt) viral pseudoknotted RNAs, this is a niche subsection of plant and animal viromes. This confers a limited use, should one endeavor to use the RNA folding prediction software on larger, more heterogeneous data sets.

Finally, those who have intellectual rights to these RNA folding web servers [21,26-30] can amend the software and change the parameters of whatever in silico modus they are using for the sake of improvement/refinement/issuing better predictions. This limits the reproducibility of this work, should someone wish to input the same values/predict the same structures used in this investigation.

Future Directions

The conclusions derived from this report further the understanding of how to predict the tertiary, 3D conformation of viral pseudoknotted RNAs (under the context of MEA and MFE prediction software). However, further work could certainly be conducted in this field, which could be brought about by either expanding the current data set or providing further analysis of the already established data set.

Addressing the former point, by softening the exclusion criteria (see Figure S1 in Multimedia Appendix 1), either by allowing more lengthy pseudoknots (nucleotides>150), allowing for a broader scope of MFE structures (MFE<–60 kcal/mol), or assaying a wider variety of RNA classes (rather than just viral tRNA-like, viral 3 UTR, and viral frameshifts), we can increase our understanding of how these moieties behave. Additionally, other RNA data sets, such as RNA STRAND [57], could be adopted in this investigation.

Addressing the latter point, further “prediction accuracy metrics” exist within computational biology that could bolster the claims this investigation made. One metric that the authors advocate for is the *M*-score (also known as the macroaveraged F_1-score), which is a form of weighted F_1-score. It is calculated by summing all F_1-scores for a data set with n classes and then dividing the total by n [62].

This macroaveraged F_1-score is most applicable when the data set in question has equal amounts of data points, for each class n (which, in this investigation, happened to be the case). Yet, data sets found in the real world often comprise skewed data, are class-imbalanced, and can encompass nonnormalized data.

In these cases, where there are limited samples in a small class n or where the data are imbalanced, when performing binary classification evaluation, a more appropriate tool to use would be the Mathews correlation coefficient (MCC) [63,64]. The following equation (considering 3 of the 4 confusion matrices, analogous to F_1-scoring):

serves to measure the relationship between predicted values and real values (TN refers to true negative). Following the Pearson correlation coefficient directly [64], this metric is commonplace in bioinformatics and has been benchmarked to a wide array of open source data sets within the literature. When applied to either imbalanced support vector machine (SVM) or the MCC-Bayes data sets, this tool offers a good balance between training time and computational efficacy.

Conclusion

To the best of our knowledge, this paper is the first attempt at applying a suite of RNA folding engines to a data set solely comprising viral pseudoknotted RNAs. The data computed in this paper were founded upon different MEA and MFE software programs that have received updates in recent years, and the accuracy of these RNA folding engines was benchmarked following Mathews’ parameters. The evidence provided suggests that viral pseudoknotted RNAs may conform to the MFE structure in some cases, rather than the MEA structure. Under the scope of these quality folding engines, pKiss provided the most accurate structures when compared to data experimentally derived from mutagenesis, sequence comparison, structure probing, and NMR, while Kinefold resulted in the least accurate structures. This indicates that the veracity of the underlying thermodynamic model parameters (eg, Turner model, Jacobson-Stockmayer model) is compromised if the auxiliary parameters are not enforced (eg, Mg^{2+} binding, dangling end options, H-type penalties).

To expedite the screening of RNAs, whether they are knotted or planer, we must achieve a better understanding of the thermodynamics associated with cellular processes and how they govern the shaping of RNA. The explored ab initio methodologies provide more accurate results than previously reported, though they do not outperform deep learning algorithms. The exploration of RNA outside the wet lab might seem counterintuitive; however, the computing power we now possess lends to efficacious predictions. Limitations are present in both in vitro and in silico methodologies, leading to the conclusion that both are necessary to further the exploration of drug targets, mRNA vaccines, thermosensors, and RNA-based genome editing.

Acknowledgments

We would like to thank Ajay Singh, Jamie M Robertson, and the Effective Writing for Healthcare program (Harvard Medical School) for reviewing and editing this work. We thank the Das and Barna laboratories (Stanford University), as well as the entirety of the EteRNA community for their contributions to the project. We would also like to thank Henri Orland for providing supplemental aid to the content of the paper. Finally, we would like to acknowledge the Eterna OpenKnot labs project for inspiring this work and the National Instate of Health for generating its Pseudokbase++ database. This research received no external funding.

Data Availability

The data analyzed in this study are present within the main paper, as well as Multimedia Appendix 1.

Authors' Contributions

Conceptualization, methodology, and writing—original draft preparation were handled by VM; formal analysis and data curation by VM and MC; and writing—review and editing by VM, SZ, and JP. All authors have read and agreed to the published version of the manuscript.

Conflicts of Interest

None declared.

Multimedia Appendix 1
Supplementary findings related to the manuscript.
[DOC File , 9458 KB - xbio_v2i1e58899_app1.doc]

References

1. Lewin AS, Hauswirth WW. Ribozyme gene therapy: applications for molecular medicine. Trends Mol Med 2001 May;7(5):221-228. [doi: 10.1016/s1471-4914(01)01965-7] [Medline: 11325634]
2. Walter NG, Engelke DR. Ribozymes: catalytic RNAs that cut things, make things, and do odd and useful jobs. Biologist (London) 2002 Oct;49(5):199-203 [FREE Full text] [Medline: 12391409]
3. Zuber J, Schroeder SJ, Sun H, Turner DH, Mathews DH. Nearest neighbor rules for RNA helix folding thermodynamics: improved end effects. Nucleic Acids Res 2022 May 20;50(9):5251-5262 [FREE Full text] [doi: 10.1093/nar/gkac261] [Medline: 35524574]
4. Wu L, Belasco JG. Let me count the ways: mechanisms of gene regulation by miRNAs and siRNAs. Mol Cell 2008 Jan 18;29(1):1-7 [FREE Full text] [doi: 10.1016/j.molcel.2007.12.010] [Medline: 18206964]
5. Leamy KA, Assmann SM, Mathews DH, Bevilacqua PC. Bridging the gap between in vitro and in vivo RNA folding. Q Rev Biophys 2016 Jan;49:e10 [FREE Full text] [doi: 10.1017/S003358351600007X] [Medline: 27658939]
6. Brierley I, Pennell S, Gilbert RJC. Viral RNA pseudoknots: versatile motifs in gene expression and replication. Nat Rev Microbiol 2007 Aug;5(8):598-610 [FREE Full text] [doi: 10.1038/nrmicro1704] [Medline: 17632571]
7. Xayaphoummine A, Bucher T, Thalmann F, Isambert H. Prediction and statistics of pseudoknots in RNA structures using exactly clustered stochastic simulations. Proc Natl Acad Sci U S A 2003 Dec 23;100(26):15310-15315 [FREE Full text] [doi: 10.1073/pnas.2536430100] [Medline: 14676318]
8. Pu H, Li J, Li D, Han C, Yu J. Identification of an internal RNA element essential for replication and translational enhancement of tobacco necrosis virus A(C). PLoS One 2013 Feb 27;8(2):e57938 [FREE Full text] [doi: 10.1371/journal.pone.0057938] [Medline: 23460916]
9. Taylor JM. Structure and replication of hepatitis delta virus RNA. In: Casey JL, editor. Hepatitis Delta Virus. Berlin, Heidelberg: Springer; 2006:1-23.
10. Tinoco I, Bustamante C. How RNA folds. J Mol Biol 1999 Oct 22;293(2):271-281. [doi: 10.1006/jmbi.1999.3001] [Medline: 10550208]
11. Nikolova EN, Zhou H, Gottardo FL, Alvey HS, Kimsey IJ, Al-Hashimi HM. A historical account of Hoogsteen base-pairs in duplex DNA. Biopolymers 2013 Dec;99(12):955-968 [FREE Full text] [doi: 10.1002/bip.22334] [Medline: 23818176]
12. Gernot A, Jinho B, Philippe DF, Henri O, Graziano V. The Oxford Handbook of Random Matrix Theory. Oxford, UK: Oxford University Press; 2011:872-897.
13. Lim CS, Brown CM. Know your enemy: successful bioinformatic approaches to predict functional RNA structures in viral RNAs. Front Microbiol 2017 Jan 4;8:2582 [FREE Full text] [doi: 10.3389/fmicb.2017.02582] [Medline: 29354101]
14. Mans RM, Pleij CW, Bosch L. tRNA-like structures. Structure, function and evolutionary significance. Eur J Biochem 1991 Oct 15;201(2):303-324 [FREE Full text] [doi: 10.1111/j.1432-1033.1991.tb16288.x] [Medline: 1935928]
15. Felden B, Florentz C, Giegé R, Westhof E. Solution structure of the 3'-end of brome mosaic virus genomic RNAs. Conformational mimicry with canonical tRNAs. J Mol Biol 1994 Jan;235(2):508-531. [doi: 10.1006/jmbi.1994.1010] [Medline: 8289279]

16. Lai D, Proctor J, Zhu J, Meyer I. R-CHIE: a web server and R package for visualizing RNA secondary structures. Nucleic Acids Res 2012 Jul;40(12):e95 [FREE Full text] [doi: 10.1093/nar/gks241] [Medline: 22434875]
17. Byun Y, Han K. PseudoViewer3: generating planar drawings of large-scale RNA structures with pseudoknots. Bioinformatics 2009 Jun 01;25(11):1435-1437. [doi: 10.1093/bioinformatics/btp252] [Medline: 19369500]
18. Larson SB, Lucas RW, McPherson A. Crystallographic structure of the T=1 particle of brome mosaic virus. J Mol Biol 2005 Feb 25;346(3):815-831 [FREE Full text] [doi: 10.1016/j.jmb.2004.12.015] [Medline: 15713465]
19. Choudhary K, Deng F, Aviran S. Comparative and integrative analysis of RNA structural profiling data: current practices and emerging questions. Quant Biol 2017 Mar;5(1):3-24 [FREE Full text] [doi: 10.1007/s40484-017-0093-6] [Medline: 28717530]
20. Lavender CA, Gorelick RJ, Weeks KM. Structure-based alignment and consensus secondary structures for three HIV-related RNA genomes. PLoS Comput Biol 2015 May;11(5):e1004230 [FREE Full text] [doi: 10.1371/journal.pcbi.1004230] [Medline: 25992893]
21. Janssen S, Giegerich R. The RNA shapes studio. Bioinformatics 2015 Feb 01;31(3):423-425 [FREE Full text] [doi: 10.1093/bioinformatics/btu649] [Medline: 25273103]
22. Bindewald E, Shapiro BA. RNA secondary structure prediction from sequence alignments using a network of k-nearest neighbor classifiers. RNA 2006 Mar;12(3):342-352 [FREE Full text] [doi: 10.1261/rna.2164906] [Medline: 16495232]
23. Taufer M, Licon A, Araiza R, Mireles D, van Batenburg FHD, Gultyaev AP, et al. PseudoBase++: an extension of PseudoBase for easy searching, formatting and visualization of pseudoknots. Nucleic Acids Res 2009 Jan;37(Database issue):D127-D135 [FREE Full text] [doi: 10.1093/nar/gkn806] [Medline: 18988624]
24. Legendre A, Angel E, Tahi F. Bi-objective integer programming for RNA secondary structure prediction with pseudoknots. BMC Bioinform 2018 Jan 15;19(1):13 [FREE Full text] [doi: 10.1186/s12859-018-2007-7] [Medline: 29334887]
25. Sato K, Kato Y. Prediction of RNA secondary structure including pseudoknots for long sequences. Brief Bioinform 2022 Jan 17;23(1):bbab395 [FREE Full text] [doi: 10.1093/bib/bbab395] [Medline: 34601552]
26. Dawson WK, Fujiwara K, Kawai G. Prediction of RNA pseudoknots using heuristic modeling with mapping and sequential folding. PLoS One 2007 Sep 19;2(9):e905 [FREE Full text] [doi: 10.1371/journal.pone.0000905] [Medline: 17878940]
27. Xayaphoummine A, Bucher T, Isambert H. Kinefold web server for RNA/DNA folding path and structure prediction including pseudoknots and knots. Nucleic Acids Res 2005 Jul 01;33(Web Server issue):W605-W610 [FREE Full text] [doi: 10.1093/nar/gki447] [Medline: 15980546]
28. Zadeh JN, Steenberg CD, Bois JS, Wolfe BR, Pierce MB, Khan AR, et al. NUPACK: analysis and design of nucleic acid systems. J Comput Chem 2011 Jan 15;32(1):170-173. [doi: 10.1002/jcc.21596] [Medline: 20645303]
29. Fornace ME, Huang J, Newman CT, Porubsky NJ, Pierce MB, Pierce NA. NUPACK: analysis and design of nucleic acid structures, devices, and systems. ChemRxiv preprint Preprint posted online November 10, 2022. [doi: 10.26434/chemrxiv-2022-xv98l]
30. Hofacker IL, Fontana W, Stadler PF, Bonhoeffer LS, Tacker M, Schuster P. Fast folding and comparison of RNA secondary structures. Monatsh Chem 1994 Feb;125(2):167-188. [doi: 10.1007/bf00818163]
31. Wayment-Steele HK, Kladwang W, Strom AI, Lee J, Treuille A, Becka A, Eterna Participants, et al. RNA secondary structure packages evaluated and improved by high-throughput experiments. Nat Methods 2022 Oct 03;19(10):1234-1242 [FREE Full text] [doi: 10.1038/s41592-022-01605-0] [Medline: 36192461]
32. Zammit A, Helwerda L, Olsthoorn RCL, Verbeek FJ, Gultyaev AP. A database of flavivirus RNA structures with a search algorithm for pseudoknots and triple base interactions. Bioinformatics 2021 May 17;37(7):956-962 [FREE Full text] [doi: 10.1093/bioinformatics/btaa759] [Medline: 32866223]
33. Mlera L, Melik W, Bloom ME. The role of viral persistence in flavivirus biology. Pathog Dis 2014 Jul;71(2):137-163 [FREE Full text] [doi: 10.1111/2049-632X.12178] [Medline: 24737600]
34. Creager ANH. Tobacco mosaic virus and the history of molecular biology. Annu Rev Virol 2022 Sep 29;9(1):39-55 [FREE Full text] [doi: 10.1146/annurev-virology-100520-014520] [Medline: 35704746]
35. Du Z, Holland JA, Hansen MR, Giedroc DP, Hoffman DW. Base-pairings within the RNA pseudoknot associated with the simian retrovirus-1 gag-pro frameshift site. J Mol Biol 1997 Jul 18;270(3):464-470. [doi: 10.1006/jmbi.1997.1127] [Medline: 9237911]
36. Zwieb C, Samuelsson T. SRPDB (Signal Recognition Particle Database). Nucleic Acids Res 2000 Jan 01;28(1):171-172 [FREE Full text] [doi: 10.1093/nar/28.1.171] [Medline: 10592215]
37. De Rijk P, Robbrecht E, de Hoog S, Caers A, Van de Peer Y, De Wachter R. Database on the structure of large subunit ribosomal RNA. Nucleic Acids Res 1999 Jan 01;27(1):174-178 [FREE Full text] [doi: 10.1093/nar/27.1.174] [Medline: 9847172]
38. Van de Peer Y, De Rijk P, Wuyts J, Winkelmans T, De Wachter R. The European Small Subunit Ribosomal RNA database. Nucleic Acids Res 2000 Jan 01;28(1):175-176 [FREE Full text] [doi: 10.1093/nar/28.1.175] [Medline: 10592217]
39. Peselis A, Serganov A. Structure and function of pseudoknots involved in gene expression control. Wiley Interdiscip Rev RNA 2014;5(6):803-822 [FREE Full text] [doi: 10.1002/wrna.1247] [Medline: 25044223]
40. Lucas A, Dill KA. Statistical mechanics of pseudoknot polymers. J Chem Phys 2003 Jul 22;119(4):2414-2421. [doi: 10.1063/1.1587129]

41. Chiu JKH, Chen YP. Conformational features of topologically classified RNA secondary structures. PLoS One 2012 Jul 5;7(7):e39907 [FREE Full text] [doi: 10.1371/journal.pone.0039907] [Medline: 22792195]
42. Ferré-D'Amaré AR, Zhou K, Doudna JA. Crystal structure of a hepatitis delta virus ribozyme. Nature 1998 Oct 08;395(6702):567-574. [doi: 10.1038/26912] [Medline: 9783582]
43. Tomita K, Ishitani R, Fukai S, Nureki O. Complete crystallographic analysis of the dynamics of CCA sequence addition. Nature 2006 Oct 26;443(7114):956-960. [doi: 10.1038/nature05204] [Medline: 17051158]
44. Liberati A, Altman DG, Tetzlaff J, Mulrow C, Gøtzsche PC, Ioannidis JPA, et al. The PRISMA statement for reporting systematic reviews and meta-analyses of studies that evaluate health care interventions: explanation and elaboration. J Clin Epidemiol 2009 Oct;62(10):e1-e34 [FREE Full text] [doi: 10.1016/j.jclinepi.2009.06.006] [Medline: 19631507]
45. Mathews DH. How to benchmark RNA secondary structure prediction accuracy. Methods 2019 Jun 01;162-163:60-67 [FREE Full text] [doi: 10.1016/j.ymeth.2019.04.003] [Medline: 30951834]
46. Wang Y, Liu Y, Wang S, Liu Z, Gao Y, Zhang H, et al. ATTfold: RNA secondary structure prediction with pseudoknots based on attention mechanism. Front Genet 2020;11:612086 [FREE Full text] [doi: 10.3389/fgene.2020.612086] [Medline: 33384721]
47. An J, Meng F, Yan Z. An efficient computational method for predicting drug-target interactions using weighted extreme learning machine and speed up robot features. BioData Min 2021 Jan 20;14(1):3 [FREE Full text] [doi: 10.1186/s13040-021-00242-1] [Medline: 33472664]
48. Sun Y, Liu F, Fan C, Wang Y, Song L, Fang Z, et al. Characterizing sensitivity and coverage of clinical WGS as a diagnostic test for genetic disorders. BMC Med Genomics 2021 Apr 13;14(1):102 [FREE Full text] [doi: 10.1186/s12920-021-00948-5] [Medline: 33849535]
49. Fu L, Cao Y, Wu J, Peng Q, Nie Q, Xie X. UFold: fast and accurate RNA secondary structure prediction with deep learning. Nucleic Acids Res 2022 Feb 22;50(3):e14 [FREE Full text] [doi: 10.1093/nar/gkab1074] [Medline: 34792173]
50. Sikka J, Satya K, Kumar Y, Uppal S, Shah R, Zimmermann R. Learning based methods for code runtime complexity prediction. 2020 Presented at: Advances in Information Retrieval: 42nd European Conference on IR Research (ECIR 2020); April 14–17, 2020; Lisbon, Portugal p. 313-325. [doi: 10.1007/978-3-030-45439-5_21]
51. Mathews DH. Using an RNA secondary structure partition function to determine confidence in base pairs predicted by free energy minimization. RNA 2004 Aug;10(8):1178-1190 [FREE Full text] [doi: 10.1261/rna.7650904] [Medline: 15272118]
52. Do CB, Woods DA, Batzoglou S. CONTRAfold: RNA secondary structure prediction without physics-based models. Bioinformatics 2006 Jul 15;22(14):e90-e98 [FREE Full text] [doi: 10.1093/bioinformatics/btl246] [Medline: 16873527]
53. Xia T, SantaLucia J, Burkard ME, Kierzek R, Schroeder SJ, Jiao X, et al. Thermodynamic parameters for an expanded nearest-neighbor model for formation of RNA duplexes with Watson-Crick base pairs. Biochemistry 1998 Oct 20;37(42):14719-14735. [doi: 10.1021/bi9809425] [Medline: 9778347]
54. Bellaousov S, Mathews DH. ProbKnot: fast prediction of RNA secondary structure including pseudoknots. RNA 2010 Oct;16(10):1870-1880 [FREE Full text] [doi: 10.1261/rna.2125310] [Medline: 20699301]
55. Nussinov R, Pieczenik G, Griggs JR, Kleitman DJ. Algorithms for loop matchings. SIAM J Appl Math 1978 Jul;35(1):68-82. [doi: 10.1137/0135006]
56. Zuker M, Sankoff D. RNA secondary structures and their prediction. Bull Math Biol 1984;46(4):591-621. [doi: 10.1016/s0092-8240(84)80062-2]
57. Andronescu M, Bereg V, Hoos HH, Condon A. RNA STRAND: the RNA Secondary Structure and Statistical Analysis Database. BMC Bioinform 2008 Aug 13;9(1):340 [FREE Full text] [doi: 10.1186/1471-2105-9-340] [Medline: 18700982]
58. Holst E, Thyregod P. A statistical test for the mean squared error. J Stat Comput Simul 1999 Jul;63(4):321-347. [doi: 10.1080/00949659908811960]
59. Li H, Zhu D, Zhang C, Han H, Crandall KA. Characteristics and prediction of RNA structure. Biomed Res Int 2014;2014:690340 [FREE Full text] [doi: 10.1155/2014/690340] [Medline: 25110687]
60. Andres K. Formulas. In: Laboratory Statistics (Second Edition). Amsterdam, the Netherlands: Elsevier; 2018:1-140.
61. Jabbari H, Wark I, Montemagno C. RNA secondary structure prediction with pseudoknots: contribution of algorithm versus energy model. PLoS One 2018;13(4):e0194583 [FREE Full text] [doi: 10.1371/journal.pone.0194583] [Medline: 29621250]
62. Rainio O, Teuho J, Klén R. Evaluation metrics and statistical tests for machine learning. Sci Rep 2024 Mar 13;14(1):6086 [FREE Full text] [doi: 10.1038/s41598-024-56706-x] [Medline: 38480847]
63. Chicco D, Jurman G. The advantages of the Matthews correlation coefficient (MCC) over F1 score and accuracy in binary classification evaluation. BMC Genomics 2020 Jan 02;21(1):6 [FREE Full text] [doi: 10.1186/s12864-019-6413-7] [Medline: 31898477]
64. Boughorbel S, Jarray F, El-Anbari M. Optimal classifier for imbalanced data using Matthews correlation coefficient metric. PLoS One 2017 Jun 2;12(6):e0177678 [FREE Full text] [doi: 10.1371/journal.pone.0177678] [Medline: 28574989]

Abbreviations

FN: false negative
FP: false positive

MAE: mean absolute error
MCC: Mathews' correlation coefficient
MEA: maximum expected accuracy
MFE: minimum free energy
mRNA: messenger RNA
MSE: mean squared error
PPV: positive predictive value
PRISMA: Preferred Reporting Items for Systematic Reviews and Meta-Analyses
RNA STRAND: RNA Secondary Structure and Statistical Analysis Database
ROUT: robust outlier
tRNA: transfer RNA
UTR: untranslated region
TP: true positive

Edited by T Leung, A Schwartz; submitted 27.03.24; peer-reviewed by D Saderi, V Nagesh, RSG Mahmoud, T Olatoye, F Qudus Arogundade; comments to author 09.07.24; revised version received 31.08.24; accepted 04.10.24; published 05.11.24.

Please cite as:
Medeiros V, Pearl J, Carboni M, Zafeiri S
Exploring the Accuracy of Ab Initio Prediction Methods for Viral Pseudoknotted RNA Structures: Retrospective Cohort Study
JMIRx Bio 2024;2:e58899
URL: https://bio.jmirx.org/2024/1/e58899
doi:10.2196/58899
PMID:

Original Paper

Establishment of a Novel Fetal Ovine Heart Cell Line by Spontaneous Cell Fusion: Experimental Study

Khalid Suleiman[1], BVSc, MVSc, PhD; Mutaib Aljulidan[1], BSc; Gamaleldin Hussein[1], BVSc, MVSc, PhD; Habib Alkhalaf[1], BVSc, MVSc

Veterinary Vaccine Production Centre, Ministry of Environment, Water and Agriculture, Riyadh, Saudi Arabia

Corresponding Author:
Khalid Suleiman, BVSc, MVSc, PhD
Veterinary Vaccine Production Centre
Ministry of Environment, Water and Agriculture
PO Box 15831
Riyadh, 11454
Saudi Arabia
Phone: 966 501305563
Email: kmsuleiman67@gmail.com

Related Articles:

Companion article: https://preprints.jmir.org/preprint/53721

Companion article: https://bio.jmirx.org/2024/1/e63336/

Companion article: https://bio.jmirx.org/2024/1/e62905/

Companion article: https://bio.jmirx.org/2024/1/e62911/

Abstract

Background: The culture of immortal cell lines has become an indispensable tool in the field of modern biotechnology and has been used in the production of human and viral veterinary vaccines, therapeutic recombinant proteins, interferons, and monoclonal antibodies. Several approaches are used to immortalize cells in culture, such as transduction of cells with viral oncogenes, induced expression of telomerase reverse transcriptase, and spontaneous immortalization by serial passage of primary cell lines.

Objective: This study aimed to establish an immortal cell line by serial passage of fetal ovine heart cells that could be used to produce veterinary viral vaccines.

Methods: We serially passaged primary heart cells prepared from a fetal ovine heart till passage 140. We studied the events that led to the transformation and immortalization of the cell line under light and phase contrast microscopy. DNA samples of the cell line at passages 22 (before transformation) and 47 (after transformation) were genotyped according to single nucleotide polymorphisms (SNPs) using the OvineSNP50 BeadChip (Illumina). We sequenced the *cytochrome b* gene, control region, and *tRNA-Phe* and *12S rRNA* genes of the mitochondrial genome of the cell line at passages 26 and 59 by Sanger sequencing. The susceptibility of the cell line to sheep pox, Peste des petits ruminants (PPR), lumpy skin disease (LSD), Rift Valley fever (RVF), and camel pox viruses was investigated.

Results: We established a unique immortal cell line called fetal ovine heart–Saudi Arabia (FOH-SA) by serial passage of fetal ovine heart cells. We demonstrated that the transformation or immortalization of the cell line resulted from spontaneous cellular and nuclear fusion of 2 morphologically distinct cardiocytes at passage 29. Fused cells at passage 29 gave rise to progeny cells, which grew into multicellular filaments that persisted at passages 30, 31, and 32. Trypsinization of the filamentous multicellular growth at passage 32 gave an epithelial-type immortal heart cell line. SNP genotyping revealed 65% and 96% homozygosity in SNP genotypes of the cell line at passages 22 and 47, respectively. Partial sequencing of the mitochondrial genome of the cell line revealed mutational events in the control region and the *tRNA-Phe* and *12S rRNA* genes of the mitochondrial genome of passage 59 cells. The cell line was found to be permissive to sheep pox, PPR, LSD, RVF, and camel pox viruses.

Conclusions: We established an immortal cell line by serial passage of primary fetal ovine heart cells, which was permissive to many animal viruses. It could be used in animal virus isolation, vaccine production, and biotechnology. The study reported spontaneous cell fusion of cardiocytes as a method of cell immortalization. The findings of this study might help address the mystery of how the VERO cell line evolved.

(JMIRx Bio 2024;2:e53721) doi:10.2196/53721

KEYWORDS

fetal ovine heart; cell line; serial passage; spontaneous cell fusion; SNP genotyping; mitochondrial genome sequencing

Introduction

Cell culture has become an indispensable tool in the field of modern biotechnology and has been used in the production of human and veterinary viral vaccines, therapeutic recombinant proteins, interferons (IFNs), and monoclonal antibodies [1-3]. Cell culture has also been used to study intracellular reactions through the creation of in vitro models for research and study the cytotoxicity of pharmaceuticals and bacterial toxins [4,5]. Recently, cell culture has emerged as a future candidate for the creation of cell-based meat intended for human consumption [6].

Primary cells obtained from mature or embryonic human and animal organs usually undergo a limited number of passages, after which they enter replicative senescence that is characterized by degenerative changes such as cell rounding, cell enlargement, decreased capacity to proliferate, and detachment from the monolayer [7,8]. At the molecular level, senescent cells show distinctive markers of senescence, such as increased expression of p53, p21, p16, and other cyclin-dependent kinase inhibitors like p27 and p15 [9-11].

In rare cases, some mammalian cells under continuous subculture escape replicative senescence and become spontaneously immortal, resulting in a continuous cell line [12,13]. The Madin-Darby bovine kidney (MDBK) and Madin-Darby ovine kidney (MDOK) cell lines were spontaneously immortalized by serial passage of cells from the renal tissues of *Bos taurus* and *Ovis aries*, respectively [14]. Recently, an ovine kidney cell line (FLK-N3) was also spontaneously established by serial passage of primary fetal lamb kidney cells from a fetus of a normal sheep [15]. The ubiquitous African green monkey cell line (VERO) was also spontaneously immortalized by serial passage of kidney cells of the African green monkey, and it has been deposited at the American Type Culture Collection (ATCC) at passage 113 to establish a bank for availability [16].

Over the last 35 years, numerous types of primary cell cultures have been used at the Veterinary Vaccine Production Centre in Riyadh, Saudi Arabia, to produce the sheep pox vaccine, which included ovine cells from the testicles, aortic endothelium, kidneys, and heart. Although the titers of the produced vaccine were satisfactory, the disadvantages associated with primary cultures, such as the risk of contamination, tediousness, inconsistency of cell characteristics, ethics of slaughtering animals and using organs to prepare cell cultures, and limited production capacity, created hurdles in the production wheel, especially in the face of increased demand in Saudi Arabia for this vaccine. Trials were required over the years to establish a continuous cell line to overcome the difficulties and disadvantages associated with the use of primary cultures in vaccine production. The objective of this study was to establish a continuous cell line by serial passage of the primary cells of the fetal ovine heart, which could be used in vaccine production.

Methods

Preparation of the Primary Cell Culture

In March 2013, a single pregnant ewe (*Harri* breed) was euthanized by exsanguination in accordance with the Implementing Regulations of the Law of Ethics of Research on Living Creatures of the NCBE (Article, 38) for the collection of fetal organs to prepare primary cell cultures necessary for the production of the sheep pox vaccine. The fetal heart was aseptically incised and used to prepare primary cell cultures. The heart muscle was cut to 0.5-1.0 cm, washed 3 times with 1× MEM (Minimum Essential Medium; Gibco), and digested under stirring with 0.25% trypsin 10 times for 30 minutes each time. After each cycle of digestion, the suspension was allowed to settle, and the supernatant was sieved through a sterile gauze and centrifuged at 1000 rpm for 5 minutes. The supernatant was then discarded, and the cell pellet was cultured in nonvented Roux flasks containing complete growth medium (CGM) consisting of 1× MEM (Gibco), 10% fetal bovine serum (FBS) (Gibco), 1% GlutaMAX (Gibco), and 50 µg/mL of gentamycin, and a pH of 7.2-7.4 was maintained with 5.6% sodium bicarbonate. The flasks were incubated at 37 °C in a normal incubator.

Established Cell Lines

Primary heart cell cultures obtained from extractions 1 to 8 were initially subcultured after 5 days and then after every 3 days, and this cell line was used for producing the sheep pox vaccine. A second cell line was established from heart extractions 9 and 10, which was first subcultured after 9 days and then serially passaged every 3 days. Samples of the second heart cell line at different passages were cryopreserved in Recovery Cell Culture Freezing Medium (Gibco) in liquid nitrogen at −80 °C. The second cell line derived from heart extractions 9 and 10 was named the fetal ovine heart–Saudi Arabia (FOH-SA) cell line.

Cell Morphology and Cell Line Transformation

Initially, the morphologies of the 2 cell lines were studied under an inverted bright field microscope (Olympus), and later, the morphology of the second cell line (extractions 9 and 10) was studied under an inverted phase contrast microscope (Olympus).

Cryopreserved cells at passages 20 to 27 were resuscitated and subcultured to study the transformation event under a phase contrast microscope (Olympus CKX53) with a camera (DP74, software CellSens). Cultured flasks were fixed with tape on the microscope stage in a walk-in normal incubator at 37 °C. We photographed fixed fields of passages 28, 29, 30, 32, and 33 every 3 hours for 24 hours and then every 24 hours for a total of 72 hours for each passage.

Growth Curve and Population Doubling Time

Three-day-old cultures of heart cell line passages 25 (before transformation) and 36 (after transformation) were seeded into 25-cm^2 nonvented Roux flasks at densities of 9144 cells/cm^2 and 6485 cells/cm^2, respectively. Flasks were incubated at 37 °C in a normal incubator, and cells were counted after day 1, 2, 4, 6, 8, and 10 using a Handheld Automated Cell Counter (Millipore). The growth curves of the 2 passages were constructed by plotting the log of growth against time, and the population doubling time was calculated using a standard formula [17].

Extended Incubation of the Cell Line at 37 °C

We observed that the monolayer of the cell line established after transformation (passage 33 and above) could be maintained at 37 °C for 3-4 weeks without showing signs of cell degeneration. To confirm this observation, we incubated passage 59 cultures at 37 °C for 6 months, with the growth medium being changed every 3 weeks. During storage, the monolayer was examined under an inverted microscope every week. At the end of the storage period, flasks were subcultured, and the sensitivity of the cells to sheep pox virus was determined.

DNA Preparation

DNA was extracted from a cell suspension containing approximately 5×10^5 cells/mL, using the MagNA Pure 96 DNA and Viral NA Small Volume Kit as instructed by the manufacturer (Roche). The DNA concentration was measured using the NanoDrop 2000 instrument (Thermo Scientific; 260 nm). DNA extracted from cells in passages 22, 26, 47, and 59 was aliquoted and stored at −80 °C.

Authentication and Mycoplasma Testing

A DNA sample at passage 22 was shipped to the European Collection of Authenticated Cell Cultures (ECACC), United Kingdom, for authentication of the cell line by mitochondrial DNA barcoding and detection of mycoplasma contamination. Currently, DNA barcoding is used to authenticate animal cell lines, and it uses the mitochondrial cytochrome c oxidase subunit I (*COXI*) gene as a barcode. The test is performed by polymerase chain reaction (PCR) amplification of a 617-bp segment of the mitochondrial *COXI* gene, followed by sequencing of the product and matching of the finding to a library of reference sequences [18].

Single Nucleotide Polymorphism Genotyping

We shipped aliquots of DNA samples of cell line passages 22 (before transformation) and 47 (after transformation) to the GeneSeek Laboratory of NEOGEN for single nucleotide polymorphism (SNP) genotyping using the OvineSNP50 BeadChip (Illumina). The OvineSNP50 BeadChip is a high-throughput microarray system developed by Illumina in collaboration with the International Sheep Genomics Consortium. The OvineSNP50 BeadChip map contains 54,241 ovine SNPs spanning all 26 autosomal chromosomes, the sex chromosomes, and the mitochondria. The bead chip uses the Infinium HD Assay to analyze DNA samples. Briefly, the Infinium Assay work-flow consists of an initial PCR-free amplification of DNA samples on day 1, followed by enzymatic fragmentation of the amplified samples, application of the fragmented samples to the bead chip, and incubation of the chip overnight for samples to hybridize on day 2. On day 3, hybridized samples are extended, fluorescently stained, and imaged by the iScan System (Illumina). The genotyping data of the DNA samples at passages 22 and 47 generated by the Infinium Assay of the bead chip on the iScan System were analyzed using Illumina GenomeStudio version 2.0.2 and Illumina GenCall Version 7.0.0, with a low GenCall score cutoff equal to 0.050.

Partial Sequencing of the Cell Line Mitochondrial Genome

We sequenced 2 segments of the FOH-SA cell line mitochondrial genome at passages 26 (before transformation) and 59 (after transformation) using Sanger sequencing with the 3730xl DNA Analyzer and BigDye Terminator v3.1 Cycle Sequencing Kit (Applied Biosystems). Two pairs of primers designed by Meadows et al [19] from the complete ovine mitochondrial DNA [20] were used to amplify the segments. The first pair of primers (Cytb-F: 5′-GTCATCATCATTCTCACATGGAATC-3′ and Cytb-R: 5′-CTCCTTCTCTGGTTTACAAGACCAG-3′) was used for amplifying a 1272-bp region of the ovine mitochondrial *cytochrome b* gene (AF010406 positions 14078 to 15349). The second pair of primers (mtCR-F2: 5′-AACTGCTTGACCGTACATAGTA-3′ and mtCR-R1: 5′-AGAAGGGTATAAAGCACCGCC-3′) was used to amplify a 1246-bp fragment spanning part of the control region, the complete sequence of the *tRNA-Phe* gene, and the partial sequence of the *12S rRNA* coding RNA gene (AF010406 positions 15983 to 592).

Susceptibility of the Cell Line to Viruses

The sensitivity of the FOH-SA cell line to viruses was investigated by infecting it with several animal viral vaccine strains, including sheep pox virus (Romanian strain), Peste des petits ruminants (PPR) (Nigerian 75/1), Rift Valley fever (RVF) virus (Smithburn strain), lumpy skin disease (LSD) virus (Neethling strain), and a local attenuated isolate of the camel pox virus. Passage 36 cells were inoculated at a multiplicity of infection (MOI) of 0.01, and flasks were incubated at 37 °C. The monolayers were examined daily under an inverted microscope for the development of the cytopathic effect (CPE). Flasks were harvested when the CPE reached 90%-95%, and the tissue culture infective dose 50 ($TCID_{50}$) for each virus was determined by the Karber method [21].

Production of the Sheep Pox Vaccine

We have used the FOH-SA cell line since 2013 for producing sheep pox (Romania strain) and camel pox vaccines (local attenuated isolate). Cells were propagated in Roux (125, 175, and 225 cm^2) and roller flasks (850 and 1700 cm^2), and inoculation was performed with a MOI of 0.01. The viral suspensions were harvested when about 90% CPE was reached.

Cell Line Deposition at the ATCC for Patenting

Thirty cryotubes each containing more than 10^6 cells of the fetal heart cell line (FOH-SA) at passage 51 each were shipped on dry ice to the Foreign Animal Disease Diagnostic Laboratory (FADDL), United States Department of Agriculture (USDA) in Plum Island for safety testing of foot and mouth disease, PPR, sheep pox, and camel pox viruses as a prerequisite by the USDA prior to deposition at the ATCC. After passing safety testing, 25 cryotubes were shipped from the FADDL to the ATCC for deposition for the purpose of patenting under the Budapest Treaty on the International Recognition of the Deposit of Microorganisms for the Purposes of Patent Procedure.

Data Analysis

Images of DNA samples of the heart cell line at passages 22 and 47 generated by the iScan System in the Infinium Assay were analyzed with Illumina GenomeStudio software (GSGT version 2.0.2), which was used to call and report the genotypes of the SNP loci on the OvineSNP50 BeadChip. The number of SNPs called; the frequencies of A/A, A/B, and B/B SNP genotypes; the minor allele frequency (MAF); and the 50% GenCall Score for each sample were calculated using GenCall version 7.0.0 software [22]. Data of the partial sequencing of the mitochondrial genome were controlled for quality and trimmed by DNA Baser Assembler (v5.15.0; Heracle BioSoft), and pairwise sequence alignment (PSA) of mitochondrial DNA sequences was carried out with an EMBOSS Needle [23].

BLASTn was used to compare the sequences of *Cytb*, the control region, and the *tRNA-Phe* and *12S rRNA* genes of cell line passages 26 and 59 to the *Ovis aries* mitochondrial genome sequence database.

Ethical Considerations

A single pregnant ewe was used in the study, and it was handled in compliance with the Implementing Regulations of the Law of Ethics of Research on Living Creatures of the National Committee of Bioethics (NCBE) for the use of animals in experiments (Article, 38) [24]. The authors confirm that all the methods used in the study were approved by the Ministry of Environment, Water and Agriculture (MEWA). The authors also confirm that all the procedures and the experimental protocols were in accordance with the regulations and guidelines of the MEWA.

Results

Cell Line and Morphology

The first cell line obtained from heart extractions 1 to 8 consisted of fibroblast-like cells. The monolayer became confluent in 5 days, and cells were then subcultured every 3 days. This cell line was used for producing the sheep pox vaccine till it reached replication senescence at passage 11.

The second cell line derived from heart extractions 9 and 10 (FOH-SA) initially showed scanty growth; however, it was confluent after 9 days. The cell line revealed 2 cell morphologies (epithelial-like and fibroblast-like cells), and these prevailed to passage 28. Thereafter, the cells transformed in passages 29 through 32. Cells after passage 33 exhibited a constant epithelial morphology and were smaller in size compared to the mother cells. The FOH-SA cell line was successfully subcultured every 3 days till passage 140.

Transformation of the Ovine Heart Cells

Bright Field Microscopy

During serial passage of the heart cell line, a constant cell transformation event was documented under bright field microscopy, which began at passage 27 by increased cell density of fibroblast-like cells. In passage 29, the 2 cell morphologies disappeared and were replaced by a filament monolayer. We documented that cells in passage 29 became connected with tubules detectable 3 hours after incubation, which led to cell fusion, and the nuclei of connected cells moved to a central location in the connecting tubule and became coupled to each other. Then, huge amounts of mitochondria from fused cells migrated and accumulated around the nuclei of fused cells. This was followed by the separation of fused cells into 2 progeny cells. After 72 hours of incubation in passage 29, a monolayer appeared in the form of filaments. The filamentous cell morphology was also documented in passages 30, 31, and 32. At passage 33, the cell line stopped growing in filaments, and thereafter, the morphology remained constant till the highest passage reached (passage 140).

The cell line that evolved after transformation consisted of 1 phenotype, had an increased proliferative potential, and showed a different CPE pattern to the sheep pox virus compared with the cells before transformation.

Phase Contrast Microscopy

Further details of the heart cell morphologies and the cell fusion process demonstrated by light microscopy were revealed by investigating the cell line under phase contrast microscopy. The fibroblast-like cells consistently produced long threads that were detectable 3 hours after incubation and remained demonstrable after 24 hours but became disintegrated and could not be detected after 48 hours of incubation (Figure 1). In passage 28, the 2 cell phenotypes appeared as islets of epithelial-like cells surrounded by fibroblast-like cells (Figure 2).

In passage 29, instead of growing and multiplying, the fibroblast-like cells projected their threads that reached the epithelial-like cells, resulting in the establishment of connections that developed into tubules connecting the 2 cell types. When the 2 cell phenotypes existed close to each other, they directly fused, and such fusion points could be detected 3 hours after incubation of passage 29 cells. The nuclei of the fused cells appeared coupled together with huge amounts of mitochondria accumulating around them (Figure 3A-D).

When mitochondrial recruitment was complete, the 2 nuclei became confined and compressed in part of the cytosol of the 2 fused cells and became completely delineated from the rest of the cytosol of the fused cells. This was followed by a reaction in which complete fusion of the 2 nuclei was documented, characterized by the disappearance of the nucleoli and increased brightening of the fused nuclei. We described this event as a "nuclear fusion reaction." When the nuclear fusion reaction was complete, the fused nuclei amalgamated with part of the cytosol of the fused cells to create the body of evolving progeny cells that eventually separated into 2 daughter cells (Figure 4A-F).

The first progeny cells from spontaneous cell fusion came into existence about 9 hours after incubation. It was observed that horizontally coupled nuclei gave rise to nascent cells with epithelial cell–like morphology, while fibroblast-like progeny cells evolved from the vertically coupled nuclei (Figure 5A and B).

The process of cell fusion and the appearance of new progeny cells continued in passage 29 cells, and 24 hours after incubation, approximately 95% of the cell population had completed spontaneous cell fusion and produced progeny cells (Figure 6A). Each progeny cell resulting from cell fusion in passage 29 then grew and multiplied, and 72 hours after incubation, progeny cells appeared as long multicellular filaments (Figure 6B-D). Trypsinization of the 72-hour culture at passage 29 resulted in single cells (Figure 7), and these cells when cultured (passage 30) grew into multicellular filaments. The pattern of multicellular filamentous growth was also documented in passages 31 and 32. Finally, when the passage 32 cells grown for 72 hours were trypsinized and cultured (passage 33), the progeny cells stopped growing into multicellular filaments, and thereafter, the cell morphology remained constant till the highest passage reached (passage 140) (Figure 8).

Although the final cell line had an epithelial-like morphology, there were 2 morphological types of cells (fibroblast-like cells and epithelial-like cells) similar in morphology to the parent cells, but this distinction could only be detected during the first 3-5 hours of culture incubation, after which the cell line appeared to have only 1 cell morphology.

When we examined many fields of the passage 30 culture, points of cell fusion surrounded by a matrix of second-generation growing progeny cells were detected. These fused cells represented cells that had failed to fuse in passage 29 due to physical distancing. These cells possessed exceptionally large nuclei with prominent nucleoli. The events following cell fusion proceeded as described before. Moreover, the nuclear fusion was preceded by the clear disintegration of the nuclear membranes of the fusing nuclei and obvious blending of the genetic material of the 2 nuclei. In addition, the nuclear reaction was accompanied by a very brilliant glow indicative of the high energy provided by the mitochondria to complete the fusion reaction (Figure 9A-F). A schematic summary of the spontaneous cell fusion process is shown in Figure 10.

In general, during the study of spontaneous cell fusion between the 2 heart cell phenotypes, we observed that the cell fusion process was photosensitive, and prolonged exposure of a fixed field during documentation by photography resulted in delay and sometimes abortion of the cell fusion process in the specific field under examination.

Figure 1. Morphology of the heart cell line at passage 22. (A) A 3-hour culture showing fibroblast-like cells developing long threads and epithelial-like cells appearing rounded in shape. (B) The same culture in A after 48 hours of incubation showing both cell types with fibroblast-like cells without threads. Imaging was performed using a phase contrast microscope (×200).

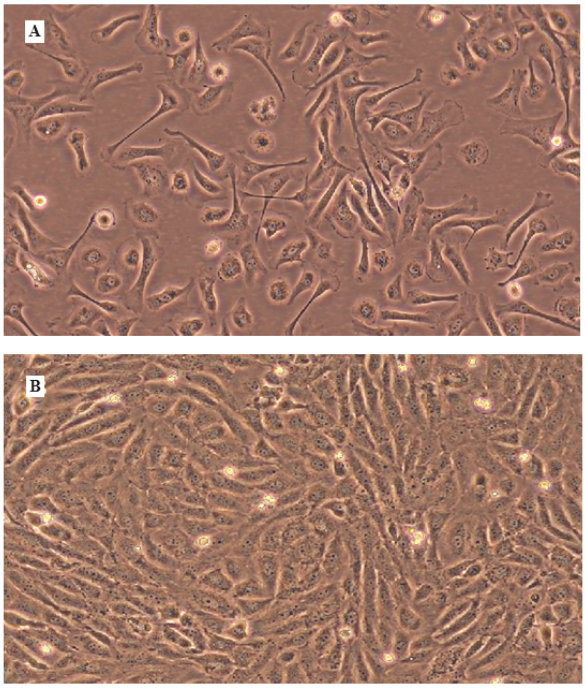

Figure 2. Morphology of the heart cell line. (A) Passage 26 culture showing fibroblast-like cells in a bundle growing diagonal to the field and epithelial-like cells above and below the bundle. (B) Passage 28 culture showing epithelial-like cells surrounded by bundles of fibroblast-like cells. Imaging was performed using a phase contrast microscope (×200).

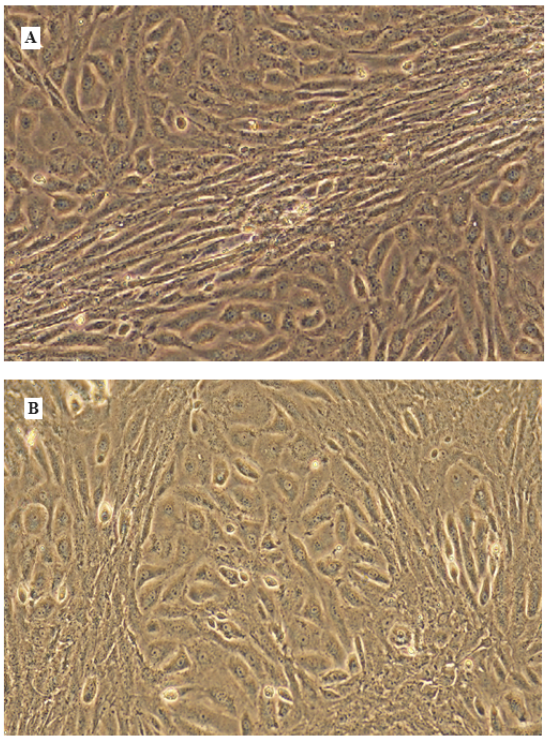

Figure 3. A 3-hour culture of the heart cell line at passage 29. (A, B) Heart cell phenotypes connected by tubules and points of spontaneous cell fusion with aggregated mitochondria around coupled nuclei of fused cells. (C, D) Two points of cell fusion after 3 and 6 hours of incubation. Imaging was performed using a phase contrast microscope (×200).

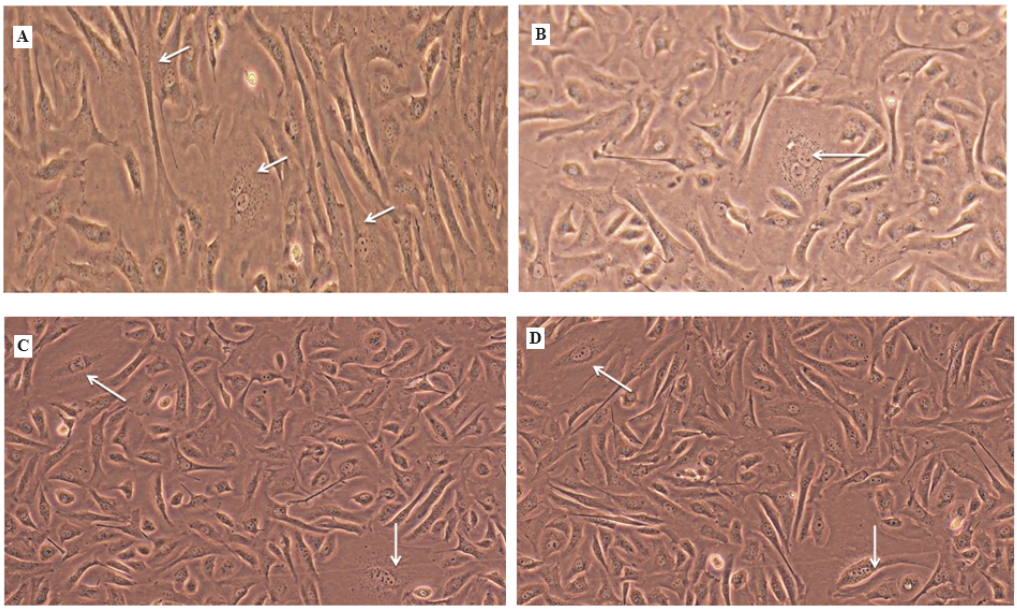

Figure 4. Stepwise progression of the spontaneous cell fusion process in passage 29 heart cells. (A) A 3-hour postincubation culture showing the point of cell fusion and coupling of nuclei. (B) A 7-hour postincubation culture showing the coupled nuclei becoming demarcated with part of the cytosol. (C) An 8-hour postincubation culture showing the nuclear fusion reaction. (D) An 11-hour postincubation culture showing the nucleoli of the 2 progeny cells. (E) An 18-hour postincubation culture showing the nuclei of the progeny cells becoming prominent. (F) A 21-hour postincubation culture showing the 2 nuclei of the progeny cells settling beside each other. Imaging was performed using a phase contrast microscope (×200).

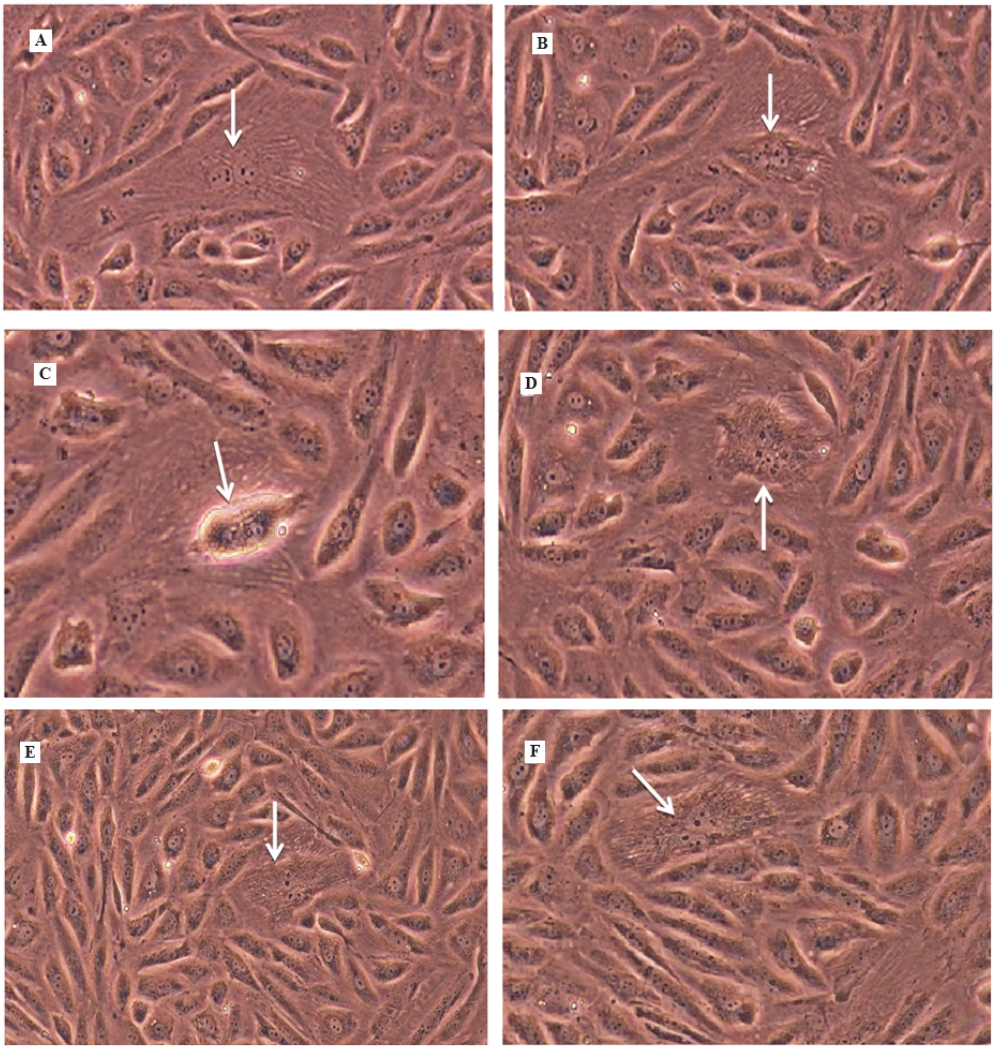

Figure 5. Heart cell line at passage 29. (A) A 6-hour postincubation culture showing 2 points of cell fusion (white arrows). (B) A 9-hour postincubation culture (the same field) showing 2 fibroblast-like cells and 2 epithelial-like cells that developed from the 2 fusion points in A (white arrows) and showing 2 new cell fusion points in the field (black arrows). Imaging was performed using a phase contrast microscope.

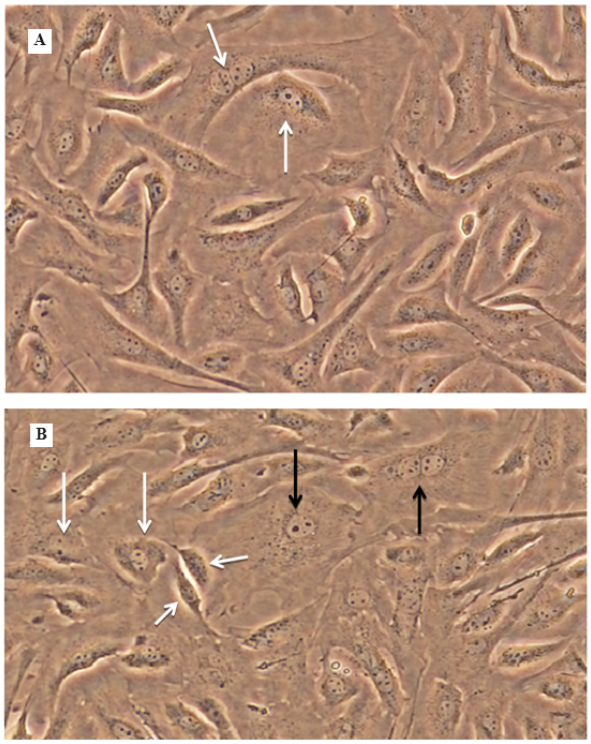

Figure 6. Growth of the progeny cells that developed after spontaneous cell fusion in passage 29 (same culture as in Figure 5). (A) Progeny cells 24 hours after incubation. (B) Growing progeny cells 36 hours after incubation. (C) Cells 48 hours after incubation. (D) The progeny cells have grown into long multicellular filaments 72 hours after incubation. Imaging was performed using a phase contrast microscope (×200).

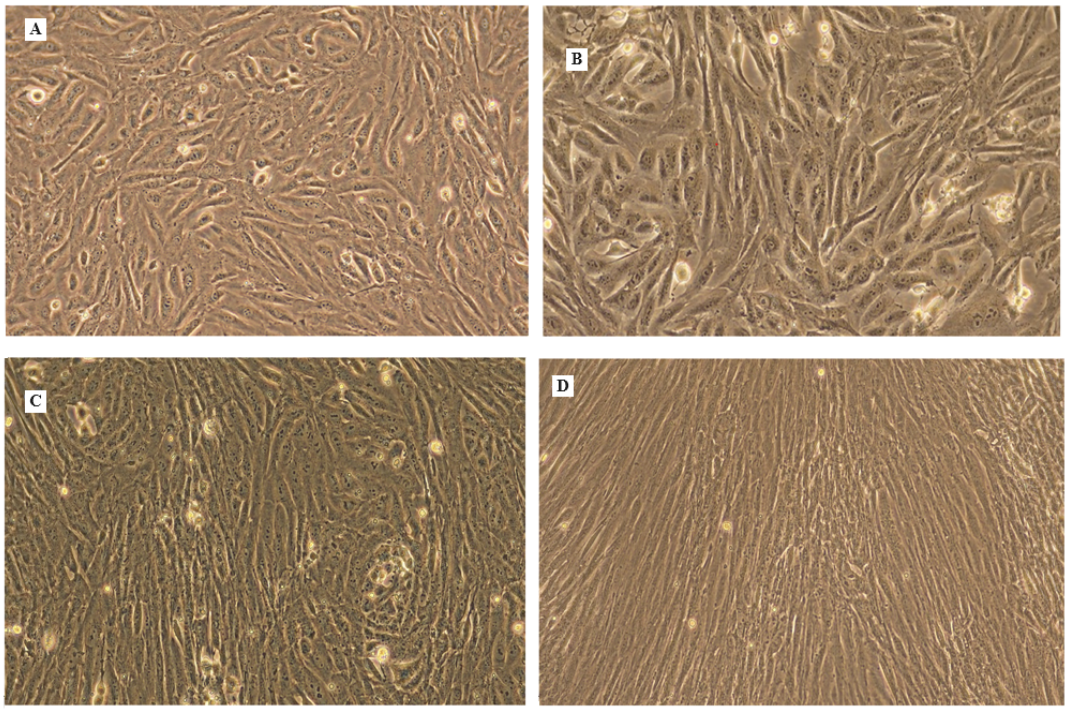

Figure 7. The heart cell line at passage 30 (3 hours after incubation). This is the first generation of cells after spontaneous cell fusion in passage 29, which resulted after trypsinization of the 72-hour multicellular filamentous growth in passage 29. Imaging was performed using a bright field microscope (×200).

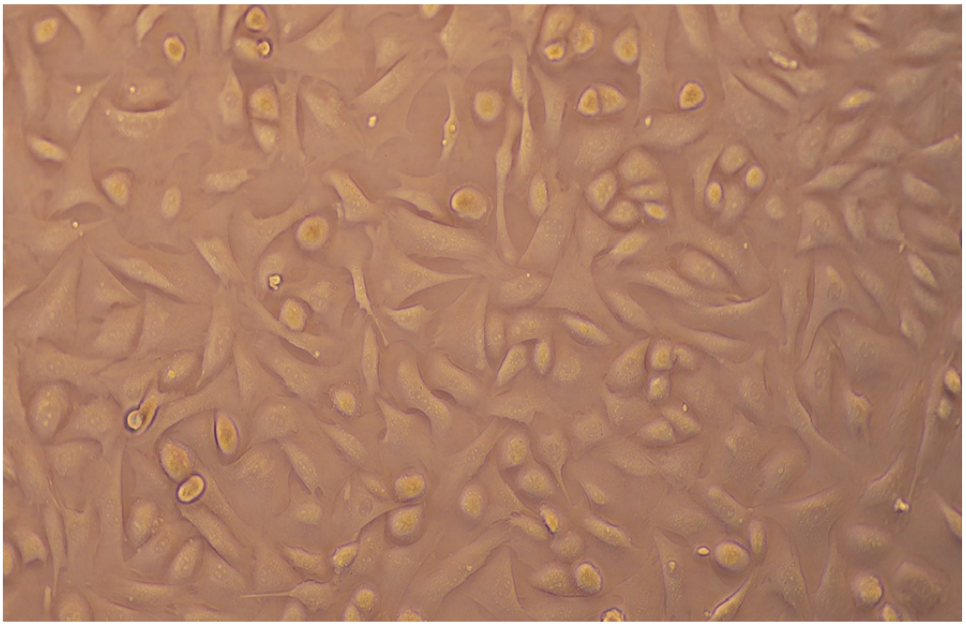

Figure 8. Morphology of the heart cell line at passage 33 after 48 hours of incubation. This morphology remained constant in the subsequent subcultures till passage 140. Imaging was performed using a phase contrast microscope (×100).

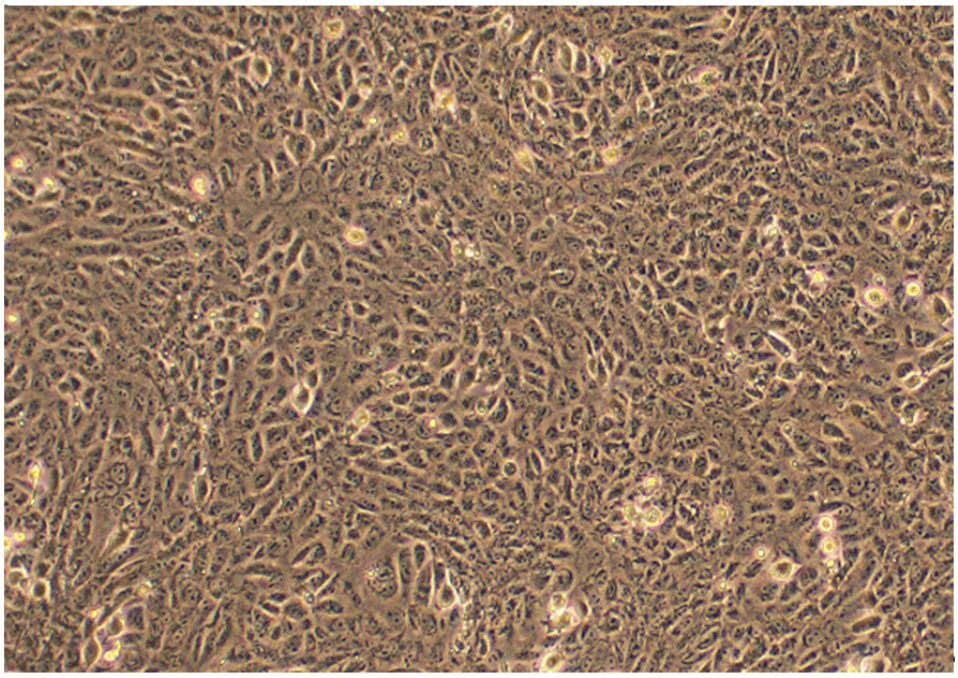

Figure 9. Point of spontaneous cell fusion in passage 30. (A) A 24-hour postincubation culture showing cell fusion and coupling of nuclei with accumulation of mitochondria around them. (B) A 46-hour postincubation culture showing disintegration of the nuclear membranes of the 2 nuclei and rearrangement of their genetic material. (C) A 48-hour postincubation culture showing complete mix up of the genetic material of the 2 cells. (D) A 49-hour postincubation culture showing a nuclear fusion reaction with massive liberation of energy (burning of the genetic material). (E) A 50-hour postincubation culture showing cooling down of the nuclear fusion reaction and reappearance of the genetic material in the developing progeny cells. (F) The 2 nuclei separate at the end of the nuclear fusion reaction (photographed from a different culture). Imaging was performed using a phase contrast microscope (×200).

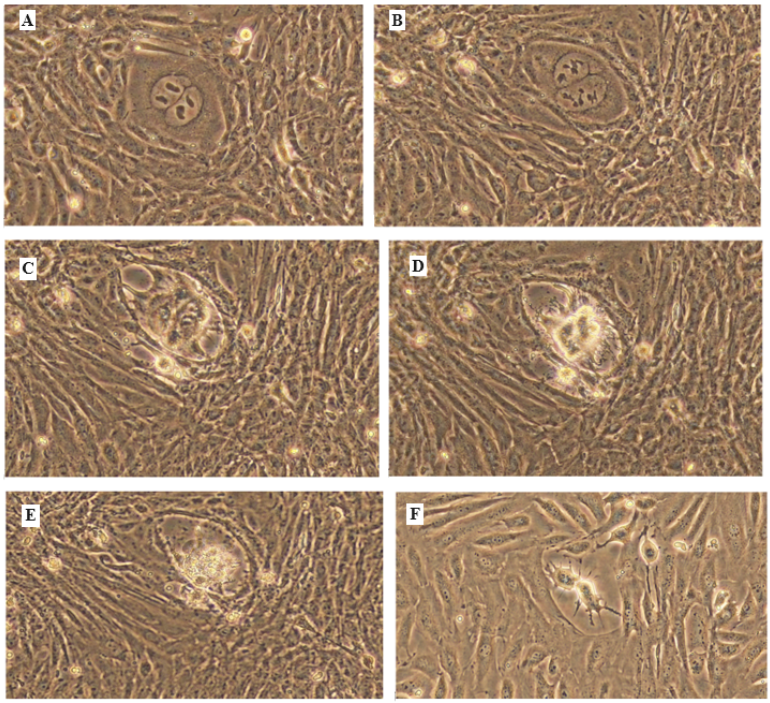

Figure 10. Schematic summary of the phenomenon of spontaneous cell fusion between fetal ovine heart cells in vitro.

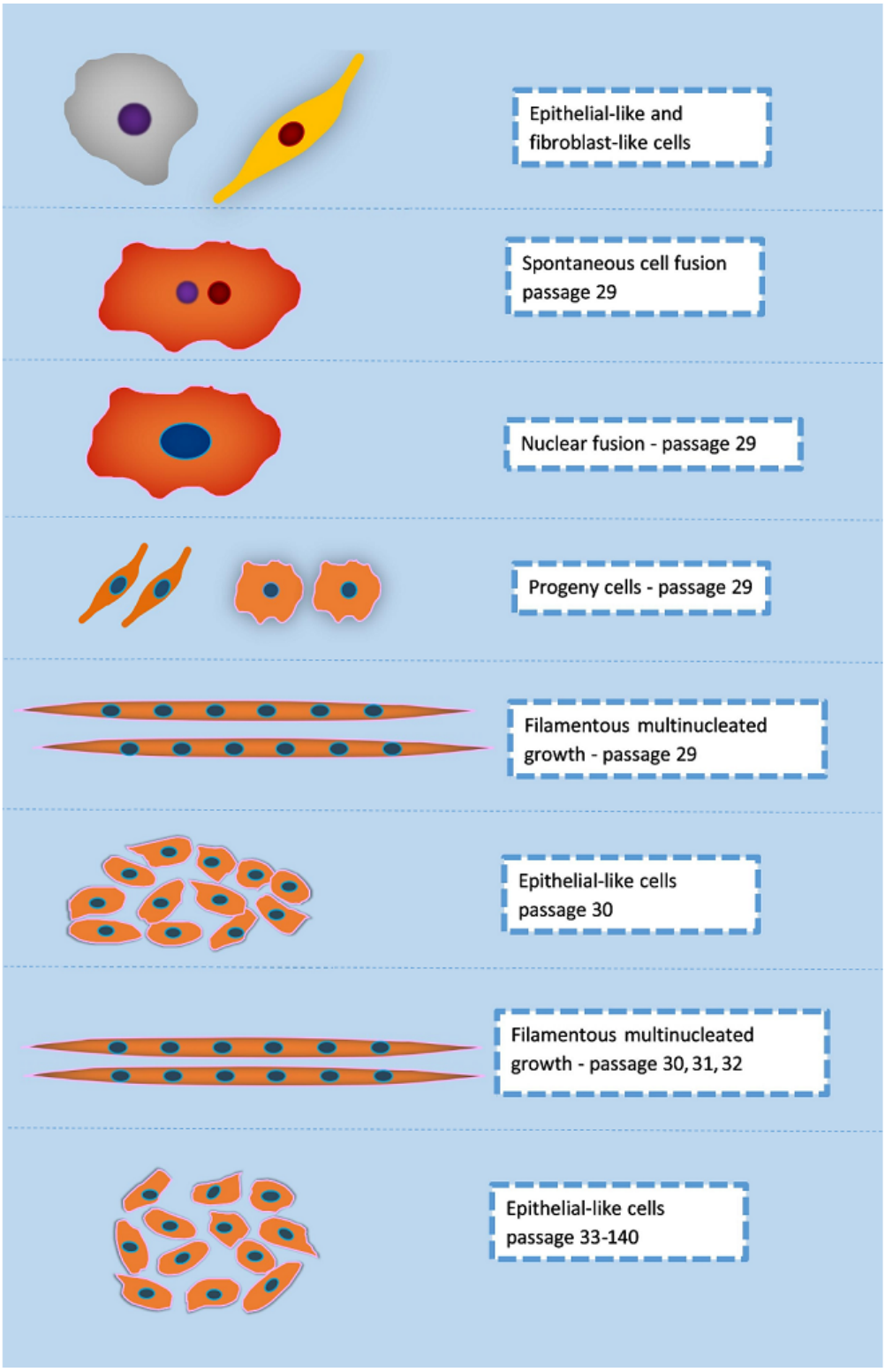

Growth Curve and Population Doubling Time

A characteristic growth curve of cells after transformation was established using a 3-day-old culture at passage 36. The curve showed no lag phase. The highest growth rate was in the first 24 hours, and the log phase continued for 10 days. Transformed cells had a population doubling time of 14.5 hours compared to 25.8 hours for cells before transformation. The growth curve of the heart cell line at passage 36 is shown in Figure S1 in Multimedia Appendix 1.

Extended Incubation at 37 °C

The FOH-SA cell line was successfully subcultured after 6 months of storage at 37 °C; however, trypsinization of the culture required 30 minutes rather than the usual 5 minutes, and the whole monolayer came out as 1 sheet, which was broken down after rigorous shaking and pipetting. During the storage

period, the cell monolayer showed no signs of degeneration; however, numerous islets could be detected in the monolayer, in which the cells again acquired the ability to multiply in multicellular filaments, similar to the filamentous cell morphology reported in the transitional passages 29-32 (Figure S2 in Multimedia Appendix 1). After storage, the cells remained sensitive to sheep pox virus, and the CPE pattern remained similar to that of the original cells.

Cell Line Authentication

Authentication of the ovine heart cell line at the ECACC revealed that the mitochondrial DNA barcode of passage 22 cells matched 99% to *Ovis aries* (top 100 results on BLAST). The result of mycoplasma PCR analysis at the ECACC documented that the heart cell line was free of mycoplasma.

SNP Genotyping

Of 54,241 SNPs on the bead chip, 50,653 (93.4%) in the DNA sample of passage 22 cells were called. The genotype frequencies of the SNP alleles in the sample were 0.65 homozygous and 0.35 heterozygous.

In the DNA sample of passage 47 cells, 45,774 SNPs were called, which represented 84.4% of the total number of SNPs on the bead chip. The genotype frequencies of the alleles in the sample were 0.96 homozygous and 0.04 heterozygous.

The total number of SNPs called, the genotypes of the SNPs, the minor allele frequencies, and the 50% GenCall Score of each of the DNA samples are shown in Table 1.

A total of 4879 SNPs called in passage 22 were not called in passage 47. The no-call SNPs were distributed throughout the chromosomes. The highest numbers were reported in chromosomes 3, 2, 1, 5, and 9. The no-call SNPs occurred singly and in succession of 2, 3, 4, and 5 SNPs. The genes spanning the 3, 4, and 5 successive no-call SNPs were identified by inserting the location of each set of SNPs in ENSEMBL (Table S1 in Multimedia Appendix 1).

The genetic conversion was also documented in the mitochondrial SNPs *mt.7729*, *CytB_1505.1*, and *CytB_1745.1*. The alleles of these SNPs were 100% BB homozygous in passage 22 cells (before transformation) and became 67% AA and 33% BB homozygous in passage 47 cells (after transformation).

The single SNP in the Y chromosome (*oY1.1*; index 37199 in the SNP map) was not called in the cell line either before transformation or after transformation. Accordingly, we concluded that the cell line was established from a female ovine fetus as the sex of the fetus was not checked during the preparation of the primary cultures.

Table 1. OvineSNP50 BeadChip genotyping of the fetal ovine heart cell line.

DNA sample	SNPs[a] called[b], n	A/A frequency[c]	A/B frequency[d]	B/B frequency[e]	MAF[f]	50% GenCall Score
Passage 22[g]	50,653	0.30	0.35	0.35	0.48	0.903
Passage 47[h]	45,774	0.95	0.04	0.01	0.03	0.875

[a]SNP: single nucleotide polymorphism.

[b]SNPs in each sample with a GenCall Score above the no-call threshold.

[c]The number of A/A SNP genotype calls divided by the total number of calls.

[d]The number of A/B SNP genotype calls divided by the total number of calls.

[e]The number of B/B SNP genotype calls divided by the total number of calls.

[f]MAF: minor allele frequency.

[g]Cell line before cell fusion.

[h]Cell line after cell fusion.

Sequencing of the Cytochrome b Gene

Sequencing of the *Cytb* gene of the heart cell line at passages 26 and 59 produced sequences of 1078 bp and 1061 bp, respectively. After quality control and trimming, the length of the *Cytb* gene was 834 bp for passage 26 cells and 858 bp for passage 59 cells. BLASTn analysis of *Cytb* of passage 26 cells revealed 99.28% identity to 100 BLAST hits of the *Ovis aries* complete mitogenome. Pairwise alignment of the partial sequences of the *Cytb* gene of the 2 cell passages showed 93.8% similarity with 6.2% gaps (Figure S3 in Multimedia Appendix 1). BLASTn analysis of the partial sequence of the *Cytb* gene of passage 59 cells showed 99.88% identity to the top 100 BLAST hits of the *Ovis aries* mitogenome, and this sequence was deposited in the GenBank database (GenBank accession: ON811684).

Sequencing of the Control Region and the tRNA-Phe and 12S rRNA Genes

The partial sequencing of the control region and the *tRNA-Phe* and *12S rRNA* genes of the heart cell line mitogenome resulted in a sequence of 1088 bp for passage 26 cells and 1083 bp for passage 59 cells. However, after trimming and quality control, the size of the sequences was 828 bp for passage 26 cells and only 305 bp for passage 59 cells. The 100 top BLAST hits for the passage 26 partial sequence revealed 98.67%-99.88% identity to the *Ovis aries* control region and the *tRNA-Phe* and *12S rRNA* mitogenome genes. PSA of the 828 bp sequence of passage 26 cells and 305 bp sequence of passage 59 cells revealed only 25.6% similarity with 67.9% gaps (Figure S4 in Multimedia Appendix 1).

Susceptibility to Viruses

The FOH-SA cell line was found to be highly susceptible and permissive to all tested viruses. The CPE of the RVF virus was detected within 48 hours in the form of cell elongation, syncytia formation, and monolayer disruption. The RVF virus suspension was harvested after 4 days, and the $TCID_{50}$ was $10^{7.1}$/mL. The CPE of the PPR virus was detected within 72 hours in the form of cell rounding, syncytia formation, and adherence of the monolayer to the surface. The virus was harvested after 5 days, and the $TCID_{50}$ of the harvest reached $10^{7.3}$/mL. The LSD virus showed a CPE similar to that of the PPR virus; however, it dismantled the monolayer sheet. The virus was harvested after 5 days, and the $TCID_{50}$ of the harvest was $10^{7.5}$/mL. The CPE of the camel pox virus was detected after 48 hours in the form of cell rounding, large syncytia, and monolayer detachment. After 3 days, the $TCID_{50}$ of the harvest was $10^{7.5}$/mL. The CPE of the sheep pox virus was detected after 48 hours. The virus was harvested after 5 days, and the $TCID_{50}$ of the harvest was $10^{7.5}$/mL. The CPEs of the sheep pox, camel pox, and PPR viruses are shown in Figure S5 in Multimedia Appendix 1.

Production of the Sheep Pox Vaccine

The cell line was used since its establishment in 2013 mainly for producing sheep pox and camel pox vaccines. Over the years, production was carried out in cell line passages ranging from 38 to 115, and satisfactory viral suspensions with $TCID_{50}$ values of $10^{7.1}$/mL to $10^{7.5}$/mL were obtained for both vaccines.

ATCC Cell Line Deposition

The FOH-SA cell line passed all the safety tests performed by the FADDL, including freedom from FMD, PPR, and sheep and camel pox viruses. Thereafter, it was shipped to the ATCC where it was processed in accordance with the Budapest Treaty, and the relevant international Budapest Treaty forms were issued. The cell line was deposited under the patent accession number PTA-125751.

Discussion

Establishment of a Fetal Ovine Heart Cell Line

This study describes the establishment of a continuous cell line by serial passage of fetal ovine heart cells. The cell line consistently transforms at passage 29 because of spontaneous cell fusion between 2 distinct heart cell types. The progeny cells resulting from the fusion process grow in the form of multicellular filaments in passages 29, 30, 31, and 32, after which the cell line shows an epithelial morphology.

Comparative SNP genotyping of the cell line before and after cell fusion revealed large-scale genetic conversion resulting in high homozygosity in the progeny cells. Partial sequencing of the mitochondrial genome of the cell line showed mutational events in the control region and the *tRNA-Phe* and *12S rRNA* genes of the mitochondrial genome in the progeny cells. The cell line was permissive to sheep pox, PPR, LSD, RVF, and camel pox viruses.

Spontaneous Cell Fusion

Spontaneous immortalization of mammalian cells is a rare event where spontaneous upregulation of the telomerase reverse transcriptase enzyme or low expression of p15, p16, or Rb allows cells to escape replication senescence and become immortal [25-27].

Although numerous animal cell lines have been spontaneously immortalized by serial passage, the exact mechanisms causing cell immortalization remain unexplained. For instance, the mechanisms that led to the establishment of the VERO cell line, which was derived from the serial passage of normal kidney cells, remain unexplained, although the cell line was established decades ago.

The transformation event documented in this study passed undetected during the initial serial passaging to establish an immortal heart cell line; however, the sufficient amount of cells stored before transformation allowed us to repeatedly derive the cells through passage 29, which enabled us to precisely observe and explain the events that led to cell transformation. If this approach was not followed, the transformation event reported in this study would have remained unexplained. Ogle et al [28] stated that the origin of a cell as the product of a fusion event can be difficult or impossible to deduce.

In this study, we established an immortal fetal ovine heart cell line through serial passage and we described the unprecedented method of cell immortalization in which 2 heart cell phenotypes spontaneously fused and then segregated into 2 progeny cells that had a different morphology and a smaller size compared with the parent cells, had an increased proliferation potential, exhibited a transitional phase of filamentous growth, showed immortality, and were susceptible to numerous animal viruses.

Fusion of cells of the same type or different types and fusion of their nuclei were found to occur in vivo, yielding hybrid cells known as heterokaryons (multinuclear) or synkaryons (mononuclear). In synkaryons, resorting and recombination of chromosomal DNA could occur, and the mononuclear daughter cells resulting from the hybrid cells have been found to express all the genetic material of the parental cells [29,30].

In this study, spontaneous cell fusion between the fibroblast-like and epithelial-like heart cell phenotypes was repeatedly documented at passage 29 (cells were subcultured every 3-4 days) and was not detected at any earlier passage. This could mean that these cell types became mature and competent for fusion at this specific age (29 passages), possibly by expressing the necessary cell fusion proteins and having mature mitochondria capable of providing the energy necessary for the nuclear fusion reaction. Recent work has identified fusion proteins (fusogens) as indispensable molecules in the fusion process between mammalian myoblast cells [29,31]. Similar fusogens might have mediated the fusion of the heart cells documented in this study.

In this study, we observed 2 types of spontaneous cell fusions. Adjacent fusion occurred when the 2 phenotypes existed in the neighborhood and was detected within 3-5 hours after incubation of passage 29 cells. The second type of cell fusion occurred when the cell types were distantly placed from each other. In

this type, the fibroblast-like cells protruded projections reaching the epithelial-like cells, and eventually, a tubule was established connecting the 2 cells. Shortly after cell fusion, coupling of the nuclei of the fused cells occurred, which triggered the migration of the mitochondrial population of the 2 cells to the site of nuclear coupling. The force driving the 2 nuclei to a coupling site at the tubular junction between the 2 cells could not be explained in this study. The mitochondrial migration was found to be crucial for initiating the nuclear fusion process, and it was only triggered when all the mitochondria of the fusing cells accumulated at the site of the coupled nuclei.

Cell fusion in vitro was induced by treating human lymphocytes with polyethylene glycol [32]. A second approach for cell fusion in vitro, known as electrofusion, was experimented by applying electric impulses to cells suspended in an appropriate electrofusion buffer [33,34]. Both methods resulted in hybrid cells with 2 or 3 nuclei; however, no nuclear fusion between the nuclei of the hybrid cells was demonstrated in these studies. Hence, the spontaneous cell fusion and nuclear fusion described in this study are novel unprecedented phenomena in cell biology.

In this study, the spontaneous cell fusion between the 2 heart cell phenotypes at passage 29 could be viewed as a type of cell mating (sexual reproduction), which was followed by a form of cell multiplication that could be considered asexual reproduction, in which each progeny cell grew into multiple cells that remained connected to each other and formed filaments. This pattern of cell multiplication was documented in the transitional passages 29, 30, 31, and 32 and could be described as resembling septate hyphae resulting from asexual reproduction in fungi. An early report described in vitro mating between 2 clonal lines of mouse fibroblasts that resulted in hybrid cells with evidence of segregation after mating; however, research in cell mating was discontinued and no other reports are available [35].

SNP Genotyping

The OvineSNP50 BeadChip has been used in many applications, including genome-wide selection, comparative genetic studies, and breed characterization for evaluating biodiversity [36-38]. It was validated by Illumina for genotyping of more than 3000 samples from diverse *Ovis aries* domestic and wild breeds [19]. In this study, we used the bead chip to compare the genotype of the cell line before and after cell fusion. SNP genotyping of DNA of the heart cell line at passage 22 revealed 50,653 polymorphic loci representing 93.4% of the SNPs on the bead chip, which was higher than the highest number of polymorphic loci reported in all domestic ovine breeds (*Rasa aragonesa* breed of sheep exhibited the highest polymorphic loci of 48,676) during the validation of the bead chip by Illumina. The *Harri* sheep breed, the sheep breed from which the heart cell line was established, was not included in the buildup of the bead chip.

SNP genotyping of passage 47 cells showed 0.95 A/A and 0.01 B/B SNP genotype frequencies compared to 0.30 A/A and 0.35 B/B genotype frequencies in the DNA samples at passage 22, while the frequencies for heterozygosity were 0.35 and 0.04 for passages 22 and 47, respectively. These results indicate that the spontaneous cell fusion resulted in large-scale genetic conversion in progeny cells involving about 65% of the alleles, resulting in 96% homozygosity. Osada et al [39] identified the single nucleotide variants of the African green monkey (*Chlorocebus sabaeus*) cell line (VERO) nuclear genome and reported 87.7% homozygosity. They attributed the high homozygosity to the evolutionary divergence between the genus *Macaca* and *Chlorocebus* from approximately 8-12 million years ago.

The MAF of the heart cell line before cell fusion was 0.48 and after cell fusion was 0.03 The MAF of 0.03 for the FOH-SA cell line after cell fusion indicated that the FOH-SA cell line was a rare variant possessing high levels of rare alleles, which is consistent with the fact that spontaneous cell fusion in animal cells is a rare event.

Partial Mitochondrial Genome Sequencing

The ovine mitochondrial *Cytb* gene and a fragment of the ovine mitogenome containing the control region have been used to haplotype sheep breeds and to study genetic diversity among and between sheep breeds [20,21,40]. In this study, we partially sequenced the *Cytb* gene and the mitochondrial fragment containing the control region and the *tRNA-Phe* and *12S rRNA* genes of the heart cell line to explore whether the spontaneous cell fusion led to mutational events in the mitogenome of the progeny cells. PSA of the partial sequences of the cell line at passages 26 and 59 revealed 54 gaps caused by an insertion of 35 bp in the 5′ end and a deletion of 15 bp in the 3′ end of the partial sequence of the *Cytb* gene in passage 59 cells. These insertion and deletion events in the *Cytb* gene of passage 59 cells might have caused changes in the genotype of *Cytb* gene SNPs as they were documented by the ovine bead chip genotyping of passage 47 cells of the FOH-SA cell line.

There was a similarity of 25.6% in the mitogenome segments spanning the control region and the *tRNA-Phe* and *12S rRNA* genes of the heart cell line at passages 26 and 59. The low similarity was caused by 583-bp gaps resulting from major deletion events in the segment of the mitogenome of passage 59 cells. The results of partial sequencing of the mitogenome of the heart cell line substantiated the results of SNP genotyping for the occurrence of large-scale genetic conversion in the progeny cells following spontaneous cell fusion. Osada et al [39] sequenced the complete mitogenome of the VERO cell line, and it was phylogenetically so diverse from *Chlorocebus sabaeus* (the species from which it was established) that the VERO cell line could be clustered as a separate species.

We believe that the events associated with FOH-SA cell line development and VERO cell line establishment were analogous, that is, both cell lines evolved by spontaneous cell fusion. This reality was ascertained by several findings. First, a 3-hour culture of FOH-SA cells and that of VERO cells looked morphologically identical, with both showing an endothelial-like morphology (Figure S6 in Multimedia Appendix 1). Second, the endothelial-like morphology of the 3-hour culture of both cell lines was because both cell lines consisted of 2 cell types. One type descended from fibroblast-like cells usually showing rudimentary projections a few hours after incubation that soon disappeared with growth, and the other type descended from epithelial-like cells with morphological features indicative of the ancestors of the 2 cell lines. A comparison of the 3-hour

culture of VERO cells with heart cells at passage 22 (before transformation) strikingly demonstrated this fact (Figure S7 in Multimedia Appendix 1). Third, large-scale genetic conversion in both cell lines resulted in high levels of homozygosity in both cell lines, which could only be ascribed to spontaneous cell fusion. Fourth, major mutational events were detected in the mitogenomes of both cell lines. Future comparative studies of the mitogenomes of the FOH-SA and VERO cell lines will confirm the existence in the animal body of cell phenotypes that could spontaneously fuse and give rise to progeny cells that are genetically highly divergent from the parent cells.

Susceptibility of the Cell Line to Viruses

The cell line was found to be highly permissive to the RVF, PPR, LSD, camel pox, and sheep pox viruses; hence, it could be used for the isolation of these viruses as well as the development and production of vaccines. Cell immortalization was found to be associated with silencing or deletion of the IFN gene cluster [12], and the sensitivity of VERO cells to numerous viruses was also ascribed to the deletion of the IFN gene cluster [39]. Similarly, the sensitivity of FOH-SA cells to these viruses might be attributed to the deletion of the IFN gene cluster. A future genome landscape assessment of the cell line is expected to disclose this fact. SARS-CoV-2 and SAR-CoV-1 use angiotensin-converting enzyme 2 (ACE2) as a receptor for cell entry, and the ACE2 receptor is abundantly expressed on cardiocytes, cardiofibroblasts, and coronary endothelial cells [41,42]. Hence, the FOH-SA cell line derived from heart tissue would be a good candidate for the propagation of SARS-CoV-2 and SARS-CoV-1 viruses.

Extended Incubation at 37 °C

A unique property of the FOH-SA cell line was the possibility of storing cultured cells at 37 °C for months provided that the growth medium was changed every 3 weeks. This property could be exploited as a short storage mechanism to avoid the cumbersome and risky cryopreservation of cells when they are needed within months, and this property could be useful in the propagation of slow-growing viruses. Shipment of this cell line could be done using cultures, which is more practical and economical than shipping on dry ice or liquid nitrogen. The capacity of FOH-SA cells stored at 37 °C to revert to multicellular filamentous growth similar to the filamentous growth documented in passages 29 to 32 is an important differentiating characteristic of this cell line.

Future studies on the FOH-SA cell line should investigate the molecular mechanisms of spontaneous cell fusion, the genome landscape of the cell line, the mitochondrial genome sequences of the cell line, the genes and pathways involved in immortalization, and the safety of the cell line in vaccine production, especially at high passages.

Acknowledgments

We would like to acknowledge Mohamed M Alfuhaid, who is the Director General of the General Administration of Laboratories, for his continuous support, encouragement, and enthusiasm. We greatly appreciate the close follow-up and the unlimited support of Dr Khaled S Abuhimed, Director of the Veterinary Vaccine Production and Evaluation Centre. We also greatly appreciate the help of Dr Hussain Al-Ghadeer and Dr Elgazali Guma, Veterinary Diagnostic Laboratory, Ministry of Environment, Water and Agriculture, Riyadh, in preparing DNA samples.

Data Availability

The partial sequence of the *cytochrome b* gene of the fetal ovine heart–Saudi Arabia (FOH-SA) cell line at passage 59 was submitted to NCBI GenBank and is available under accession number ON811684. The cell line at passage 51 was deposited at the American Type Culture Collection under the Budapest Treaty under patent accession number 125751 for availability.

Authors' Contributions

KS designed the study, performed the investigation, and analyzed the results. KS prepared the manuscript and revised it. MA participated in the preparation of the primary cell culture, passaging, and cryopreservation. GH collaborated in preparing the primary cell culture and testing the sensitivity of the cell line to viruses. HA participated in designing the study and supervised it.

Conflicts of Interest

None declared.

Multimedia Appendix 1
Supplementary findings.
[PDF File (Adobe PDF File), 1109 KB - xbio_v2i1e53721_app1.pdf]

References

1. Eibl R, Eibl D, Pörtner R, Catapano G, Czermak P. Cell and Tissue Reaction Engineering. Berlin, Heidelberg: Springer; 2009.

2. Swain P. Basic techniques and limitations in establishing cell culture: a mini review. Adv Anim Vet Sci 2014;2(4S):1-10. [doi: 10.14737/journal.aavs/2014/2.4s.1.10]
3. Verma A, Verma M, Singh A. Animal tissue culture principles and applications. In: Animal Biotechnology. Cambridge, MA: Academic Press; 2020:269-293.
4. Assanga I. Cell growth curves for different cell lines and their relationship with biological activities. Int J Biotechnol Mol Biol Res 2013 Aug 31;4(4):60-70. [doi: 10.5897/ijbmbr2013.0154]
5. Suleiman K, Boehnel H, Babiker S, Zaki A. Cytotoxic activity in fermenter culture supernatants of Corynebacterium seudotuberculosis. J Anim Vet Ad 2006;5:939-942 [FREE Full text]
6. Soice E, Johnston J. Immortalizing cells for human consumption. Int J Mol Sci 2021 Oct 28;22(21):11660 [FREE Full text] [doi: 10.3390/ijms222111660] [Medline: 34769088]
7. Hayflick L, Moorhead P. The serial cultivation of human diploid cell strains. Exp Cell Res 1961;25(3):585-621. [doi: 10.1016/0014-4827(61)90192-6]
8. Hayflick L. The cell biology of aging. J Invest Dermatol 1979 Jul;73(1):8-14 [FREE Full text] [doi: 10.1111/1523-1747.ep12532752] [Medline: 448179]
9. Kuilman T, Michaloglou C, Mooi WJ, Peeper DS. The essence of senescence. Genes Dev 2010 Nov 15;24(22):2463-2479 [FREE Full text] [doi: 10.1101/gad.1971610] [Medline: 21078816]
10. Alessio N, Squillaro T, Cipollaro M, Bagella L, Giordano A, Galderisi U. The BRG1 ATPase of chromatin remodeling complexes is involved in modulation of mesenchymal stem cell senescence through RB-P53 pathways. Oncogene 2010 Oct 07;29(40):5452-5463. [doi: 10.1038/onc.2010.285] [Medline: 20697355]
11. Kumari R, Jat P. Mechanisms of cellular senescence: cell cycle arrest and senescence associated secretory phenotype. Front Cell Dev Biol 2021 Mar 29;9:645593 [FREE Full text] [doi: 10.3389/fcell.2021.645593] [Medline: 33855023]
12. Fridman AL, Tainsky MA. Critical pathways in cellular senescence and immortalization revealed by gene expression profiling. Oncogene 2008 Oct 09;27(46):5975-5987 [FREE Full text] [doi: 10.1038/onc.2008.213] [Medline: 18711403]
13. Shay JW, Wright WE. Telomeres and telomerase: three decades of progress. Nat Rev Genet 2019 May 13;20(5):299-309. [doi: 10.1038/s41576-019-0099-1] [Medline: 30760854]
14. Madin SH, Darby NB. Established kidney cell lines of normal adult bovine and ovine origin. Experimental Biology and Medicine 1958 Jul 01;98(3):574-576. [doi: 10.3181/00379727-98-24111]
15. Matsuura K, Inoshima Y, Kameyama K, Murakami K. Establishment of a novel ovine kidney cell line for isolation and propagation of viruses infecting domestic cloven-hoofed animal species. In Vitro Cell Dev Biol Anim 2011 Aug 22;47(7):459-463 [FREE Full text] [doi: 10.1007/s11626-011-9434-3] [Medline: 21695582]
16. Sheets R. History and characterization of the Vero cell line. A report prepared by CDR Rebecca Sheets, Ph.D., USPHS. CBER/OVRR/DVRPA/VVB for the Vaccines and Related Biological Products Advisory Committee Meeting to be held on May 12, 2000. ResearchGate. URL: https://www.researchgate.net/profile/Awatif_Issa/post/Does_Vero_cell_possess_Fc_receptor/attachment/59d635e479197b80779935f0/AS:386030961217536%401469048361106/download/Verocell.pdf [accessed 2024-06-27]
17. Davis JM. Basic Cell Culture: A Practical Approach. Oxford, England: Oxford University Press; 1994.
18. Hebert PDN, Cywinska A, Ball SL, deWaard JR. Biological identifications through DNA barcodes. Proc Biol Sci 2003 Feb 07;270(1512):313-321 [FREE Full text] [doi: 10.1098/rspb.2002.2218] [Medline: 12614582]
19. Meadows J, Li K, Kantanen J, Tapio M, Sipos W, Pardeshi V, et al. Mitochondrial sequence reveals high levels of gene flow between breeds of domestic sheep from Asia and Europe. J Hered 2005;96(5):494-501. [doi: 10.1093/jhered/esi100] [Medline: 16135704]
20. Hiendleder S, Lewalski H, Wassmuth R, Janke A. The complete mitochondrial DNA sequence of the domestic sheep (Ovis aries) and comparison with the other major ovine haplotype. J Mol Evol 1998 Oct;47(4):441-448. [doi: 10.1007/pl00006401] [Medline: 9767689]
21. Kärber G. Beitrag zur kollektiven Behandlung pharmakologischer Reihenversuche. Archiv f experiment Pathol u Pharmakol 1931 Jul;162(4):480-483. [doi: 10.1007/bf01863914]
22. OvineSNP50 Genotyping BeadChip. Illumina. URL: https://www.illumina.com/documents/products/datasheets/datasheet_ovinesnp50.pdf [accessed 2024-06-27]
23. Madeira F, Pearce M, Tivey A, Basutkar P, Lee J, Edbali O, et al. Search and sequence analysis tools services from EMBL-EBI in 2022. Nucleic Acids Res 2022 Jul 05;50(W1):W276-W279 [FREE Full text] [doi: 10.1093/nar/gkac240] [Medline: 35412617]
24. National Committee of BioEthics Implementing Regulations of the Law of Ethics of Research on Living Creatures. National Committee of BioEthics. 2022. URL: https://tinyurl.com/bye2xwef [accessed 2024-06-27]
25. Shay J, Wright W. Senescence and immortalization: role of telomeres and telomerase. Carcinogenesis 2005 May;26(5):867-874. [doi: 10.1093/carcin/bgh296] [Medline: 15471900]
26. Lundberg AS, Hahn WC, Gupta P, Weinberg RA. Genes involved in senescence and immortalization. Curr Opin Cell Biol 2000 Dec;12(6):705-709. [doi: 10.1016/s0955-0674(00)00155-1] [Medline: 11063935]

27. Smeets SJ, van der Plas M, Schaaij-Visser T, van Veen EA, van Meerloo J, Braakhuis BJ, et al. Immortalization of oral keratinocytes by functional inactivation of the p53 and pRb pathways. Int J Cancer 2011 Apr 01;128(7):1596-1605. [doi: 10.1002/ijc.25474] [Medline: 20499310]
28. Ogle BM, Cascalho M, Platt JL. Biological implications of cell fusion. Nat Rev Mol Cell Biol 2005 Jul 15;6(7):567-575. [doi: 10.1038/nrm1678] [Medline: 15957005]
29. Zhang H, Ma H, Yang X, Fan L, Tian S, Niu R, et al. Cell fusion-related proteins and signaling pathways, and their roles in the development and progression of cancer. Front Cell Dev Biol 2021 Feb 1;9:809668 [FREE Full text] [doi: 10.3389/fcell.2021.809668] [Medline: 35178400]
30. Alvarez-Dolado M. Cell fusion: biological perspectives and potential for regenerative medicine. Front Biosci 2007 Jan 01;12(1):1-12. [doi: 10.2741/2044] [Medline: 17127279]
31. Bi P, Ramirez-Martinez A, Li H, Cannavino J, McAnally JR, Shelton JM, et al. Control of muscle formation by the fusogenic micropeptide myomixer. Science 2017 Apr 21;356(6335):323-327 [FREE Full text] [doi: 10.1126/science.aam9361] [Medline: 28386024]
32. Pedrazzoli F, Chrysantzas I, Dezzani L, Rosti V, Vincitorio M, Sitar G. Cell fusion in tumor progression: the isolation of cell fusion products by physical methods. Cancer Cell Int 2011 Sep 20;11(1):32 [FREE Full text] [doi: 10.1186/1475-2867-11-32] [Medline: 21933375]
33. Kandušer M, Ušaj M. Cell electrofusion: past and future perspectives for antibody production and cancer cell vaccines. Expert Opin Drug Deliv 2014 Dec 10;11(12):1885-1898. [doi: 10.1517/17425247.2014.938632] [Medline: 25010248]
34. Ramos C, Teissié J. Electrofusion: a biophysical modification of cell membrane and a mechanism in exocytosis. Biochimie 2000 May;82(5):511-518. [doi: 10.1016/s0300-9084(00)00200-5] [Medline: 10865136]
35. Littlefield JW. election of hybrids from mating of fibroblasts in vitro and their presumed recombinants. Science 1964 Aug 14;145(3633):709-710. [doi: 10.1126/science.145.3633.709] [Medline: 14168277]
36. Sandenbergh L, Cloete S, Roodt-Wilding R, Snyman M, Bester-van der Merwe A. Evaluation of the OvineSNP50 chip for use in four South African sheep breeds. SA J. An. Sci 2016 Apr 05;46(1):89. [doi: 10.4314/sajas.v46i1.11]
37. Ilori B, Rosen B, Sonstegard T, Bankole O, Durosaro S, Hanotte O. Assessment of OvineSNP50 in Nigerian and Kenyan sheep populations. Nigerian J Biotechnol 2019 Mar 25;35(2):176. [doi: 10.4314/njb.v35i2.21]
38. Cao Y, Song X, Shan H, Jiang J, Xiong P, Wu J, et al. Genome-wide association study of body weights in hu sheep and population verification of related single-nucleotide polymorphisms. Front Genet 2020 Jul 3;11:588 [FREE Full text] [doi: 10.3389/fgene.2020.00588] [Medline: 32719712]
39. Osada N, Kohara A, Yamaji T, Hirayama N, Kasai F, Sekizuka T, et al. The genome landscape of the african green monkey kidney-derived vero cell line. DNA Res 2014 Dec;21(6):673-683 [FREE Full text] [doi: 10.1093/dnares/dsu029] [Medline: 25267831]
40. Othman O, Germot A, Khodary M, Petit D, Maftah A. Cytochrome b diversity and phylogeny of six Egyptian sheep breeds. Annu Res Rev Biol 2018 Jan 18;22(4):1-11. [doi: 10.9734/arrb/2018/38879]
41. Tai W, He L, Zhang X, Pu J, Voronin D, Jiang S, et al. Characterization of the receptor-binding domain (RBD) of 2019 novel coronavirus: implication for development of RBD protein as a viral attachment inhibitor and vaccine. Cell Mol Immunol 2020 Jun;17(6):613-620 [FREE Full text] [doi: 10.1038/s41423-020-0400-4] [Medline: 32203189]
42. Patel VB, Zhong J, Grant MB, Oudit GY. Role of the ACE2/angiotensin 1–7 axis of the renin–angiotensin system in heart failure. Circ Res 2016 Apr 15;118(8):1313-1326. [doi: 10.1161/circresaha.116.307708]

Abbreviations

ACE2: angiotensin-converting enzyme 2
ATCC: American Type Culture Collection
CPE: cytopathic effect
ECACC: European Collection of Authenticated Cell Culture
FADDL: Foreign Animal Disease Diagnostic Laboratory
FOH-SA: fetal ovine heart–Saudi Arabia
IFN: interferon
LSD: lumpy skin disease
MAF: minor allele frequency
MEM: Minimum Essential Medium
MEWA: Ministry of Environment, Water and Agriculture
MOI: multiplicity of infection
NCBE: National Committee of Bioethics
PCR: polymerase chain reaction
PPR: Peste des petits ruminants
PSA: pairwise sequence alignment
RVF: Rift Valley fever

SNP: single nucleotide polymorphism
TCID50: tissue culture infective dose 50
USDA: United States Department of Agriculture

Edited by T Leung, G Eysenbach; submitted 17.10.23; peer-reviewed by R Pillai, S Chakraborty, H Rafi, A Mukherjee; comments to author 22.03.24; revised version received 11.04.24; accepted 29.05.24; published 18.07.24.

Please cite as:
Suleiman K, Aljulidan M, Hussein G, Alkhalaf H
Establishment of a Novel Fetal Ovine Heart Cell Line by Spontaneous Cell Fusion: Experimental Study
JMIRx Bio 2024;2:e53721
URL: https://bio.jmirx.org/2024/1/e53721
doi:10.2196/53721
PMID:

Original Paper

Establishing Antimicrobial Resistance Surveillance in the Water and Environment Sector in a Resource-Limited Setting: Methodical Qualitative and Quantitative Description of Uganda's Experience From 2021 to 2023

Godfrey Katumba[1*], MSc; Herman Mwanja[2*], BEHS; Jonathan Mayito[2*], MBChB, MMed, PhD; Betty Mbolanyi[1], MSc; Fred Isaasi[2], MPH; Daniel Kibombo[2], MPH; Judith Namumbya[1], MSc; David Musoke[3], PhD; Jonathan Kabazzi[2,4], BMLS; Musa Sekamatte[5], MPH; Lillian Idrakua[1], MSci; Richard Walwema[2], MBA; Mohammed Lamorde[2], PhD; Francis Kakooza[2], PhD; Simon Etimu[1], MSci

[1]Ministry of Water and Environment, Government of Uganda, Kampala, Uganda
[2]Infectious Diseases Institute, Makerere University, Kampala, Uganda
[3]School of Public Health, Makerere University, Kampala, Uganda
[4]National Health Laboratory and Diagnostics Services, Ministry of Health, Kampala, Uganda
[5]One Health Coordination Office, Ministry of Health, Uganda, Kampala, Uganda
[*]these authors contributed equally

Corresponding Author:
Herman Mwanja, BEHS
Infectious Diseases Institute
Makerere University
Makerere University Main Campus
Kampala, P.O. Box 22418
Uganda
Phone: 256 0770781589
Email: hmwanja@idi.co.ug

Related Articles:

Companion article: https://preprints.jmir.org/preprint/50588

Companion article: https://bio.jmirx.org/2024/1/e58901/

Companion article: https://bio.jmirx.org/2024/1/e58903/

Companion article: https://bio.jmirx.org/2024/1/e58949/

Abstract

Background: Antimicrobial irrational use and poor disposal in the human and animal sectors promote antimicrobial resistance (AMR) in the environment as these antimicrobials and their active ingredients, coupled with resistant microbes, are released into the environment. While AMR containment programs in the human and animal sectors are well established in Uganda, those in the water and environment sector still need to be established and strengthened. Therefore, the Ministry of Water and Environment set out to establish an AMR surveillance program to bolster the One Health efforts for the containment of AMR under the National Action Plan 2018-2023.

Objective: This study aims to describe Uganda's experience in establishing AMR surveillance in the water and environment sector.

Methods: A methodical qualitative and quantitative description of the steps undertaken between August 2021 and March 2023 to establish an AMR surveillance system in the water and environment sector is provided. The Uganda Ministry of Water and

Environment used a stepwise approach. Governance structures were streamlined, and sector-specific AMR surveillance guiding documents were developed, pretested, and rolled out. The National Water Quality Reference Laboratory infrastructure and microbiology capacity were enhanced to aid AMR detection and surveillance using conventional culture-based methods. A passive and targeted active surveillance hybrid was used to generate AMR data. Passive surveillance used remnants of water samples collected routinely for water quality monitoring while targeted active surveys were done at selected sites around the Kampala and Wakiso districts. Excel and Stata 15 statistical software were used for data analysis.

Results: A sector-specific technical working group of 10 members and focal persons is in place, providing strategic direction and linkage to the national AMR surveillance program. The National Water Quality Reference Laboratory is now at biosafety level 2 and conducting microbiology testing using conventional culture-based techniques. Up to 460 water samples were processed and 602 bacterial isolates were recovered, of which 399 (66.3%) and 203 (33.7%) were priority pathogens and nonpriority pathogens, respectively. Of the 399 priority pathogens, 156 (39.1%), 140 (35.1%), 96 (24.1%), and 7 (1.8%) were *Escherichia coli*, *Klebsiella* species, *Enterococcus* species, and *Salmonella* species, respectively. *E coli* showed resistance to ampicillin (79%), ciprofloxacin (29%), and ceftriaxone (29%). Similarly, *Klebsiella* species showed resistance to ampicillin (100%), ciprofloxacin (17%), and ceftriaxone (18%). *Enterococcus* species showed resistance to ciprofloxacin (52%), vancomycin (45%), and erythromycin (56%). Up to 254 (63.7%) of the priority pathogens recovered exhibited multiple and extensive resistance to the different antibiotics set.

Conclusions: Initial efforts to establish and implement AMR surveillance in the water and environment sector have succeeded in streamlining governance and laboratory systems to generate AMR data using conventional culture-based methods.

(JMIRx Bio 2024;2:e50588) doi:10.2196/50588

KEYWORDS

antimicrobial resistance; surveillance system; water and environment sector

Introduction

Antimicrobial resistance (AMR) occurs when microorganisms survive after exposure to antimicrobials that would normally kill them, inhibit their metabolism, or stop their growth [1]. This also includes antibiotic resistance in bacteria [2]. As a result, antibiotics become ineffective against disease-causing bacteria, leading to AMR evolving into a silent pandemic [2,3], which is projected to account for over 10 million human deaths by 2050 [3]. This imparts a substantial financial burden on the health care system [4]. AMR is a “One Health” issue, highlighting the complex interconnectedness between the health and well-being of animals, people, plants, and their shared environment [5]. This results from the transmission of resistant microorganisms, their genes, or mobile genetic elements between these compartments [6]. Thus, making AMR one of the top threats to global health, with increasing trends in resistant infections in humans and animals, tending toward a postantibiotic era [7].

Globally, AMR in the environment has been a neglected issue whose public health importance, burden, and implication are yet to be explored comprehensively [8], especially in resource-limited settings [9]. Over the past decades, global health research has increasingly shown that the environment plays a key role in the proliferation and exacerbation of AMR and its effects [9-12]. Most antimicrobials used in humans and animals are excreted or indiscriminately disposed of into the environment in their raw or active forms [13]. Sublethal levels of antimicrobials, contaminants, and resistant bacteria in effluents from pharmaceutical industries, households, agricultural runoffs, and health care settings are released into the environment [3,14]. This creates an unnatural selective pressure in the environment [3,15] that, coupled with direct contact between natural bacterial communities and the discharged resistant bacteria, drives the evolution, selection, and emergence of resistant strains within the environment [3,13,16].

In Uganda, AMR surveillance and containment efforts have mainly focused on the human and animal sectors [17], partly due to the lack of a structured surveillance program with consensus on standard methodologies and targets in the water and environment sector on both the national and global scale [7]. Currently, there is no benchmarking or threshold data in the sector to inform epidemiological, evolutionary, and risk modeling efforts [7,12]. The Uganda Ministry of Water and Environment (MWE) and its partners, therefore, undertook efforts to establish an AMR surveillance program in the water and environment sector to bolster a One Health approach in curbing AMR, guided by the AMR National Action Plan 2018-2023. Instituting AMR surveillance in the sector was done in cognizance of the country’s environmental concerns, local contexts, and a structured framework [13,18-20]. We, therefore, present Uganda’s experience in establishing an AMR surveillance program and the emerging data on the status of AMR in the environment sector between August 2021 and March 2023.

Methods

Overview

A methodical qualitative and quantitative description of the steps undertaken between August 2021 and March 2023 to establish an AMR surveillance system in the water and environment sector is provided. Several surveillance documents, guidelines, and reports were reviewed to collect data appropriately aligned to AMR surveillance in a low-resource setting [21]. The description below provides the steps (processes and methods) undertaken to set up the program.

AMR Governance Establishment and Enhancement

The Government of Uganda, through the MWE, with support from the Infectious Diseases Institute at Makerere University through the Fleming Fund Country Grant 2 project, instituted a stepwise approach with incremental targets and sequential phases from August 2021. This involved establishing a foundation, consolidating and refining gains, scaling up, and further expanding the surveillance system.

A 10-member sector-specific AMR technical working group (TWG) with focal persons was established to coordinate the AMR containment efforts, including surveillance activities in the sector. The TWG developed AMR surveillance documents (plan, protocol, and standard operating procedures) focused on the monitoring of priority environmental bacteria (*Escherichiacoli*, *Klebsiella* species, *Enterococcus* species, and *Salmonella* species) in water samples. These documents were aligned to the different international and national guidelines [22-25]. The National Water Quality Reference Laboratory (NWQRL) was identified as the sentinel site for AMR surveillance in the sector using conventional culture-based techniques. One sample type (water samples) was also designated for the initial AMR surveillance efforts. The TWG also reviewed the generated AMR data to inform AMR programming and policy formulation in the sector.

Enhancement of the Microbiology Capacity of the NWQRL

The NWQRL microbiology section was equipped and its infrastructure was enhanced. The human resource capacity was enhanced through in-service microbiology, biosecurity and biosafety, and laboratory quality management system trainings and mentorships. This capacity enhancement was done through a One Health approach, leveraging the established AMR surveillance capacity in the human and animal sectors. The NWQRL was also enrolled in the national laboratory external quality assessment and proficiency testing scheme of the Uganda National Health Laboratory and Diagnostic Services to enhance the microbiology testing quality.

Pretest and Rollout of the AMR Surveillance Documents

The developed sector-specific AMR surveillance documents were pretested through an active survey. This involved the collection of samples from the Kampala-Wakiso region and analyzing them at the NWQRL. A total of 9 strategic surface water (nonpoint sources) and wastewater (point sources) sampling sites were identified in Kampala and Wakiso, and 15 grab samples were collected using the standard procedures as stipulated in the different surveillance documents. The samples were transported to the NWQRL under appropriate conditions and analyzed using standard, conventional, culture-based procedures. The lessons learned during the pretest were used to refine the surveillance documents.

The documents were then rolled out to generate AMR surveillance data through a hybrid of passive and active surveillance. The initial efforts focused on nonpoint sources or surface water sources (rivers, streams, and other open channels), drinking water (national water grid and other potable water), and point sources or wastewater (sewer, wastewater treatment plants and ponds, and septic tanks) samples. Passive surveillance used remnants of samples routinely referred from across the country to the NWQRL for water quality monitoring. Active surveillance used samples collected through quarterly targeted surveys from strategic sites (shown in the map provided in Multimedia Appendix 1) in the Kampala-Wakiso region as stipulated in the surveillance protocol. This region was chosen because it has vast human economic activities that involve the intense use of antibiotics and thus provided an ideal setting for integrated AMR surveillance in the sector.

Conventional culture-based bacteriology techniques were used for the enumeration, isolation, and identification of priority bacteria. Water sample enrichment was done by inoculating 2-5 ml of the sample into 10 ml of brain heart infusion and incubating for 16-18 hours at 37 °C. Following the enrichment, culture media and biochemical tests were used to isolate and identify the bacteria.

For *E coli* and *Klebsiella* species, MacConkey agar with crystal violet was used for the primary culture and purity plating. The distinct colonies (*E coli*: pink/red lactose-fermenting colonies; *Klebsiella* species: pink-yellow mucoid lactose-fermenting colonies) that grew after 18-24 hours of incubation at 37 °C were subjected to Gram stain (microscopy) and biochemical tests including oxidase, urea, citrate, triple sugar iron, and sulfide indole motility tests using standard procedures.

For *Salmonella* species, MacConkey agar with crystal violet was used for the primary culture. The distinct colonies (colorless colonies) that grew after 18-24 hours of incubation at 37 °C were purity plated on xylose lysine deoxycholate media. The distinct colonies (red colonies with black centers) that grew after 18-24 hours of incubation at 37 °C were subjected to Gram stain and biochemical tests including oxidase, urea, citrate, triple sugar iron, and sulfide indole motility tests using standard procedures. For *Enterococcus* species, Slanetz and Bartley agar was used for the primary culture. The distinct colonies (red or purple colonies) that grew after 18-24 hours of incubation at 37 °C were purity plated on 5% sheep blood agar media. The distinct colonies (white or gray colonies) that grew after incubation were subjected to Gram stain (microscopy) and biochemical tests including catalase and bile esculin tests.

Other than the priority bacterial isolates, we also recovered other bacteria species including *Citrobacter freundii*, *Enterobacter*, *Pseudomonas*, *Proteus*, *Providencia*, and *Raoultella* species.

AMR Data Generation

Antimicrobial susceptibility testing was done using the Kirby-Bauer disc diffusion method with the appropriate isolate-antibiotic combinations and techniques as stipulated in the 31st edition of the Clinical and Laboratory Standards Institute guidelines [26]. Penicillins, fluoroquinolones, cephalosporins, aminoglycosides, carbapenems, glycopeptides, macrolides, oxazolidinones, folates (sulphonamide-trimethoprim), tetracycline, and phenicols were the antibiotic classes considered. Isolates were cryopreserved in a 20% glycerol and brain heart infusion and archived at the Uganda National Biorepository at the Central Public Health

Laboratories and National Animal Diseases Diagnostics and Epidemiology Center laboratory at –80 °C.

Data Analysis

Excel 2016 (Microsoft Corporation) and Stata 16 (StataCorp) were used for data entry, cleaning, and analysis. The percentage resistance of the isolates to each antibiotic was generated and visuals (charts and graphs) were developed. The chi-square test and binary logistic regression were used to test whether the resistance of the priority pathogens (*Ecoli*, *Klebsiella*, and *Enterococcus* species) to the different antibiotics was significantly different across the point and nonpoint sources. A *P* value <.05 indicated a significant statistical difference.

Ethical Statement

The work reported here is part of the Uganda National AMR surveillance program that was approved by the National AMR Sub-Committee of the National One Health Platform.

Results

Streamlining of AMR Governance in the Water and Environment Sector

The sector-specific TWG was constituted and comprised of 10 members from the three directorates of the MWE, including the directorates of water resources management, water development, and environmental affairs. Focal persons for AMR surveillance in the sector were identified. The TWG finalized the sector surveillance documents that stipulate the target priority pathogens and sample type, designated the NWQRL as the sentinel site, designed the routine and targeted surveys, and reviewed and reported the AMR data generated to the MWE. The TWG also published a report on the AMR burden in the sector in the annual Natural Resources, Environment, Climate Change, Land and Water Management Program Performance Report 2022 [27]. Further, the TWG functioned as a linkage for the sector surveillance program to the national AMR surveillance program under the National AMR Sub-Committee of the National One Health Platform, the human and animal sector-specific AMR surveillance programs, the academia, and implementing partners.

Microbiology Laboratory Capacity Enhancement in the Sector

Following the infrastructural and equipment enhancement, the NWQRL now houses a fully-fledged biosafety level 2 microbiology laboratory, the minimum level required for AMR surveillance. The laboratory has staff trained in microbiology, including antimicrobial susceptibility testing, biosafety biosecurity, AMR data management, and laboratory quality management systems. These staff have supported the laboratory analysis of environmental samples to generate AMR data.

Bacterial Isolates Recovered

Up to 460 samples were collected and processed at the NWQRL between August 2021 and March 2023, of which 363 (78.9%) were from passive surveillance while 97 (21.1%) were from active surveillance. Of the 460 samples, 158 (34.3%) were from point sources (wastewater samples), while 284 (61.7%) were from nonpoint sources: 108 (23.5%) ground, 95 (20.7%) surface, and 81 (17.6%) drinking water samples. Up to 328 (71.3%) samples had significant growth and yielded 602 bacterial isolates, of which, 399 (66.3%) and 203 (33.7%) were priority and nonpriority pathogens, respectively. Of the 602 isolates, 223 (37%), 166 (27.6%), 132 (21.9%), and 67 (11.1%) were from waste, surface, ground, and drinking water sources, respectively. Of the 602 isolates, 399 (66.3%) were priority pathogens: 156 (39.1%) *E coli*, 140 (35.1%) *Klebsiella* species, 96 (24.1%) *Enterococcus* species, and 7 (1.8%) *Salmonella* species. The 203 nonpriority isolates were *Citrobacter* species (n=57, 28.1%), *Enterobacter* species (n=52, 25.6%), *Proteus* species (n=23, 11.3%), *Pseudomonas* species (n=19, 9.4%), *Acinetobacter* species (n=8, 3.9%), and other bacterial species (n=44, 21.7%).

The Burden of AMR in the Water and Environment Sector

E coli (n=156) had a resistance of 79% to ampicillin, 55% to trimethoprim/sulfamethoxazole, 29% to ceftriaxone and ciprofloxacin, 18% to cefepime and chloramphenicol, 11% to imipenem, and 0% to amikacin and meropenem. Other antibiotic resistance is shown in Table 1.

Klebsiella species isolates (n=140) had a resistance of 100% to ampicillin, 33% to trimethoprim/sulfamethoxazole, 28% to amoxicillin-clavulanate, 27% to cefuroxime, 17% to ciprofloxacin, 2% to imipenem, and 0% to amikacin. *Salmonella* species isolates (n=7) had a resistance of over 50% to ampicillin, ciprofloxacin, ceftriaxone, trimethoprim/sulfamethoxazole, and tetracycline. *Enterococcus* species (n=96) had a resistance of 45% to vancomycin, 56% to erythromycin, 54% to tetracycline, and 52% to ciprofloxacin (Table 1).

Overall, there was no significant difference between the resistance observed in *E coli* and *Klebsiella* species isolates recovered from point and nonpoint sources. Among the *Enterococcus* species isolates, a significant difference (odds ratio 5.318182, 95% CI 1.793498-15.76977; *P*=.003) was observed in the resistance to chloramphenicol between the isolates recovered from point and nonpoint sources. The *Enterococcus* isolates recovered from point sources were 5 times more likely to be resistant to chloramphenicol than those recovered from nonpoint sources.

Several isolates recovered exhibited nonsusceptibility to more than one antibiotic and to two or more antibiotic classes, a phenomenon referred to as multidrug resistance (MDR) and extensive drug resistance, respectively. Up to 254 (63.7%) of the 399 priority pathogens recovered exhibited MDR or extensive drug resistance, of which 99 (39%), 85 (33.5%), 65 (25.6%), and 5 (2%) were *E coli*, *Enterococcus* species, *Klebsiella* species, and *Salmonella* species, respectively. Of the MDR *E coli* isolates (n=99), 40 (40%), 25 (25%), 18 (18%), 12 (12%), 1 (1%), and 3 (3%) showed resistance to 2, 3, 4, 5, 6, and 7 antibiotics from different classes, respectively. Of the MDR *Enterococcus* species isolates (n=85), 27 (32%), 34 (40%), 16 (19%), and 8 (9%) showed resistance to 2, 3, 4, and 5 antibiotics from different classes, respectively. Of the MDR *Klebsiella* species isolates (n=65), 36 (55%), 20 (32%), 2 (3%),

6 (9%), and 1 (2%) showed resistance to 2, 3, 4, 5, and 7 antibiotics from different classes, respectively (Table 2).

Table 1. Antimicrobial resistance profiles for the different isolates recovered between August 2021 and March 2023

Isolate name, antibiotic class, and antibiotic name	Isolates tested for AST[a], n	Resistance (%)
Escherichia coli **(n=156)**		
Penicillins		
Ampicillin	151	79
Fluoroquinolones		
Ciprofloxacin	141	29
Levofloxacin	38	21
Cephalosporins		
Cefuroxime	38	39
Ceftriaxone	115	29
Ceftazidime	38	26
Cefepime	66	18
Aminoglycosides		
Gentamicin	150	9
Amikacin	38	0
Carbapenems		
Meropenem	38	0
Imipenem	148	11
Beta-lactamase		
Piperacillin-tazobactam	53	4
Amoxicillin-clavulanate	38	13
Sulfonamide-trimethoprim		
Trimethoprim/sulfamethoxazole	146	55
Tetracyclines		
Tetracycline	50	30
Amphenicols		
Chloramphenicol	94	18
Glycyclines		
Tigecycline	50	30
Klebsiella **species (n=140)**		
Penicillins		
Ampicillin	137	100
Fluoroquinolones		
Ciprofloxacin	89	17
Levofloxacin	71	7
Cephalosporins		
Ceftriaxone	92	18
Ceftazidime	71	15
Cefepime	80	11
Aminoglycosides		
Gentamicin	134	4
Amikacin	71	0

Isolate name, antibiotic class, and antibiotic name	Isolates tested for AST[a], n	Resistance (%)
Carbapenems		
Meropenem	71	1
Imipenem	134	2
Beta-lactamase		
Piperacillin-tazobactam	75	3
Amoxicillin-clavulanate	71	28
Sulfonamide-trimethoprim		
Trimethoprim/sulfamethoxazole	135	33
Tetracyclines		
Tetracycline	10	30
Amphenicols		
Chloramphenicol	56	4
Glycyclines		
Tigecycline	71	4
***Salmonella* species (n=7)**		
Penicillins		
Ampicillin	7	86
Fluoroquinolones		
Ciprofloxacin	7	71
Cephalosporins		
Ceftriaxone	5	60
Carbapenems		
Imipenem	7	29
Sulfonamide-trimethoprim		
Trimethoprim/sulfamethoxazole	7	57
Tetracyclines		
Tetracycline	4	75
Amphenicols		
Chloramphenicol	7	43
***Enterococcus* species (n=96)**		
Penicillins		
Ampicillin	74	30
Fluoroquinolones		
Ciprofloxacin	60	52
Gentamicin-Syn	51	0
Glycopeptides		
Vancomycin	88	45
Macrolides		
Erythromycin	88	56
Oxazolidinones		
Linezolid	51	2
Sulfonamide-trimethoprim		

Isolate name, antibiotic class, and antibiotic name	Isolates tested for AST[a], n	Resistance (%)
Trimethoprim/sulfamethoxazole	66	89
Tetracyclines		
Tetracyclines	80	54
Amphenicols		
Chloramphenicol	40	50
Glycyclines		
Tigecycline	71	0

[a]AST: antimicrobial susceptibility testing.

Table 2. Isolates that exhibited multidrug resistance and extensive drug resistance tendencies among the priority isolates recovered.

Number of antibiotics for which resistance is shown	Frequency of resistant isolates
Two antibiotics	
Enterococcus species	27
Klebsiella species	36
Escherichia coli	40
Three antibiotics	
Enterococcus species	34
Klebsiella species	20
Escherichia coli	25
Four antibiotics	
Enterococcus species	16
Klebsiella species	02
Escherichia coli	18
Five antibiotics	
Enterococcus species	8
Klebsiella species	6
Escherichia coli	12
Six antibiotics	
Enterococcus species	0
Klebsiella species	0
Escherichia coli	1
Seven antibiotics	
Enterococcus species	0
Klebsiella species	1
Escherichia coli	3

Discussion

AMR surveillance in the Uganda water and environment sector is taking shape, including the streamlining of the sector AMR governance structures. This has expanded the One Health approach to AMR surveillance in the country. A TWG, a national AMR reference laboratory, and an AMR focal person were constituted and provided with terms of reference. This is in alignment with the road map for the participation of low- and middle-income countries in the Global Antimicrobial Surveillance System [21]. This program has been established using a phased/stepwise approach where one sentinel site, the NWQRL, was identified and its capacity enhanced and is now used for AMR surveillance. This is a prerequisite for establishing targeted and well-monitored public health surveillance of AMR in low-income settings [21,28]. The alignment of the efforts in the sector with national and international guidelines allows national and international

comparisons of established surveillance systems to identify areas of improvement [29].

The program has succeeded in profiling the resistance patterns of the bacterial pathogens recovered from different water types from both point and nonpoint sources of AMR determinants in the environment as categorized by Khurana and Sinha [30]. Wastewater samples represent the point sources as the resistant microorganisms in these samples either emerge directly or after antimicrobials reach and contaminate the different environment compartments. The ground, drinking, and surface water samples constitute the nonpoint sources of resistant organisms since these indicate the interface and spillage of resistant microorganisms from the environment to the human and animal populations [30].

The program used culture-based methods as these were better aligned with the current laboratory infrastructure in the Uganda water and environment sector and the country at large. Liguori et al [7] have described the methods as fairly standardized and an avenue for further analysis of the recovered isolates including sensitivity testing, sequence-based typing, and whole genome sequencing, which aid in detecting and identifying antibiotic-resistant genes and genetic elements. However, these culture-based methods recover fewer microorganisms as the majority of the environmental microbes are not readily cultured, yet they may pose public health challenges [31]. Thus, the AMR surveillance systems in the sector require appropriate expansion to include whole genome sequencing and environmental wastewater sequencing.

E coli, *Klebsiella* species, *Enterococcus* species, and *Salmonella* species used for surveillance in the Ugandan sector are globally recommended for the environment sector [32,33]. An expert survey conducted among 105 experts from different fields and parts of the world found that Enterobacterales (mainly *E coli* and *Salmonella* species) and *Enterococcus* species were the most selected culture target microorganisms for AMR surveillance in the environment [7]. These microorganisms are similar to those recommended for AMR surveillance in the human [34,35] and animal health [36] sectors. This makes the comparison, quantification, and evaluation of the occurrence of these organisms across the different sectors in low-resource settings feasible [3,37]. They are classified as the major clinically relevant multidrug-resistant pathogens prevalent in the different environmental compartments [3,32,33,38] that can cause life-threatening illnesses in humans and animals [24].

The high *E coli* resistance to ampicillin and trimethoprim/sulfamethoxazole observed in our evaluation is similar to that observed in South Africa, where *E coli* had high resistance to sulfamethoxazole (100%) and ampicillin (90%) [39]. Moges et al [40] in Ethiopia observed that the recovered *E coli* had 100% resistance to ampicillin and 38% resistance to trimethoprim/sulfamethoxazole. This ampicillin resistance is similar to that found by Nabadda et al [41] among recovered *E coli* isolates from human samples in Uganda, which had more than 90% resistance to ampicillin. Amaya et al [42] also found that some *E coli* recovered from groundwater from wells in León, Nicaragua showed very high resistance of 100% to ampicillin, ciprofloxacin, and trimethoprim/sulfamethoxazole. This indicates a similarity in the resistance of *E coli* recovered from humans and the environment, which requires further assessment using whole genome sequencing techniques to elucidate the interrelatedness.

The high resistance of *Klebsiella* species against ampicillin observed in the Uganda program correlates to the high ampicillin intrinsic resistance (100%) observed in the *Klebsiella* species isolates from environmental samples in a study in Pakistan from 2017 to 2019 [43]. Holt et al [44] similarly found 100% resistance to ampicillin among the different *Klebsiella* species recovered [45]. This phenomenon of *Klebsiella* species' intrinsic resistance to ampicillin is demonstrated in the Clinical and Laboratory Standards Institute guidelines [26] and the European Committee on Antimicrobial Susceptibility Testing guidelines [46,47]. The moderate *Klebsiella* species resistance (below 50%) to gentamicin, imipenem, and trimethoprim/sulfamethoxazole observed in the program is consistent with that observed in an Iraqi study on the resistance patterns of *Klebsiella* species isolates from clinical and environmental samples [48].

Resistant *Salmonella* species isolated from some of the samples indicate contamination of these sources by human and animal waste [49,50]. This points to a potential risk for an outbreak of salmonellosis within the animal or human populations residing in the surroundings of the sample source [51,52]. Such an observation can be used to predict the health profile of the human and animal populations in a given catchment area using environmental samples [20].

Enterococcus species resistance to tetracycline (54%), vancomycin (45%), erythromycin (56%), and ciprofloxacin (52%) in this program were all higher (in some instances double) than the resistance of the *Enterococcus* species from environmental samples in an area of intensive poultry production in Canada [53]. Another study in France also showed high resistance of *Enterococcus* species isolates to erythromycin (100%), vancomycin (85.7%), and tetracycline (57.1%) [54].

The MDR exhibited by the isolates recovered in the program is consistent with the findings of studies conducted in several parts of the world. For example, a 96.4% MDR occurrence was observed in the bacterial strains recovered from samples collected from different aquatic environments in a study in France [54]. Another study in Ghana by Odonkor and Addo [55] found that 63% of the *E coli* strains recovered were resistant to at least 3 antibiotics from different classes. Further, a study conducted in the United States also found that 65% of the isolates recovered from combined sewage overflows (wastewater) were resistant to 6 or more antibiotics from different classes [56]. Human and animal exposure to and infection with such highly resistant bacteria in the environment through complex interactions impacts the economy of countries as such infections are harder to treat. This increases medical costs, hospital stays, the risk of infection spread, severity, and mortality rates [57].

Our evaluation had one major limitation. The representativeness of the AMR data generated is still limited as the active surveys are conducted in only the Kampala-Wakiso region. Therefore, the data may not be sufficient to generalize the prevalence of

AMR in Uganda's water and environment sector. However, the data marks the first efforts to generate AMR data in the sector, but more efforts are required to increase the quantity of the sector AMR data.

Efforts to implement AMR surveillance in the water and the environment sector succeeded in streamlining AMR surveillance governance and isolating resistant pathogens from different water types (waste, drinking, surface, and groundwater). The program needs to be consolidated and expanded to include more sentinel sites, sample types, advanced AMR surveillance methodologies and techniques, and the surveillance of antimicrobial residues. Sustained surveillance in the sector and interlinkages with the human and animal sectors' surveillance systems are also required to inform concerted strategies to control AMR in the country.

Acknowledgments

The authors of this work would like to show appreciation to the members of the Uganda Ministry of Water and Environment (MWE) senior management, the National AMR Sub-Committee of the National One Health Platform, and the staff at the National Water Quality Reference Laboratory for their support during the execution of this work.

The Fleming Fund Country Grant (RFP/CG2/Uganda, grant FF78-484) to the Infectious Diseases Institute from UKaid funded this work through the Mott Mac Donald management agency.

Data Availability

The data generated from the water and environment sector is a preserve of the Uganda MWE. It can be accessed by placing a request and concept on use to the Commissioner Water Quality Management Department in the Directorate of Water Resources Management, MWE.

Conflicts of Interest

None declared.

Multimedia Appendix 1
Map showing the environment sector antimicrobial resistance surveillance sampling points in Kampala and Wakiso.
[PNG File , 656 KB - xbio_v2i1e50588_app1.png]

References

1. Prestinaci F, Pezzotti P, Pantosti A. Antimicrobial resistance: a global multifaceted phenomenon. Pathog Glob Health 2015;109(7):309-318. [doi: 10.1179/2047773215Y.0000000030] [Medline: 26343252]
2. Frieri M, Kumar K, Boutin A. Antibiotic resistance. J Infect Public Health 2017;10(4):369-378. [doi: 10.1016/j.jiph.2016.08.007] [Medline: 27616769]
3. Samreen, Ahmad I, Malak HA, Abulreesh HH. Environmental antimicrobial resistance and its drivers: a potential threat to public health. J Glob Antimicrob Resist 2021 Dec;27:101-111. [doi: 10.1016/j.jgar.2021.08.001] [Medline: 34454098]
4. Tillotson GS, Zinner SH. Burden of antimicrobial resistance in an era of decreasing susceptibility. Expert Rev Anti Infect Ther 2017 Jul;15(7):663-676. [doi: 10.1080/14787210.2017.1337508] [Medline: 28580804]
5. Robinson TP, Bu DP, Carrique-Mas J, Fèvre EM, Gilbert M, Grace D, et al. Antibiotic resistance is the quintessential One Health issue. Trans R Soc Trop Med Hyg 2016 Jul;110(7):377-380. [doi: 10.1093/trstmh/trw048] [Medline: 27475987]
6. Larsson DJ, Andremont A, Bengtsson-Palme J, Brandt KK, de Roda Husman AM, Fagerstedt P, et al. Critical knowledge gaps and research needs related to the environmental dimensions of antibiotic resistance. Environ Int 2018 Aug;117:132-138. [doi: 10.1016/j.envint.2018.04.041] [Medline: 29747082]
7. Liguori K, Keenum I, Davis BC, Calarco J, Milligan E, Harwood VJ, et al. Antimicrobial resistance monitoring of water environments: a framework for standardized methods and quality control. Environ Sci Technol 2022 Jul 05;56(13):9149-9160. [doi: 10.1021/acs.est.1c08918] [Medline: 35732277]
8. Taneja N, Sharma M. Antimicrobial resistance in the environment: the Indian scenario. Indian J Med Res 2019 Feb;149(2):119-128. [doi: 10.4103/ijmr.IJMR_331_18] [Medline: 31219076]
9. Fletcher S. Understanding the contribution of environmental factors in the spread of antimicrobial resistance. Environ Health Prev Med 2015 Jul;20(4):243-252. [doi: 10.1007/s12199-015-0468-0] [Medline: 25921603]
10. Musoke D, Namata C, Lubega GB, Niyongabo F, Gonza J, Chidziwisano K, et al. The role of Environmental Health in preventing antimicrobial resistance in low- and middle-income countries. Environ Health Prev Med 2021 Oct 05;26(1):100. [doi: 10.1186/s12199-021-01023-2] [Medline: 34610785]
11. Vassallo A, Kett S, Purchase D, Marvasi M. Antibiotic-resistant genes and bacteria as evolving contaminants of emerging concerns (e-CEC): is it time to include evolution in risk assessment? Antibiotics (Basel) 2021 Sep 03;10(9):1066. [doi: 10.3390/antibiotics10091066] [Medline: 34572648]

12. Larsson DGJ, Flach C. Antibiotic resistance in the environment. Nat Rev Microbiol 2022 May;20(5):257-269. [doi: 10.1038/s41579-021-00649-x] [Medline: 34737424]
13. Frontiers 2017: emerging issues of environmental concern. United Nations Environment Programme. 2017. URL: https://www.unep.org/resources/frontiers-2017-emerging-issues-environmental-concern [accessed 2023-02-01]
14. Puvača N, Vapa Tankosić J, Ignjatijević S, Carić M, Prodanović R. Antimicrobial resistance in the environment: review of the selected resistance drivers and public health concerns. J Agron Technol Eng Manag 2022 Sep 30;5(5):793-802. [doi: 10.55817/CSCQ3326]
15. Holmes AH, Moore LSP, Sundsfjord A, Steinbakk M, Regmi S, Karkey A, et al. Understanding the mechanisms and drivers of antimicrobial resistance. Lancet 2016 Jan 09;387(10014):176-187. [doi: 10.1016/S0140-6736(15)00473-0] [Medline: 26603922]
16. Irfan M, Almotiri A, AlZeyadi ZA. Antimicrobial resistance and its drivers-a review. Antibiotics (Basel) 2022 Oct 05;11(10):1362. [doi: 10.3390/antibiotics11101362] [Medline: 36290020]
17. Kivumbi M, Standley C. Efforts to identify and combat antimicrobial resistance in Uganda: a systematic review. Trop Med Infect Dis 2021 May 24;6(2):86. [doi: 10.3390/tropicalmed6020086] [Medline: 34074031]
18. Food and Agriculture Organization of the United Nations, World Organisation for Animal Health, World Health Organization, United Nations Environment Programme. Strategic Framework for Collaboration on Antimicrobial Resistance: Together for One Health. Rome, Italy: Food & Agriculture Organization; Apr 6, 2022.
19. McEwen S, Collignon PJ. Antimicrobial resistance: a One Health perspective. Microbiol Spectr 2018 Mar;6(2):A. [doi: 10.1128/microbiolspec.ARBA-0009-2017] [Medline: 29600770]
20. Huijbers PM, Flach C, Larsson DJ. A conceptual framework for the environmental surveillance of antibiotics and antibiotic resistance. Environ Int 2019 Sep;130:104880. [doi: 10.1016/j.envint.2019.05.074] [Medline: 31220750]
21. Seale AC, Gordon NC, Islam J, Peacock SJ, Scott JAG. AMR surveillance in low and middle-income settings - a roadmap for participation in the Global Antimicrobial Surveillance System (GLASS). Wellcome Open Res 2017;2:92. [doi: 10.12688/wellcomeopenres.12527.1] [Medline: 29062918]
22. Global action plan on antimicrobial resistance. World Health Organization. 2015. URL: https://apps.who.int/iris/rest/bitstreams/864486/retrieve [accessed 2020-12-12]
23. Strategic and operational guidance for national action plan on antimicrobial resistance for developing countries focusing on animal and environment aspects. Centre for Science and Environment. 2016. URL: https://cdn.cseindia.org/userfiles/strategic-and-operational-guidance-NAP-on-AMR-for-Developing-Countries.pdf [accessed 2023-02-01]
24. National action plan for antimicrobial resistance. Central Public Health Laboratories of the Republic of Uganda Ministry of Health. 2018. URL: https://www.cphl.go.ug/sites/default/files/2020-02/Uganda%20National%20Action%20Plan%20for%20Antimicrobial%20Resistance%202018-%202023-compressed_0.pdf [accessed 2023-02-01]
25. Uganda One Health strategic plan 2018-2022. Ministry of Health Republic of Uganda. 2018. URL: https://health.go.ug/sites/default/files/Uganda%20OHSP%20Final%20Launched%2015-02-2018%20%281%29.pdf [accessed 2023-02-01]
26. M100 performance standards for antimicrobial susceptibility testing. Clinical & Laboratory Standards Institute. 2021 Mar. URL: https://clsi.org/media/z2uhcbmv/m100ed31_sample.pdf [accessed 2024-04-23]
27. NRECCLWM programme management report 2022. Ministry of Water and Environment Republic of Uganda. 2022. URL: https://www.mwe.go.ug/library/nrecclwm-programme-management-report-2022 [accessed 2023-02-01]
28. Nsubuga P, White ME, Thacker SB, Anderson MA, Blount SB, Broome CV, et al. Public health surveillance: a tool for targeting and monitoring interventions. In: Jamison DT, Breman JG, Measham AR, Alleyne G, Claeson M, Evans DB, et al, editors. Disease Control Priorities in Developing Countries. 2nd edition. Washington, DC: The International Bank for Reconstruction and Development; 2006.
29. Queenan K, Häsler B, Rushton J. A One Health approach to antimicrobial resistance surveillance: is there a business case for it? Int J Antimicrob Agents 2016 Oct;48(4):422-427. [doi: 10.1016/j.ijantimicag.2016.06.014] [Medline: 27496533]
30. Khurana A, Sinha R. Tackling AMR starts with the environment. Sanitation Environment 2019:78-80.
31. Rizzo L, Manaia C, Merlin C, Schwartz T, Dagot C, Ploy MC, et al. Urban wastewater treatment plants as hotspots for antibiotic resistant bacteria and genes spread into the environment: a review. Sci Total Environ 2013 Mar 01;447:345-360. [doi: 10.1016/j.scitotenv.2013.01.032] [Medline: 23396083]
32. Martinez JL. Environmental pollution by antibiotics and by antibiotic resistance determinants. Environ Pollut 2009 Nov;157(11):2893-2902. [doi: 10.1016/j.envpol.2009.05.051] [Medline: 19560847]
33. Berendonk TU, Manaia CM, Merlin C, Fatta-Kassinos D, Cytryn E, Walsh F, et al. Tackling antibiotic resistance: the environmental framework. Nat Rev Microbiol 2015 May;13(5):310-317. [doi: 10.1038/nrmicro3439] [Medline: 25817583]
34. Iskandar K, Molinier L, Hallit S, Sartelli M, Hardcastle TC, Haque M, et al. Surveillance of antimicrobial resistance in low- and middle-income countries: a scattered picture. Antimicrob Resist Infect Control 2021 Mar 31;10(1):63. [doi: 10.1186/s13756-021-00931-w] [Medline: 33789754]
35. Pandey R, Mukherjee R, Chang CM. Antimicrobial resistance surveillance system mapping in different countries. Drug Target Insights 2022;16:36-48. [doi: 10.33393/dti.2022.2482] [Medline: 36479338]

36. Amin MA, Pasha MH, Hoque MN, Siddiki AZ, Saha S, Kamal MM. Methodology for laboratory-based antimicrobial resistance surveillance in animals. Vet World 2022 Apr;15(4):1066-1079. [doi: 10.14202/vetworld.2022.1066-1079] [Medline: 35698528]
37. Jorge M, Awa AK. THE ESBL tricycle amr surveillance project: a simple, ONE HEALTH approach to global surveillance. AMR Control. 2017. URL: http://resistancecontrol.info/2017/the-esbl-tricycle-amr-surveillance-project-a-simple-one-health-approach-to-global-surveillance/ [accessed 2022-02-01]
38. Martínez JL. Antibiotics and antibiotic resistance genes in natural environments. Science 2008 Jul 18;321(5887):365-367. [doi: 10.1126/science.1159483] [Medline: 18635792]
39. Genthe B, Ndlela L, Madlala T. Antimicrobial resistance screening and profiles: a glimpse from the South African perspective. J Water Health 2020 Dec;18(6):925-936. [doi: 10.2166/wh.2020.034] [Medline: 33328364]
40. Moges F, Endris M, Belyhun Y, Worku W. Isolation and characterization of multiple drug resistance bacterial pathogens from waste water in hospital and non-hospital environments, Northwest Ethiopia. BMC Res Notes 2014 Apr 05;7:215. [doi: 10.1186/1756-0500-7-215] [Medline: 24708553]
41. Nabadda S, Kakooza F, Kiggundu R, Walwema R, Bazira J, Mayito J, et al. Implementation of the World Health Organization Global Antimicrobial Resistance Surveillance System in Uganda, 2015-2020: mixed-methods study using national surveillance data. JMIR Public Health Surveill 2021 Oct 21;7(10):e29954. [doi: 10.2196/29954] [Medline: 34673531]
42. Amaya E, Reyes D, Paniagua M, Calderón S, Rashid M, Colque P, et al. Antibiotic resistance patterns of Escherichia coli isolates from different aquatic environmental sources in León, Nicaragua. Clin Microbiol Infect 2012 Sep;18(9):E347-E354. [doi: 10.1111/j.1469-0691.2012.03930.x] [Medline: 22738232]
43. Aslam B, Chaudhry TH, Arshad MI, Muzammil S, Siddique AB, Yasmeen N, et al. Distribution and genetic diversity of multi-drug-resistant at the human-animal-environment interface in Pakistan. Front Microbiol 2022;13:898248. [doi: 10.3389/fmicb.2022.898248] [Medline: 36147844]
44. Holt KE, Wertheim H, Zadoks RN, Baker S, Whitehouse CA, Dance D, et al. Genomic analysis of diversity, population structure, virulence, and antimicrobial resistance in Klebsiella pneumoniae, an urgent threat to public health. Proc Natl Acad Sci U S A 2015 Jul 07;112(27):E3574-E3581. [doi: 10.1073/pnas.1501049112] [Medline: 26100894]
45. Bouza E, Cercenado E. Klebsiella and enterobacter: antibiotic resistance and treatment implications. Semin Respir Infect 2002 Sep;17(3):215-230. [doi: 10.1053/srin.2002.34693] [Medline: 12226801]
46. Leclercq R, Cantón R, Brown DFJ, Giske CG, Heisig P, MacGowan AP, et al. EUCAST expert rules in antimicrobial susceptibility testing. Clin Microbiol Infect 2013 Feb;19(2):141-160. [doi: 10.1111/j.1469-0691.2011.03703.x] [Medline: 22117544]
47. Sánchez-Bautista A, Coy J, García-Shimizu P, Rodríguez JC. From CLSI to EUCAST guidelines in the interpretation of antimicrobial susceptibility: What is the effect in our setting? Enferm Infecc Microbiol Clin (Engl Ed) 2018 Apr;36(4):229-232. [doi: 10.1016/j.eimc.2017.03.003] [Medline: 28479139]
48. Jabbar Ibrahim IA, Kareem Hameed TA. Isolation, characterization and antimicrobial resistance patterns of lactose-fermenter Enterobacteriaceae isolates from clinical and environmental samples. Open J Med Microbiology 2015;05(04):169-176. [doi: 10.4236/ojmm.2015.54021]
49. Abakpa G, Umoh V, Ameh J, Yakubu S, Kwaga J, Kamaruzaman S. Diversity and antimicrobial resistance of Salmonella enterica isolated from fresh produce and environmental samples. Environ Nanotechnology Monitoring Manage 2015 May;3:38-46. [doi: 10.1016/j.enmm.2014.11.004]
50. Singh S, Yadav AS, Singh SM, Bharti P. Prevalence of Salmonella in chicken eggs collected from poultry farms and marketing channels and their antimicrobial resistance. Food Res Int 2010 Oct;43(8):2027-2030. [doi: 10.1016/j.foodres.2010.06.001]
51. Bell RL, Kase JA, Harrison LM, Balan KV, Babu U, Chen Y, et al. The persistence of bacterial pathogens in surface water and its impact on global food safety. Pathogens 2021 Oct 27;10(11):1391. [doi: 10.3390/pathogens10111391] [Medline: 34832547]
52. Dewey-Mattia D, Manikonda K, Hall AJ, Wise ME, Crowe SJ. Surveillance for foodborne disease outbreaks - United States, 2009-2015. MMWR Surveill Summ 2018 Jul 27;67(10):1-11. [doi: 10.15585/mmwr.ss6710a1] [Medline: 30048426]
53. Furtula V, Jackson C, Farrell E, Barrett J, Hiott L, Chambers P. Antimicrobial resistance in Enterococcus spp. isolated from environmental samples in an area of intensive poultry production. Int J Environ Res Public Health 2013 Mar 12;10(3):1020-1036. [doi: 10.3390/ijerph10031020] [Medline: 23481592]
54. Pérez-Etayo L, González D, Leiva J, Vitas AI. Multidrug-resistant bacteria isolated from different aquatic environments in the North of Spain and South of France. Microorganisms 2020 Sep 16;8(9):1425. [doi: 10.3390/microorganisms8091425] [Medline: 32947947]
55. Odonkor ST, Addo KK. Prevalence of multidrug-resistant isolated from drinking water sources. Int J Microbiol 2018;2018:7204013. [doi: 10.1155/2018/7204013] [Medline: 30210545]
56. Balasa G, Levengood E, Battistelli J, Franklin R. Diversity of multidrug-resistant bacteria in an urbanized river: a case study of the potential risks from combined sewage overflows. Water 2021 Aug 01;13(15):2122. [doi: 10.3390/w13152122]
57. Pezzani MD, Tornimbene B, Pessoa-Silva C, de Kraker M, Rizzardo S, Salerno ND, et al. Methodological quality of studies evaluating the burden of drug-resistant infections in humans due to the WHO Global Antimicrobial Resistance Surveillance

System target bacteria. Clin Microbiol Infect 2021 Jan 13;27(5):687-696. [doi: 10.1016/j.cmi.2021.01.004] [Medline: 33450389]

Abbreviations

AMR: antimicrobial resistance
MDR: multidrug resistance
MWE: Ministry of Water and Environment
NWQRL: National Water Quality Reference Laboratory
TWG: technical working group

Edited by T Leung, G Eysenbach; submitted 06.07.23; peer-reviewed by G Mboowa, H Borhany; comments to author 04.10.23; revised version received 08.11.23; accepted 22.03.24; published 07.05.24.

Please cite as:
Katumba G, Mwanja H, Mayito J, Mbolanyi B, Isaasi F, Kibombo D, Namumbya J, Musoke D, Kabazzi J, Sekamatte M, Idrakua L, Walwema R, Lamorde M, Kakooza F, Etimu S
Establishing Antimicrobial Resistance Surveillance in the Water and Environment Sector in a Resource-Limited Setting: Methodical Qualitative and Quantitative Description of Uganda's Experience From 2021 to 2023
JMIRx Bio 2024;2:e50588
URL: https://bio.jmirx.org/2024/1/e50588
doi:10.2196/50588
PMID:

Original Paper

In-Silico Works Using an Improved Hovorka Equations Model and Clinical Works on the Control of Blood Glucose Levels in People With Type 1 Diabetes: Comparison Study

Ayub Md Som[1*], MSc, PhD; Nur Amanina Mohd Sohadi[1*], BEng, MSc; Noor Shafina Mohd Nor[2*], MB BCh BAO, BMedSc, MRCP; Sherif Abdulbari Ali[1*], MSc, PhD; Mohd Aizad Ahmad[1*], BEng, MSc, PhD

[1]School of Chemical Engineering, College of Engineering, Universiti Teknologi MARA, Shah Alam, Malaysia

[2]Department of Peadiatrics, Faculty of Medicine, Universiti Teknologi MARA, Sungai Buloh, Malaysia

[*]all authors contributed equally

Corresponding Author:
Ayub Md Som, MSc, PhD
School of Chemical Engineering
College of Engineering
Universiti Teknologi MARA
Block 5, Level 10 Engineering Complex
Shah Alam, 40450
Malaysia
Phone: 60 173211463
Email: ayub522@uitm.edu.my

Related Articles:

Companion article: https://www.biorxiv.org/content/10.1101/2022.09.23.509189v1

Companion article: https://bio.jmirx.org/2024/1/e63851

Companion article: https://bio.jmirx.org/2024/1/e64403

Companion article: https://bio.jmirx.org/2024/1/e64442

Abstract

Background: People with type 1 diabetes (T1D) depend on external insulin to regulate their blood glucose level (BGL) within the normoglycemic range between 4.0 to 7.0 mmol/L. Patients with T1D routinely conduct self-monitoring of blood glucose through finger pricks before insulin injections. An artificial pancreas is an innovative device that mimics the function of a healthy pancreas. Despite its recent advancement, the control algorithms used in an artificial pancreas are still lagging in delivering the proper insulin dosage to patients with T1D. Previous researchers attempted to improve the interrelation between parameters and variables in the original Hovorka equations model, later known as the improved Hovorka equations model; however, the improved equations model has not been tested in terms of its usability to regulate and control the BGL in a safe range for 2 or more people with T1D.

Objective: This study aimed to simulate the improved Hovorka equations model using actual patients' data via MATLAB programming coupled with enhanced model-based predicted control and determine the optimum bolus insulin. The study then compares the performance results obtained from in-silico and clinical works.

Methods: Data from 3 patients were collected from clinic 1—Clinical Training Centre, Universiti Teknologi MARA Hospital, Sungai Buloh, Selangor—upon getting approval from the Universiti Teknologi MARA Ethics Committee. The inclusion criteria for participation were, namely having T1D, age 11-14 years, and highly dependent on insulin injection with four or more finger pricks or self-monitoring of blood glucose for BGL measurements per day. The patients with T1D typically received meals three times per day: breakfast, lunch, and dinner. A closed-loop algorithm (enhanced model-based predicted control) was used for the

in-silico test, whereas an open-loop therapy was used for the clinical validation. As for the data analysis of patients, *P* values from a multiple linear regression were used to model the relationship between meal, insulin, and BGL.

Results: The optimum bolus insulins for patient 1 were 83.33, 33.33, and 16.67 mU/min; for patient 2 were 66.67, 50.01, and 33.33 mU/min; and for patient 3 were 100.02, 83.33, and 66.67 mU/min for breakfast, lunch, and dinner, respectively. As for the in-silico works, the percentages of time that the BGL was on target for patients 1, 2, and 3 were 79.59%, 87.76%, and 71.43%, respectively, as compared to the clinical works with <50%. A small *P* value (*P*<.001) indicated that the variables were significant. However, when compared to the BGL profile, both profiles were not comparable in simulating the BGL for patients with T1D.

Conclusions: The in-silico work was not comparable to the clinical work in simulating the BGL for patients with T1D due to the different methodologies used and the insufficient information that was reported to reproduce the calculation of the optimal bolus insulin.

(JMIRx Bio 2024;2:e43662) doi:10.2196/43662

KEYWORDS

blood glucose level; closed-loop system; Hovorka model; in-silico work; meal disturbance; type 1 diabetes mellitus

Introduction

Diabetes is a chronic disease that is characterized by high blood glucose levels (BGLs). It occurs when beta cells in the pancreas produce insufficient insulin or cells are unable to use insulin effectively. Insulin is crucial in blood glucose regulations by promoting glucose uptake, consequently lowering the BGL [1], which should be regulated within the normoglycemic range between 4.0 and 7.0 mmol/L [2]. Maintaining BGLs in a safe range can help prevent long-term complications related to hyperglycemia (high BGL) and hypoglycemia (low BGL). A lack of insulin production in patients with type 1 diabetes (T1D) thus disrupts blood glucose regulation. T1D commonly occurs in children and adolescents. The incidence of T1D is more prevalent in Northern Europe than in the rest of the world. The International Diabetes Federation reported 977 cases of T1D in Malaysian children ages 0 to 19 years in 2019 [3]. People with T1D must monitor their BGL via finger pricks and either perform self-monitoring of blood glucose (SMBG) or take multiple daily injections (MDI) of insulin to regulate their BGL.

The current practice for blood glucose management is invasive, which causes distress to patients. Thus, the introduction of an artificial pancreas device (APD), also known as a closed-loop system, has improved the quality of life for people with T1D for the last few decades. An APD has the potential to impact millions of people by helping regulate BGLs. Additionally, being able to estimate this (even a low-end estimate) with modeling work reduces material costs, time, and patient risk. Despite the recent advancements in APDs, the control algorithms used are still lagging in delivering the proper insulin dosage to people with T1D. Previous works had modified some equations in the subsections of the Hovorka model [4], which is also known as the improved Hovorka equations model, in regulating the BGL within a normoglycemic range (4.0-7.0 mmol/L) [5,6]. However, the improved Hovorka equations model has not yet been tested in terms of its usability to regulate and control the BGLs in a safe range for two or more people with T1D. This study aims to simulate the improved Hovorka equations model using actual patients' data via MATLAB programming (in-silico works) coupled with enhanced model-based predicted control (eMPC) and compare its performances with clinical works. This study is a continuation of preliminary in-silico works from the previous studies [7-9] carried out on a single patient with T1D using the improved Hovorka equations model.

Methods

Ethics Approval on Data Collection for Clinical Works

Ethical approval for this study (REC/435/19) was granted by the Universiti Teknologi MARA (UiTM) Ethics Committee before data collection commenced (reference letter 600-TNCPI (5/1/6) dated 29 October 2019). The data collection and patients' information required in this study were obtained from clinic 1—Clinical Training Centre, UiTM Medical Specialist Centre, UiTM Hospital, Sungai Buloh, Selangor. Information sheets were given, and formal consent for participation from the parents or legal guardians of patients with T1D was obtained since the patients were all younger than 18 years. During the appointment, parents or guardians of participants (ie, patients with T1D) were allowed to ask questions before signing the consent form. The participants could withdraw from the study at any time without penalty. Participants' details, such as names or other personal identifiers, remain confidential in the data used by the researchers.

A total of 3 patients with T1D were recruited following informed consent. The inclusion criteria of patients were patients with T1D; age 11-14 years; and highly dependent on insulin injection with four or more finger pricks or SMBG for BGL measurements per day, MDI of insulin, and a well-documented bolus insulin requirement. The exclusion criteria were patients with T1D with evidence of hypoglycemia unawareness; known or suspected allergy to insulin; or established neuropathy, nephropathy, and retinopathy. Patients with T1D attended the clinic every 3 months and required blood taking as routine follow-up care. The amount of blood taken by the pediatrician was 5 mL each for fasting glucose and fasting insulin and was taken once. The additional data required included the patient's name, age, gender, race, body weight, BMI, type and amounts of meals consumed (specifically carbohydrates), meal time and duration, T1D history (years diagnosed with T1D), fasting plasma glucose level, fasting plasma insulin level, bolus insulin administered, and other relevant information. The patients with T1D typically received meals three times per day: breakfast, lunch, and dinner. The patients' data were termed clinical data

(clinical work) throughout the study. Table 1 summarizes the demographic profiles of the patients with T1D, including gender, age, and body weight.

Table 2 provides a 24-hour meal summary for all patients that includes meal time and duration, and amounts of meals consumed (in grams of carbohydrates).

Table 1. Demographic profiles of patients with type 1 diabetes.

Patient	Gender	Age (years) in 2020	Body weight (kg)
1	Male	13	27.0
2	Female	11	26.3
3	Male	14	49.9

Table 2. Meal summaries for patients 1-3 over 24 hours.

Meal	Mealtime (hours passed since simulation started at 5 AM)	Meal duration (min)	Total carbohydrates (g)
Patient 1			
Breakfast	7:30 AM (2.5 h)	30	36
Lunch	1:30 PM (8.5 h)	30	36
Dinner	7 PM (14 h)	30	47
Patient 2			
Breakfast	6 AM (1 h)	10	30
Lunch	1 PM (8 h)	20	41
Dinner	8 PM (15 h)	20	49
Patient 3			
Breakfast	8:15 AM (3.5 h)	30	67
Lunch	3 PM (10 h)	10	124
Dinner	8:45 PM (15.5 h)	15	47

Mathematical Model for In-Silico Works

The improved Hovorka equations [5,7] based on the Hovorka model [4] are specifically designed for people with T1D. The diagram of the improved Hovorka equations model is illustrated in Figure 1 [7]. The model has two inputs: meal disturbances and bolus insulin. It comprises three subsystems: the glucose subsystem, insulin subsystem, and insulin action subsystem. Equations 1 and 2 are used for the glucose subsystem:

where Q_1 (mmol) is the mass of glucose in an accessible compartment; Q_2 (mmol) is the mass of glucose in a nonaccessible compartment; k_{w1}, $k_{w11,}$ k_{w2}, k_{w22}, k_{w3}, and k_{w33} (min^{-1}) are activation rates; k_{12} (min^{-1}) is the transfer rate; EGP_0 is the endogenous glucose production (EGP) extrapolated to zero insulin concentration; V_G (L/kg) is the glucose distribution volume; G (mmol/L) is the glucose concentration; x_1, x_2, and x_3 are the effects of insulin on glucose transport and distribution, glucose disposal, and EGP, respectively; $F_{01}{}^c$ ($mmol\ min^{-1}\ kg^{-1}$) is the total non–insulin-dependent glucose flux; and F_R (mmol/min) is the renal glucose clearance.

When a meal is consumed, the carbohydrate content will be broken down into glucose before being converted into energy, thus increasing the BGL. Equation 5 was used for observing the effect of meal disturbances on BGLs.

where D_G is the amount of carbohydrates digested (mmol), A_G is the carbohydrate availability, and $t_{max,G}$ is the time-to-maximum of carbohydrate absorption (min).

Equations 6-8 show the insulin subsystem. Insulin is administered subcutaneously. This method is less invasive than the intravenous method, in which insulin is injected directly into the bloodstream.

The insulin absorption rate in the bloodstream is given in equation 9.

where S_1 and S_2 (mU) are the insulin sensitivity in accessible and nonaccessible compartments, respectively; u(t) (mU/min) is the insulin infusion rate; $t_{max,I}$ (min) is the time-to-maximum of insulin absorption; U_I (mU/min) is the insulin absorption rate; V_I (L/kg) is the insulin distribution volume; and k_e (min^{-1}) is the fractional elimination rate.

The insulin action subsystem is shown in equations 10-12. The insulin-glucose interaction can be observed in this subsystem.

The constants and parameters involved in the equations are shown in Tables 3 and 4, respectively.

Figure 1. Schematic diagram of the improved Hovorka equations model.

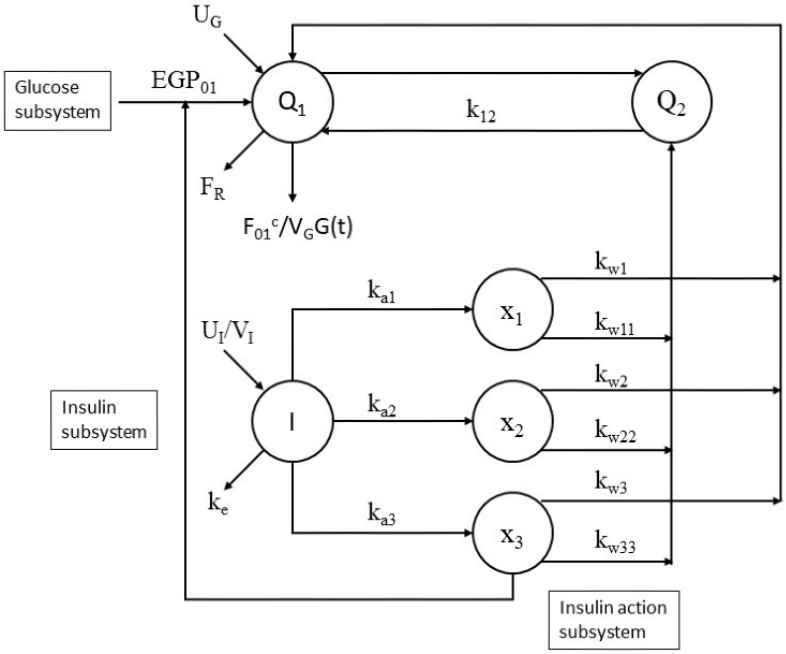

Table 3. Constant values of the improved Hovorka equations model [7,10].

Symbol	Constant	Value and unit
k_{12}	Transfer rate from nonaccessible to accessible compartment	0.066 min^{-1}
k_{a1}	Deactivation rate of glucose	0.006 min^{-1}
k_{a2}	Deactivation rate of glucose	0.06 min^{-1}
k_{a3}	Deactivation rate of glucose	0.03 min^{-1}
k_{w1}	Activation rate of glucose	50.1 min^{-1}
k_{w11}	Activation rate of glucose	–10 min^{-1}
k_{w2}	Activation rate of glucose	50.1 min^{-1}
k_{w22}	Activation rate of glucose	–0.01 min^{-1}
k_{w3}	Activation rate of glucose	50.1 min^{-1}
k_{w33}	Activation rate of glucose	–0.01 min^{-1}
k_e	Insulin elimination from plasma	0.138 min^{-1}
V_I	Insulin distribution volume	0.12 Lkg^{-1}
V_G	Glucose distribution volume	0.16 Lkg^{-1}
A_G	Carbohydrate bioavailability	0.8 (unitless)
$t_{max,G}$	Time-to-maximum of carbohydrate absorption	40 min

Table 4. Parameter values of the improved Hovorka equations model [7,10].

Symbol	Parameter	Value and unit
EGP_0	Endogenous glucose production extrapolated to zero insulin concentration	0.0161 mmol kg^{-1} min^{-1}
F_{01}	Non–insulin-dependent glucose flux	0.0097 mmol kg^{-1} min^{-1}
$t_{max,I}$	Time-to-maximum of absorption of subcutaneously injected short-acting insulin	55 min

Meals and Insulin Requirement

The in-silico work on the meal disturbances was based on the patients' daily meal intake. Table 5 shows an example of the amount of daily meal intake, specifically carbohydrates, suggested for 13-year-old male patients. The suggested meal intake is based on the total daily calorie requirement, which varies according to age and gender (refer to Table 6). It consists of breakfast, lunch, and dinner, which are adopted into the in-silico work using the improved Hovorka equations model. Generally, 50% of the calorie intake comes from carbohydrates [11].

Table 5. Example of amount of carbohydrate (CHO) intake for a 13-year-old male patient.[a]

Meal	Time	CHO (g)	CHO (mol)	CHO (mmol)
Breakfast	6 AM	60	2.068	2068
Lunch	12 PM	90	3.102	3102
Dinner	7 PM	90	3.102	3102
Total	__[b]	240	8.272	8272

[a]Source: patient with type 1 diabetes at clinic 1—Clinical Training Centre, Universiti Teknologi MARA Medical Specialist Centre, Sungai Buloh.
[b]Not applicable.

Table 6. Daily energy (calorie) requirement by weight for children and adolescents [12].

Age	Energy (kcal/kg/day)
0-6 months	≥108
7-12 months	≥98
1-3 years	102
4-6 years	90
7-10 years	70
11-14 years	Male: 55; female: 47
15-18 years	Male: 45; female: 40

The calculations of carbohydrate intake and insulin requirement can be further explained in the following example.

For a 13-year-old male patient with T1D and a body weight of 36 kg, the daily energy (calorie) requirement by weight based on Table 6 for male patients ages 11-14 years can be calculated as:

Referring to the previous calculation, a patient with a body weight of 36 kg required approximately 240 grams of carbohydrates. The bolus (exogenous) insulin required per day can be calculated based on this value. If excess insulin is infused, patients may experience hypoglycemia (low BGL) [13]. Generally, 1 unit of rapid-acting insulin can cover 10-15 grams of carbohydrates [14]. However, this range can vary from 6 to 30 grams depending on the individual's sensitivity to insulin, and insulin sensitivity for an individual may vary for a different period [14]. The total daily dose (TDD) of insulin can be calculated based on the insulin-to-carbohydrate ratio used, which is 1:15, as shown in equation 13.

TDD = Total amount of CHO intake **(13)**

÷ 15 g of CHO disposed of by 1 unit of insulin

Therefore,

TDD = 240 g CHO ÷ 15 g of CHO disposed of by 1 unit of insulin

TDD = 16 units of rapid-acting insulin

The TDD of insulin required to cover 240 grams of carbohydrate intake is 16 units based on the above calculation. In addition, a few parameters related to the patient's body weight are being considered, including V_I, V_G, EGP_0, and F_{01} as seen in Tables 3 and 4. Another calculation example is shown below.

For patient 1, with a body weight of 27 kg, the following parameter values were used:

The same equations were applied to patients 2 and 3 with a body weight of 26.3 kg and 49.9 kg, respectively.

Consequently, all simulated data via in-silico works for the 3 patients with T1D were collected and plotted to produce profiles of BGL versus time for each patient. Upon completion of data collection and construction of sufficient BGL versus time profiles for both clinical and in-silico works, these two results were analyzed and compared for any similarities or differences.

Enhanced Model Predictive Control

The eMPC used in this study is an extension of MPC, which uses a mathematical model of a system to predict its future behavior over a certain period. The prediction was then used to determine the optimal control to achieve the desired objective. To control the BGL in patients with T1D, eMPC was integrated into the improved Hovorka equations model meant for patients with T1D to predict BGLs in response to different insulin dosages and other inputs, thus optimizing the insulin dosing in real time. The model considers factors that influence the outcome of the BGL profile such as the current BGL, amount of carbohydrates consumed, and time and duration of meals and insulin. The eMPC algorithm uses these predictions to calculate the optimal insulin dosage so patients can achieve a desired BGL target range.

Figure 2 [15] illustrates the general concept of MPC. The prediction horizon, P, would be the outcome of the BGL based on the previous inputs, u, insulin infusion rate, and meal disturbances. Constraints were imposed such that the target range for BGL, G(t), was within the normoglycemic range of 4.0 to 7.0 mmol/L. The set point is set to 5 mmol/L. The insulin infusion rate, u(t), was between 0 to 35 U/hr based on the current insulin pump specification [16]. The control algorithm predicted the BGL output to be closer to the set point. The eMPC is prone to deliver more insulin to counter the hyperglycemia event. The controller is also able to shut down insulin pump infusion to minimize the occurrence of hypoglycemia.

Figure 2. General concept of model predictive control.

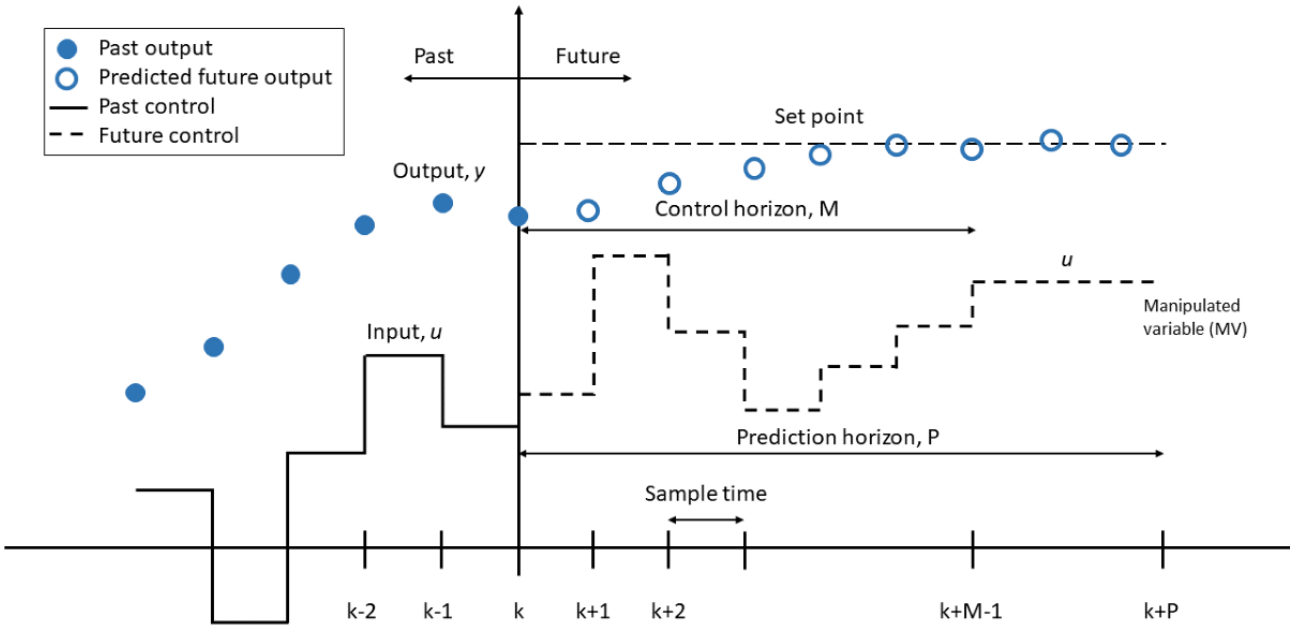

Initial values for S_1, S_2, x_1, x_2, and x_3 were set at zero since the insulin had not been injected into the patient's body, and the insulin being administered, which caused glucose transport/distribution, glucose disposal, and EGP, had not yet occurred. The bolus insulin for each meal was obtained on a trial-and-error basis to minimize the BGL to the normal range while avoiding hypoglycemia (<4.0 mmol/L). Since the blood glucose ($t_{max,G}$=40 min) reached the bloodstream sooner than the insulin ($t_{max,I}$=55 min), the bolus insulin was administered 30 minutes before a meal due to the time lag for insulin to penetrate the skin and take effect. Figures 3 and 4 show a part of the control system algorithm for glucose, G(i), and bolus insulin, u(i). When the BGL falls below the range, the insulin pump stops delivering insulin. In contrast, the insulin is continuously delivered when the BGL is above 4.0 mmol/L.

Figure 3. Part of the control system algorithm: glucose.

```
% Glucose
G(i) = Q1(i)/Vg;
if G(i)>=4.5
    Fc_01 = F01;
else
    Fc_01 = F01*G(i)/4.5;
end
if G(i)>=9
    Fr(i) = 0.003*(G(i)-9)*Vg;
else
    Fr(i) = 0;
end
```

Figure 4. Part of the control system algorithm: bolus insulin.

```
% Bolus insulin
if t(i)>=120 && t(i)<=121
     u(i) = 83.33;
elseif t(i)>=480 && t(i)<=481
    u(i) = 33.33;
elseif t(i)>=810 && t(i)<=811
    u(i) = 16.67;
else
    if G(i) <= 4
        u(i) = 0;
    else
        u(i) = u(1); %u(1)
    end
end
```

The in-silico work of BGLs against time was conducted, and the results were compared to the clinical work. The comparison focused on assessing how well the in-silico model performed in controlling BGLs. This evaluation helps determine the accuracy and effectiveness of the in-silico model in mimicking real-world BGL dynamics.

Data Analysis of Patients

Previously, the BGL profiles for both works were created. The BGL profiles in the clinical work were done manually by inserting related data and plotting the BGL profiles using Microsoft Excel 2016. Conversely, the BGL profiles in the silico work were generated using MATLAB R2015a (MathWorks). From there, the pattern of blood glucose profiles was observed and identified, such as the time of day when BGLs tend to be the highest or lowest, the frequency of hypoglycemic and hyperglycemic events, and the variability of BGLs. The BGL profiles were used to evaluate the patients' glycemic control over the selected time frame by calculating the average BGL and the percentage of time spent in different glycemic ranges, such as hypoglycemia, normoglycemia, and hyperglycemia, among other things.

Thus, Microsoft Excel 2016 was used to facilitate the data analysis work. Data such as the amounts of meals (grams of carbohydrates), mealtime and duration, and amount of plasma insulin and plasma glucose were used. A regression analysis was selected, which is a statistical method generally used to analyze the relationship between two or more variables. A multiple linear regression (MLR) is a type of regression analysis that is done to analyze the relationship between two or more independent variables and a dependent variable. In this case, the two independent variables were the amounts of meals consumed and insulin administered, while the dependent variable was the predicted BGL. The following steps were performed for the MLR.

The first step was to enter the data into the Excel spreadsheet with one column for the dependent variable and one or more columns for the independent variables. From the data tab, data analysis containing various analysis tools was selected. The regression analysis was chosen where the selected input of the y range was the BGL outcome and the inputs of the x range were meals consumed and insulin administered. A new worksheet tab appeared, giving the summary output of the regression statistics and other relevant information. The probability value (P value) and coefficient of determination (R^2) are important statistical measures used in regression analysis. The P value was used to test the research hypothesis (whether to reject or support the null hypothesis). A small P value (P<.05) indicates that the relationship between the variables is significant and the null hypothesis is rejected. R^2 measures how much the independent variables explain the variation in the dependent variable. A high R^2 value indicates a better fit of the model to the data.

Results

Simulation of Meal Disturbances

The amount of food consumed during a meal, especially carbohydrates, has been shown to impact the meal rate directly. When people consume larger meals, they tend to eat at a slower rate, taking more time to chew and swallow their food. This is likely because larger meals require more time and effort to eat, resulting in a reduced meal rate as opposed to smaller meals [17]. Besides, the meal duration also has an impact on the meal rate. A shorter meal duration is associated with a faster meal rate than a longer one [18]. The calculation of the meal rate was referred to in [19]. The meal rates were determined by dividing the total carbohydrates (in grams of carbohydrates) by meal duration (in minutes).

The meal rate calculation is as follows:

Therefore, take patient 1 as an example:

The same thing applies to other meals for all patients and is summarized in Table 7. All patients consumed each meal at a different duration between 10 to 30 minutes. The simulation started at 5 AM, and patients had their first meal at least 1 hour after, that is, at 6 AM and onward.

Table 7. Meal rates for patients 1-3.

Meal	Meal duration (min)	Carbohydrates (g)	Meal rate (g/min)
Patient 1			
Breakfast	30	36	1.20
Lunch	30	36	1.20
Dinner	30	47	1.57
Patient 2			
Breakfast	10	30	3.00
Lunch	20	41	2.05
Dinner	20	49	2.45
Patient 3			
Breakfast	30	67	2.24
Lunch	10	124	12.40
Dinner	15	47	3.00

Based on the table, patient 1 has a fixed meal duration of 30 minutes for each meal. Although patient 1 consumed a smaller meal amount, patient 1 had the lowest meal rate due to longer meal duration. Patient 2 also had a fixed meal duration of 20 minutes, except for breakfast, which took only 10 minutes. The meal rate for patient 2 was comparatively similar to patient 1 since the meal amount and duration were quite close to one another. Patient 3 did not have a fixed meal duration, varying between 10 to 30 minutes for each meal. Patient 3 also consumed the largest meal in a shorter duration during lunch, thus having the largest meal rate.

The Effect of Meal Disturbances on BGL Profiles Between Clinical and In-Silico Works for Patient 1

In this section, in-silico works of BGLs with three meals were performed for patient 1. This BGL profile between clinical and in-silico works was compared and analyzed. The BGL profile was simulated using the improved Hovorka equations model. The patients' premeal and postmeal BGLs in clinical works are shown in Table 8.

Table 8. Blood glucose reading for patient 1 in 24 hours.

Meal	Blood glucose level (mmol/L)	
	Premeal	Postmeal
Breakfast	6.3	10.1
Lunch	15.2	19.3
Dinner	12.2	17.8

Figure 5 shows the BGL profile in a day for patient 1 for both clinical and in-silico works. Each peak shown in the graphs is the BGL fluctuation during breakfast, lunch, and dinner. The red line represents the normoglycemic range of 4.0 to 7.0 mmol/L. The blue and orange lines represent BGL profiles for in-silico and clinical works, respectively.

Figure 5. Blood glucose profile in a day between clinical and in-silico works for patient 1.

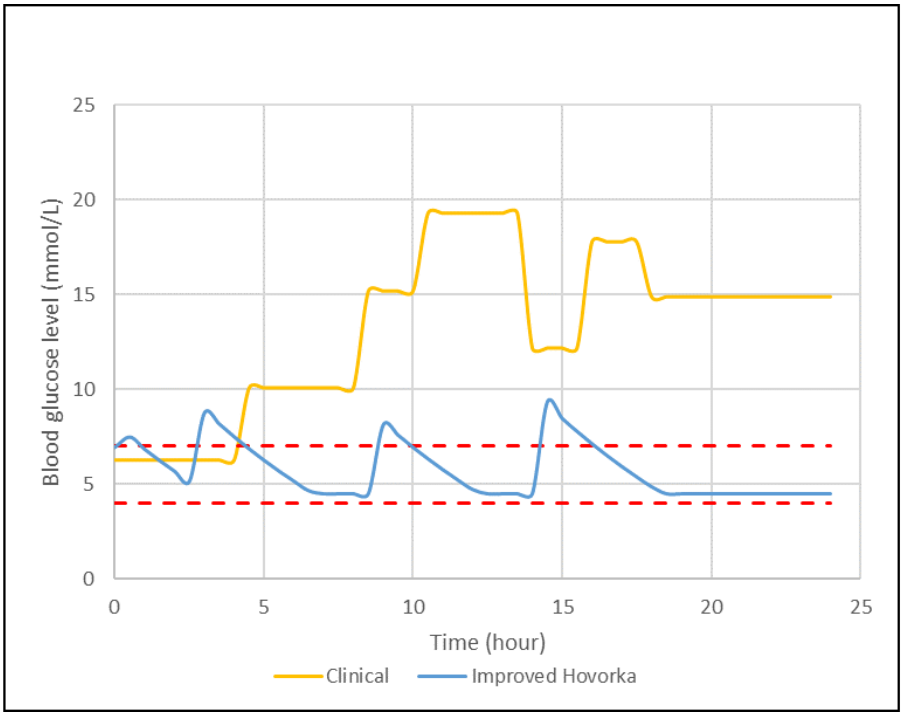

As shown in Figure 5, during the fasting stage (or no meal disturbances), patient 1 in the clinical work recorded a BGL value of 6.3 mmol/L; whereas in the in-silico work, it was 6.9 mmol/L. Initially, the BGL trends were similar during the first 3 hours. The BGL then fluctuated during breakfast, lunch, and dinner. However, the BGL in the in-silico work managed to achieve the normoglycemic range a few hours past the meal, as opposed to the patient in the clinical work who experienced hyperglycemia most of the day and only achieved normoglycemia for 18.37% of the time (ie, during breakfast). The average BGLs for the patient in the clinical and in-silico works were 13.21 mmol/L and 5.74 mmol/L, respectively. The highest BGL recorded in the clinical trials was 19.30 mmol/L post lunch. In the in-silico work, the highest BGL recorded was 9.31 mmol/L post dinner and normoglycemia was achieved 79.59% of the time.

The Effect of Meal Disturbances on BGL Profiles Between Clinical and In-Silico Works for Patient 2

In this section, in-silico works of BGL with three meals were performed for patient 2 and then compared and analyzed with the clinical works. The patient's premeal and postmeal BGLs in the clinical works are shown in Table 9.

Table 9. Blood glucose reading for patient 2 for 24 hours.

Meal	Blood glucose level (mmol/L)	
	Premeal	Postmeal
Breakfast	7.2	9.2
Lunch	9.2	7.8
Dinner	7.8	6.5

Figure 6 shows the BGL profile in a day for patient 2 for both clinical and in-silico works. As shown in the figure, the BGLs recorded for clinical and in-silico works at the fasting stage were 7.2 mmol/L and 6.9 mmol/L, respectively. It can be observed that the BGL profiles are quite similar in both works, especially post dinner. The average BGLs recorded for the patient in the clinical and in-silico works were 7.73 mmol/L and 5.29 mmol/L, respectively. The highest BGL recorded for patient 2 in the clinical work was 9.2 mmol/L, while in the in-silico work, it was 7.9 mmol/L. Patient 2 in the in-silico work stayed in the normoglycemic range for 87.76% of the time compared to the clinical work, which was 30.61% of the time. Even though patient 2 in the clinical work was unable to attain a longer duration of normoglycaemia, the BGL remained relatively low and closer to the normoglycemic range throughout the day.

Figure 6. Blood glucose profile in a day between clinical and in-silico works for patient 2.

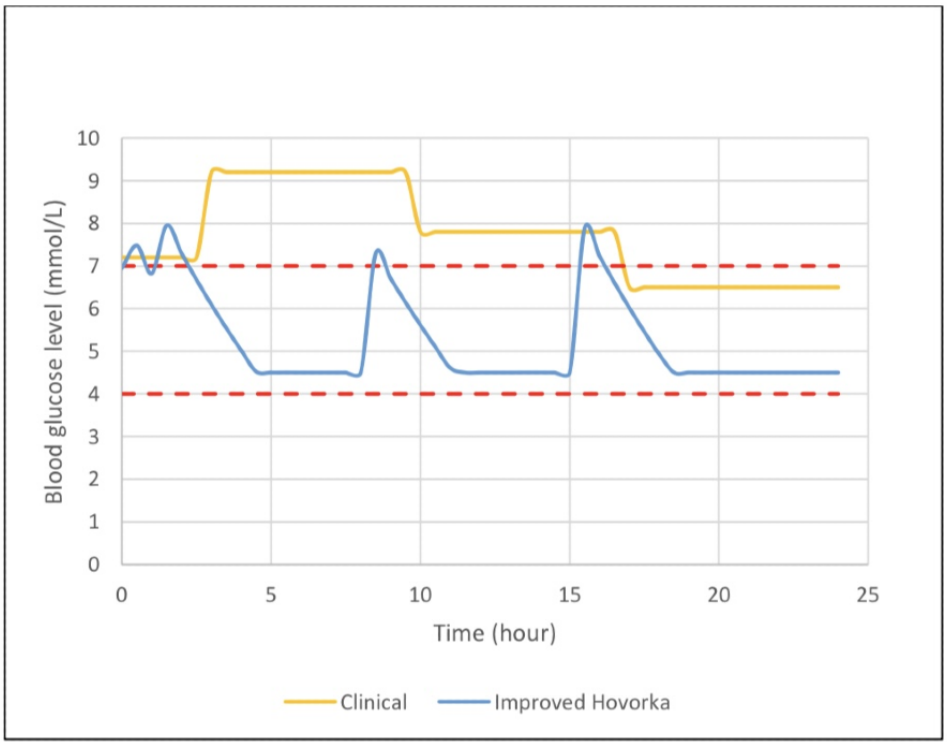

The Effect of Meal Disturbances on BGL Profiles Between Clinical and In-Silico Works for Patient 3

The in-silico works of BGL versus time with three meals were then compared and analyzed with the clinical works of patient 3. The patient's premeal and postmeal BGL in the clinical works are shown in Table 10.

Table 10. Blood glucose reading for patient 3 for 24 hours.

Meal	Blood glucose level (mmol/L)	
	Premeal	Postmeal
Breakfast	11.2	10.3
Lunch	10.3	14.3
Dinner	14.3	9.3

Figure 7 shows the BGL profile in a day for patient 3 for both clinical and in-silico works similar to the previous two patients. Initially, the BGLs recorded for the clinical and in-silico works were 11.2 mmol/L and 6.9 mmol/L, respectively. Here, one can observe that the postmeal BGLs are similar in both works. Throughout the day, the patient in the clinical work experienced hyperglycemia and was unable to reach the normoglycemic range, with the lowest BGL recorded being only 9.3 mmol/L. Conversely, normoglycemic range for the patient in the in-silico work was achieved 71.43% of the time. The average BGLs for patients in the clinical and in-silico works were 11.00 mmol/L and 6.22 mmol/L, respectively. The highest BGL recorded in the clinical and in-silico works were 14.3 mmol/L and 11.6 mmol/L, respectively.

Figure 7. Blood glucose profile in a day between clinical and in-silico works for patient 3.

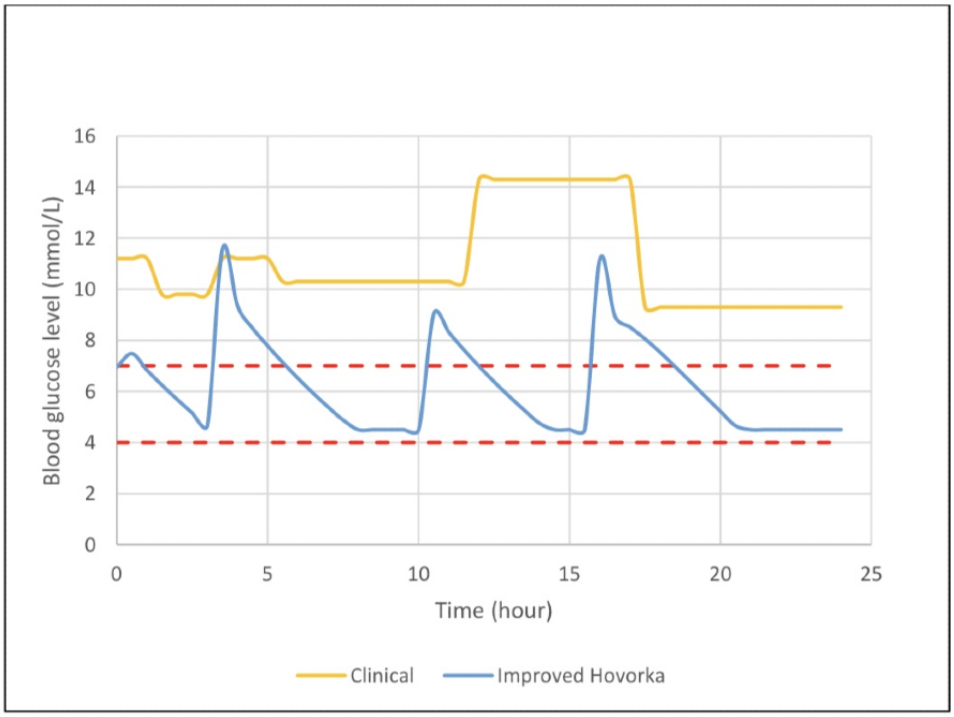

Optimum Bolus Insulin for Blood Glucose Regulations

Bolus insulin is used to control BGL at mealtime. The best time for insulin injection depends on the type of insulin used and the individual's need to achieve optimal BGL targets and reduce diabetes complications. The insulin is typically injected subcutaneously, either with a syringe or an insulin pen, and taken shortly before or after a meal [20]. The amount of bolus insulin needed depends on factors such as age, body weight, the amount of carbohydrates in the meal consumed, insulin sensitivity, and physical activity [21-23]. These factors help patients to determine the appropriate dose of bolus insulin needed.

Patients in the clinical work were given insulin during mealtime as opposed to the in-silico work in which the insulin was injected 30 minutes before a meal. Additionally, it is important to consider the timing of bolus insulin administration. Giving bolus insulin too early before a meal or too late after a meal can result in hypoglycemia and hyperglycemia, respectively. So, the bolus insulin administration was timed appropriately to match the timing of carbohydrate intake.

In this study, all patients used rapid-acting insulin to manage their BGL during mealtime to ensure their BGL would not deviate too far from the normoglycemic range (ie, 4.0-7.0 mmol/L) after each meal. Table 11 summarizes the amount of bolus insulin administered for all patients in the in-silico work.

Table 11. Amount of bolus insulin administered.

Meal	Bolus insulin (mU/min)		
	Patient 1	Patient 2	Patient 3
Breakfast	83.33	66.67	100.02
Lunch	33.33	50.01	83.33
Dinner	16.67	33.33	66.67

Data Analysis for Patients

As for the data analysis of patients between clinical and in-silico works, an MLR was used to model the relationship between meals, insulin, and BGL. The probability value (*P* value) is an important statistical element used to assess the significance of the relationship between these variables as well as to evaluate the accuracy of the simulation results. Table 12 summarizes the data analysis between clinical and in-silico works for all patients.

Table 12. Data analysis between clinical and in-silico works for all patients.

	P value	
	Clinical work	In-silico work
Patient 1	2.44×10^{-6}	4.17×10^{-7}
Patient 2	3.37×10^{-6}	4.14×10^{-6}
Patient 3	3.72×10^{-7}	9.96×10^{-5}

Discussion

Principal Findings

Observing the BGL trend for all patients in both works, the in-silico work performed better in managing BGLs as compared to the clinical work. Patients in the clinical work rarely achieved the glycemic target, 4.0 to 7.0 mmol/L. Patients 1 and 2 only achieved the target range during the morning and evening, respectively, whereas patient 3 did not achieve the target at all. The patients in the in-silico work were able to achieve the glycemic target more than 70% of the time as compared to the clinical work, which was less than 50% of the time.

The comparison of BGL against time between clinical and in-silico works can be challenging, especially when clinical data is limited, and, in this case, a continuous glucose monitoring (CGM) device is not used. Thus, the BGL profiles are different since patients in the clinical work used conventional methods to monitor their BGL (ie, SMBG and MDI); therefore, only a snapshot of BGLs at a particular time is available for comparison as seen in Figures 5-7. Studies have shown that the use of a CGM device can improve the time in range in clinical settings, thus improving the BGL profiles [24,25].

In this case, the only available data point was the focus since the clinical data was limited and did not cover the entire time span. While BGL simulations can help predict how the BGL of a patient with T1D may change under different conditions, they are not always accurate. This is because the mathematical models used in the simulations are based on assumptions about how the body works, and these assumptions may not always hold for every individual. Additionally, the simulation may not consider all the complex factors that can affect BGLs, such as exercise, stress, or illness. BGL monitoring can also be subjected to errors and variability in clinical settings. Factors such as the accuracy of the glucose meter or sensor, the timing and frequency of measurements, and the variability of patients' responses to interventions (eg, meals, physical activities, and medication) can all affect the reliability and accuracy of clinical BGL monitoring.

Based on Table 11, all patients were injected with more insulin in the morning, and the daily doses continued to decrease. Although the insulin sensitivity varies depending on the time of the day with reduced sensitivity in the evening [26,27], it can be observed that these patients have low insulin sensitivity in the morning; hence, they require more insulin doses to cater to the sudden BGL fluctuation. Patients' insulin sensitivity increases at lunch and dinner, as they require less bolus insulin to regulate the BGL. Despite larger bolus insulin doses given before mealtime, there is still a peak shortly after the meal is consumed, referring to Figures 5-7. Since the time for glucose absorption ($t_{max,G}$=40 minutes) is smaller than the time for insulin absorption to take effect ($t_{max,I}$=55 minutes), the glucose reaches the bloodstream sooner than the insulin, although insulin is infused earlier.

Among all patients, patient 3 injected the most amount of insulin compared to others since patient 3 weighed the heaviest, besides consuming the largest total amount of meals. Since increased body weight decreases insulin sensitivity, the patient's requirement for bolus insulin also increased [28]. In contrast, patients 1 and 2 in the in-silico work required less bolus insulin to control BGLs than patient 3 as they had lighter body weights and consumed meals in smaller portions. Their BGLs in the in-silico work only deviated slightly above the normoglycemic range throughout the day and were relatively more stable.

The probability value or *P* value is a statistical measure that indicates the probability of obtaining the observed results if the null hypothesis is true. The value is between 0 to 1. A *P* value <.05 is often considered statistically significant, meaning there is strong evidence against the null hypothesis, so the hypothesis is rejected. Based on Table 12, all patients in both clinical and in-silico works had a low *P* value (P<.001), which indicates that the variables are significant. However, when a comparison was made on the BGL profile, both profiles were not comparable due to different methodologies adopted in the design of the study.

Limitations of the Study

There are two main limitations discovered from the study, which in turn, make it infeasible to address the goal of determining the accuracy and effectiveness of the in-silico model in mimicking real-world BGL dynamics. First, different protocols and conditions were adopted in the methodology for the clinical and simulation works. As stated earlier, the open-loop therapy was used in the clinical work for evaluation purposes, whereas the closed-loop algorithm with eMPC was used in the in-silico test. To address this limitation for future work, it is essential to modify the simulation of the model to make the results more comparable with the clinical data. For instance, it is suggested that in the simulation work, the improved Hovorka equations model could be simulated using the same bolus, basal insulin, and meal carbohydrates used in the clinical trial. By doing so, they could compare the model output with each glucose measurement, preferably when CGM is available at our clinic for future use.

Second, the reported information was insufficient to reproduce the calculation of the optimal bolus in the in-silico simulations.

The insulin bolus was computed by trial and error as programmed earlier in its closed-loop algorithm. Since one of the main goals of the study is to determine the optimal bolus insulin, it would be advisable to detail the method followed to calculate it in the development of its new control algorithm for future works.

Conclusions

Through in-silico work using the improved Hovorka equations model and eMPC, the optimal amount of bolus insulin required to maintain BGLs within the normoglycemic range for adolescents with T1D has been determined. This approach demonstrates promising potential for precise insulin dosing strategies that aim to achieve stable glycemic control in real-world clinical scenarios. It was observed that patients had less insulin sensitivity in the morning, thus more bolus insulin was administered, and the amount gradually decreased throughout the day. The optimum bolus insulin for patient 1 was 83.33, 33.33, and 16.67 mU/min; patient 2 was 66.67, 50.01, and 33.33 mU/min; and patient 3 was 100.02, 83.33, and 66.67 mU/min for breakfast, lunch, and dinner, respectively.

Based on the comparison of BGL profiles between both clinical and in-silico works, patients in the clinical works experienced hyperglycemia most of the time and achieved the normoglycemic range less than 50% of the time. Conversely, there is a significantly increased time spent in the normoglycemic range for patients in the in-silico works using the improved Hovorka equations model with patients 1, 2, and 3 being in a normoglycemic range 79.59%, 87.76%, and 71.43% of the time, respectively. In conclusion, the in-silico work using the improved Hovorka equations model was not comparable to the clinical works to simulate BGLs with meal disturbances for people with T1D due to different methodologies adopted for both works as well as insufficient information for reproducing the calculation of the optimal bolus in the in-silico simulations. It is therefore recommended to, first, modify the simulation work of the improved model using the same bolus, basal insulin, and meal carbohydrates used in the clinical trial and, second, detail the method followed to calculate it in the development of a new control algorithm for future work.

Acknowledgments

The authors would like to thank the School of Chemical Engineering, College of Engineering, Universiti Teknologi MARA (UiTM) and the Paediatric Department, Faculty of Medicine, UiTM for all the support and assistance rendered. The authors sincerely acknowledge the participation of people with type 1 diabetes in this study.

The authors wish to acknowledge and extend their gratitude to the Ministry of Higher Education, Malaysia, and Research Management Centre, UiTM, for the financial support given under grant 600-RMC/GPK 5/3 (222/2020).

Data Availability

All data sets are presented in the main manuscript.

Authors' Contributions

NAMS conducted the programming work. AMS, NSMN, SAA, and MAA analyzed the data and supervised the overall research. NAMS and AMS wrote the paper.

Conflicts of Interest

None declared.

References

1. Lee J, Dassau E, Gondhalekar R, Seborg D, Pinsker JE, Doyle FJ. Enhanced model predictive control (eMPC) strategy for automated glucose control. Ind Eng Chem Res 2016 Nov 23;55(46):11857-11868 [FREE Full text] [doi: 10.1021/acs.iecr.6b02718] [Medline: 27942106]
2. Mayer-Davis E, Kahkoska A, Jefferies C, Dabelea D, Balde N, Gong C, et al. ISPAD Clinical Practice Consensus Guidelines 2018: definition, epidemiology, and classification of diabetes in children and adolescents. Pediatr Diabetes 2018 Oct;19 Suppl 27(Suppl 27):7-19 [FREE Full text] [doi: 10.1111/pedi.12773] [Medline: 30226024]
3. IDF Diabetes Atlas, Ninth edition. Brussels, Belgium: International Diabetes Federation; 2019.
4. Hovorka R, Canonico V, Chassin L, Haueter U, Massi-Benedetti M, Orsini Federici M, et al. Nonlinear model predictive control of glucose concentration in subjects with type 1 diabetes. Physiol Meas 2004 Aug;25(4):905-920. [doi: 10.1088/0967-3334/25/4/010] [Medline: 15382830]
5. Yusof NFM, Som AM, Ibrehem AS, Ali SA. Parameter addition in interaction of glucose and insulin for type 1 diabetes. 2012 Presented at: IEEE-EMBS Conference on Biomedical Engineering and Sciences; December 17-19, 2012; Langkawi, Malaysia. [doi: 10.1109/iecbes.2012.6498071]
6. Yusof NFM, Som AM, Ibrehem AS, Ali SA. System identification in modified diabetic model for nanochip controller. Adv Materials Res 2014 Jun;938:299-304. [doi: 10.4028/www.scientific.net/amr.938.299]

7. Som AM, Yusof NFM, Ali SA, Fuzil NS. Meal disturbance effect on blood glucose control for type 1 diabetes using improved Hovorka equations. Key Eng Materials 2019;797:158-167. [doi: 10.4028/www.scientific.net/kem.797.158]
8. Som AM, Yusof NFM, Ali SA, Sohadi NAM, Maarof AM, Nor NSM. In-silico works on the control of blood glucose level for type 1 diabetes mellitus (T1DM) using improved Hovorka equations. Int J Pharma Med Bio Sci 2020:144. [doi: 10.18178/ijpmbs.9.4.144-151]
9. Sohadi NAM, Som AM, Nor NSM, Ali SA, Pacana NDA. Control of blood glucose level for type 1 diabetes mellitus using improved Hovorka equations: comparison between clinical and in-silico works. Afr J Diabetes Med 2020 Dec;29(1):1-11.
10. Som AM, Yusof NFM, Ali SA, Zawawi N. Simulation work on blood glucose control for type 1 diabetes using modified Hovorka equations. Pertanika J Sci Technol 2019;27(4):1527-1538.
11. Dietary guidelines for Americans. Department of Health and Human Services. 2005. URL: https://health.gov/sites/default/files/2020-01/DGA2005.pdf [accessed 2007-06-07]
12. Baracco R, Kamat D. Pediatric nephrology. Pediatr Ann 2020 Jun 01;49(6):e248-e249. [doi: 10.3928/19382359-20200520-03] [Medline: 32520364]
13. Yusof NFM, Som AM, Ibrehem AS, Ali SA. A review of mathematical model describing insulin delivery system for type 1 diabetes. J Appl Sci 2014;14(13):1465-1468. [doi: 10.3923/jas.2014.1465.1468]
14. Calculating insulin dose. Diabetes Education Online. 2019. URL: https://dtc.ucsf.edu/types-of-diabetes/type1/treatment-of-type-1-diabetes/medications-and-therapies/type-1-insulin-therapy/calculating-insulin-dose/ [accessed 2024-08-01]
15. Richalet J, Rault A, Testud JL, Papon J. Model predictive heuristic control. Automatica 1978 Sep 01:413-428. [doi: 10.1016/0005-1098(78)90001-8]
16. The MiniMed™ 770G System. Medtronic Diabetes. 2023. URL: https://www.medtronicdiabetes.com/products/minimed-770g-insulin-pump-system#viewspecs [accessed 2024-08-01]
17. Bolhuis D, Forde C. Application of food texture to moderate oral processing behaviors and energy intake. Trends Food Sci Technol 2020 Dec;106:445-456. [doi: 10.1016/j.tifs.2020.10.021]
18. Robinson E, Almiron-Roig E, Rutters F, de Graaf C, Forde CG, Tudur Smith C, et al. A systematic review and meta-analysis examining the effect of eating rate on energy intake and hunger. Am J Clin Nutr 2014 Jul;100(1):123-151 [FREE Full text] [doi: 10.3945/ajcn.113.081745] [Medline: 24847856]
19. Daud NAM, Mahmud F, Jabbar MH. Meal simulation in glucose-insulin reaction analysis using Hovorka model towards system-on-chip implementation. ARPN J Eng Appl Sc 2015 Oct;10(19):8927-8935.
20. Cengiz E, Danne T, Ahmad T, Ayyavoo A, Beran D, Ehtisham S, et al. ISPAD Clinical Practice Consensus Guidelines 2022: insulin treatment in children and adolescents with diabetes. Pediatr Diabetes 2022 Dec;23(8):1277-1296. [doi: 10.1111/pedi.13442] [Medline: 36537533]
21. Bell K, King BR, Shafat A, Smart CE. The relationship between carbohydrate and the mealtime insulin dose in type 1 diabetes. J Diabetes Complications 2015;29(8):1323-1329. [doi: 10.1016/j.jdiacomp.2015.08.014] [Medline: 26422396]
22. Ozaslan B, Patek SD, Fabris C, Breton MD. Automatically accounting for physical activity in insulin dosing for type 1 diabetes. Comput Methods Programs Biomed 2020 Dec;197:105757 [FREE Full text] [doi: 10.1016/j.cmpb.2020.105757] [Medline: 33007591]
23. Weinstock RS. Patient education: type 1 diabetes: insulin treatment (beyond the basics). UpToDate. 2022. URL: https://www.uptodate.com/contents/type-1-diabetes-insulin-treatment-beyond-the-basics [accessed 2024-08-01]
24. Marigliano M, Pertile R, Mozzillo E, Troncone A, Maffeis C, Morotti E, et al. Satisfaction with continuous glucose monitoring is positively correlated with time in range in children with type 1 diabetes. Diabetes Res Clin Pract 2023 Oct;204:110895. [doi: 10.1016/j.diabres.2023.110895] [Medline: 37673191]
25. Nefs G, Bazelmans E, Marsman D, Snellen N, Tack CJ, de Galan BE. RT-CGM in adults with type 1 diabetes improves both glycaemic and patient-reported outcomes, but independent of each other. Diabetes Res Clin Pract 2019 Dec;158:107910 [FREE Full text] [doi: 10.1016/j.diabres.2019.107910] [Medline: 31678626]
26. Carrasco-Benso MP, Rivero-Gutierrez B, Lopez-Minguez J, Anzola A, Diez-Noguera A, Madrid J, et al. Human adipose tissue expresses intrinsic circadian rhythm in insulin sensitivity. FASEB J 2016 Sep;30(9):3117-3123 [FREE Full text] [doi: 10.1096/fj.201600269RR] [Medline: 27256623]
27. Yoshino J, Almeda-Valdes P, Patterson B, Okunade A, Imai S, Mittendorfer B, et al. Diurnal variation in insulin sensitivity of glucose metabolism is associated with diurnal variations in whole-body and cellular fatty acid metabolism in metabolically normal women. J Clin Endocrinol Metab 2014 Sep;99(9):E1666-E1670 [FREE Full text] [doi: 10.1210/jc.2014-1579] [Medline: 24878055]
28. Abrams P, Levitt Katz LE, Moore RH, Xanthopoulos MS, Bishop-Gilyard CT, Wadden TA, et al. Threshold for improvement in insulin sensitivity with adolescent weight loss. J Pediatr 2013 Sep;163(3):785-790 [FREE Full text] [doi: 10.1016/j.jpeds.2013.04.003] [Medline: 23706362]

Abbreviations

APD: artificial pancreas device
BGL: blood glucose level

CGM: continuous glucose monitoring
EGP: endogenous glucose production
eMPC: enhanced model-based predicted control
MDI: multiple daily injections
MLR: multiple linear regression
SMBG: self-monitoring of blood glucose
T1D: type 1 diabetes
TDD: total daily dose
UiTM: Universiti Teknologi MARA

Edited by G Eysenbach, T Leung; submitted 19.10.22; peer-reviewed by R Gore, Anonymous; comments to author 17.09.23; revised version received 28.03.24; accepted 01.07.24; published 15.08.24.

Please cite as:
Som AM, Sohadi NAM, Nor NSM, Ali SA, Ahmad MA
In-Silico Works Using an Improved Hovorka Equations Model and Clinical Works on the Control of Blood Glucose Levels in People With Type 1 Diabetes: Comparison Study
JMIRx Bio 2024;2:e43662
URL: https://bio.jmirx.org/2024/1/e43662
doi:10.2196/43662
PMID:

Peer-Review Report

Peer Review of “Exploring the Accuracy of Ab Initio Prediction Methods for Viral Pseudoknotted RNA Structures (Preprint)”

Daniela Saderi[1]; Vaishnavi Nagesh[2]; Randa Salah Gomaa Mahmoud[3]; Toba Olatoye[4]; Femi Qudus Arogundade[5]

[1]PREreview, Portland, OR, United States

[2]Mammoth Biosciences, Brisbane, CA, United States

[3]Zagazig University, Zagazig, Egypt

[4]Kwara State Teaching Service Commission, Ilorin, Nigeria

[5]ASAPBIO, Nigeria

Related Article:

Companion article: https://www.biorxiv.org/content/10.1101/2024.03.21.586060v1

(JMIRx Bio 2024;2:e65154) doi:10.2196/65154

This is a peer-review report submitted for the preprint “Exploring the Accuracy of Ab Initio Prediction Methods for Viral Pseudoknotted RNA Structures.”

This review is the result of a virtual collaborative live review discussion organized and hosted by PREreview and JMIR Publications on June 20, 2024. The discussion was joined by 11 people: 2 facilitators, 2 members of the JMIR Publications team, 1 author, and 6 live review participants, including 2 who agreed to be named: Mike Chang and Heba Abdullah Mohammed Ali. The authors of this review have dedicated additional asynchronous time over the course of 2 weeks to help compose this final report using the notes from the live review. We thank all participants who contributed to the discussion and made it possible for us to provide feedback on this preprint.

Summary

The study [1] examines the performance of 5 RNA-folding engines for predicting complex viral pseudoknotted RNA structures. This research fills a critical gap in the field by comparing the efficiency of minimal free energy (MFE) and maximum expected accuracy (MEA) using a curated dataset of 26 viral RNA sequences with known secondary structures. Contrary to prevailing assumptions favoring MEA models, their findings reveal that pKiss, an MFE-folding engine, outperforms Vsfold 5 in terms of the sensitivity, positive predictive value (PPV), and F_1-score, while laying emphasis on the importance of the PPV and sensitivity parameters in understanding and determining the superior accuracy of pKiss to predict correct base pairs and minimize incorrect predictions. The authors also point out that the engine still needed additional data to achieve high accuracy as well as a better understanding of thermodynamics at the intracellular level.

The statistical analyses used to evaluate the results were 2-way ANOVA and Tukey multiple comparisons test, which provided robust insights into the performance differences among the tested engines. The research integrates bioinformatics with statistics and advanced data science methodologies to promote our understanding of computational RNA biology. The study provides important insights into the relative advantages and disadvantages of both approaches in predicting pseudoknotted RNA structures by contrasting MFE models and MEA models. It also highlights avenues for future research to focus on the development of more sophisticated energy models and MFE engines, like pKiss, to enhance prediction capabilities, especially in the context of viral replication and gene regulation, which may lead to a better understanding of the functional roles of pseudoknotted RNA structures. Overall, this research contributes significantly to the field of computational and molecular biology.

Below, we list major and minor concerns that were discussed by participants of the live review, and where possible, we provide suggestions on how to address those issues.

List of Major Concerns and Feedback

- It would be helpful to provide more context on why percent error was chosen as the primary metric for evaluating different engines, considering alternatives like mean absolute error (MAE) and mean squared error could enhance the analysis. For instance, MAE is robust against outliers, making it a valuable metric, especially when outlier removal is part of the process. Although MAE is less sensitive to extreme values, it can offer a useful qualitative check on the models. On the other hand, the mean squared error’s sensitivity to outliers can be advantageous when the spread of the forecast is important. Including these metrics could provide a more comprehensive evaluation.
- The authors have conducted a comprehensive and insightful study, revealing important differences in prediction accuracy between Vsfold 5 and pKiss. One area that could further enhance the manuscript is the exploration of how auxiliary parameters (eg, Mg2+ binding, dangling end options, H-type penalties) are managed across the various RNA-folding

engines utilized. For example, Vsfold 5, although being an MEA model, may encounter challenges if its handling of Mg2+ binding or dangling ends significantly diverges from what is optimal for the studied RNAs. The authors' observation in section 3.1 that "the low percent error exhibited by pKiss could be the result of the pseudoknot 'enforce' constraint, but it is more likely that this outcome was multivariable, equating to the Turner energy model used, and the sensitive auxiliary parameters enforced by the program" is particularly insightful. This highlights the complexity of RNA structure prediction algorithms. To build on these findings, a structured comparative analysis of parameter handling across different software tools could be highly beneficial. This analysis would not only clarify why certain engines performed better than others but also help in identifying best practices or potential biases in prediction methodologies. Such an addition would significantly strengthen the study's conclusions and provide valuable guidance for future research in RNA structure prediction.

- To build on these findings, a structured comparative analysis of parameter handling across different software tools could be highly beneficial. This analysis would not only clarify why certain engines performed better than others but also help in identifying best practices or potential biases in prediction methodologies. Such an addition would significantly strengthen the study's conclusions and provide valuable guidance for future research in RNA structure prediction.
- In section 3.1 of the manuscript, no significant difference in percent error was identified. However, it does not specify the statistical test employed nor the method used for adjusting *P* values, which are essential details for validating the results. Additionally, the term "Vij" is introduced early in the manuscript but is not contextualized until page 13. Providing this context earlier would enhance the reader's understanding.
- It would be beneficial if "false positive" and "false negative" were more clearly defined, particularly in the context of mRNA detection. To improve clarity, the authors might consider specifying that sensitivity is the appropriate measure for detecting mRNA among known positives, while specificity is the appropriate measure for detecting mRNA among known negatives, where the probability of false positives is 1 – specificity. Additionally, using the Youden index (J), which is defined as sensitivity + specificity – 1, could provide a helpful summary of detection accuracy. This index ranges from –1 (indicating 100% incorrect detection) to 1 (indicating 100% correct detection), offering a clear metric for assessing performance [2].
- Providing the link to the dataset will allow better compliance with open science practices. Please add the link to the dataset as it appears to be missing from the reviewed version of the manuscript. When sharing the dataset, it would be important to also include the associated metadata and appropriate documentation that matches the methods described in the manuscript. For guidelines on how to share data so that it's as reusable as it can be, authors may refer to the Findability, Accessibility, Interoperability, and Reuse (FAIR) principles of data sharing [3].
- Figure 5B displays the PPV as three distinct blocks rather than continuous values, with varying sensitivity within these blocks. This nonrandom binning of PPV suggests the need for further investigation to understand the underlying causes.
- In the Discussion section, the authors stated "We have provided evidence suggesting that MEA software is not always the optimal method of topological prediction when applied to short viral pseudoknotted RNA." This is a significant claim and would benefit greatly from specific references to support the evidence provided in the study. Citing the relevant figures and results that support this claim would significantly enhance comprehension and readability. For example, "As demonstrated in Figure 4, the MEA software Vsfold 5 exhibited higher percent errors in predicting knotted base pairs compared to MFE software like pKiss." Additionally, referencing previous studies that have reported similar findings or that discuss the limitations of MEA methods in RNA structure prediction in the Discussion section would strengthen the credibility of the authors' claims by showing that similar limitations have been observed by other researchers. This helps readers understand that the study is building upon existing knowledge. For instance, "Previous studies have also highlighted the limitations of MEA methods in RNA folding predictions, particularly for pseudoknotted structures (in-text citations)."

List of Minor Concerns and Feedback

Overall, the reviewers really appreciated how clearly the figures and results were presented. Below are some minor suggested improvements.

- In the Abstract section: Please identify the abbreviation PPV as positive predictive value.
- Page 3, first paragraph after Figure 1: Definitions of pseudoknot should be referenced.
- Page 3, second paragraph after Figure 1: Please identify the NMR abbreviation as nuclear magnetic resonance.
- Page 7: The manuscript acknowledges the skewness in the data and provides a rationale for its presence. It's noted that this skewness impacts the training and testing phases, often contributing to false positives and false negatives. It would be beneficial if the authors could elaborate on how they addressed data imbalance, particularly in relation to reducing false positives and false negatives. This additional detail would enhance the understanding of the methods used to manage data skewness and improve model performance.
- Page 8, second paragraph: Mathews et al. 2019 should be corrected to Mathews, 2019 [4].
- Page 8, equation 1: Add a "%" next to *100, giving the output of x%.
- Page 10, Figure 4: In the title, "accurcy" should be corrected to "accuracy."
- Page 10, Figure 4: The bar of the SD of Vienna (knotted) is not presented.

- Page 10, Figure 4: The bars of the SD seem to be widely large, indicating significant variability in the results, so a test of the normality of data distribution should be performed before comparisons. This is also observed for the kinefold results in Figures 5 and 6.
- Page 12, Figure 6B: The color bar on the heat maps is missing.

Concluding Remarks

One of the authors of the manuscript (VM) was present during the call and provided some additional information regarding the source code, which we would like to report here as an additional resource for the reader.

Author's note: Although an original source code was not implemented within this investigation, several well-established web servers were used to generate the data present within this investigation. The link to each web server is provided below.

- VSfold5 [5]
- pKiss [6]
- Kinefold [7]
- NUPACK 3.0 [8]
- RNAfold [9]

Acknowledgments

PREreview and JMIR Publications thank the authors of the preprint for posting their work openly for feedback. We also thank all participants of the live review call for their time and for engaging in the lively discussion that generated this review.

Conflicts of Interest

DS was a facilitator of this call and one of the organizers. No other competing interests were declared by the reviewers.

References

1. Medeiros V, Pearl JM, Carboni M, Er E, Zafeiri S. Exploring the accuracy of ab initio prediction methods for viral pseudoknotted RNA structures. Preprint posted online on February 23, 2023 [FREE Full text] [doi: 10.1101/2024.03.21.586060]
2. Youden index. ScienceDirect. 2010. URL: https://www.sciencedirect.com/topics/medicine-and-dentistry/youden-index [accessed 2024-08-26]
3. FAIR principles. GO FAIR. URL: https://www.go-fair.org/fair-principles/ [accessed 2024-08-26]
4. Mathews DH. How to benchmark RNA secondary structure prediction accuracy. Methods 2019 Jun 01;162-163:60-67 [FREE Full text] [doi: 10.1016/j.ymeth.2019.04.003] [Medline: 30951834]
5. vsfold5: RNA pseudoknot prediction server. Server for Structural Biology. URL: http://www.rna.it-chiba.ac.jp/~vsfold/vsfold5/ [accessed 2024-08-26]
6. pKiss. Bielefeld BioInformatics Service. URL: https://bibiserv.cebitec.uni-bielefeld.de/pkiss [accessed 2024-08-26]
7. KineFold request form. KineFold Web Server. URL: http://kinefold.curie.fr/cgi-bin/form.pl [accessed 2024-08-26]
8. Analysis: input. NUPACK. URL: https://nupack.org/analysis/input [accessed 2024-08-26]
9. RNAfold web server. Institute for Theoretical Chemistry: ViennaRNA Web Services. URL: http://rna.tbi.univie.ac.at/cgi-bin/RNAWebSuite/RNAfold.cgi [accessed 2024-08-26]

Abbreviations

FAIR: Findability, Accessibility, Interoperability, and Reuse
MAE: mean absolute error
MEA: maximum expected accuracy
MFE: minimal free energy
PPV: positive predictive value

Edited by G Eysenbach; submitted 06.08.24; this is a non–peer-reviewed article;accepted 06.08.24; published 11.09.24.

Please cite as:
Saderi D, Nagesh V, Mahmoud RSG, Olatoye T, Arogundade FQ
Peer Review of "Exploring the Accuracy of Ab Initio Prediction Methods for Viral Pseudoknotted RNA Structures (Preprint)"
JMIRx Bio 2024;2:e65154
URL: https://bio.jmirx.org/2024/1/e65154
doi:10.2196/65154
PMID:

Publisher:
JMIR Publications
130 Queens Quay East.
Toronto, ON, M5A 3Y5
Phone: (+1) 416-583-2040
Email: support@jmir.org